Design and Construction of a Mass Loaded Tapered Quarter Wavelength Tube (ML TQWT) Using the Fostex FE-164 Full Range Driver

Martin J. King
40 Dorsman Dr.
Clifton Park, NY 12065
MJKing57@aol.com

Introduction :

I have been interested in transmission line speaker systems for many years. This interest was sparked after hearing a transmission line system, based on a Focal ten inch woofer, at the home of a local audio club member over ten years ago. Since then I have looked several times into designing and building such an enclosure only to find that the available literature was not nearly as complete as the Thiele[1] and Small[2-4] papers for designing sealed and ported speaker systems. In fact, there did not appear to be any accurate transmission line mathematical model, similar to the closed and ported box models, where one could specify the numerical values of several key parameters and predict the system response. About two years ago I came to the conclusion that if I were ever going to build a transmission line speaker system, I would have to develop my own methods for designing the enclosure.

For the next year, I worked on developing software for the design of transmission line enclosures using the MathCad[5] computer program. I purchased some Focal eight inch mid-bass drivers and constructed a test line to make the measurements required to correlate the mathematical model being formulated. Last March, I finally finished building my first transmission line speaker system. The computer model predictions and the final system measurements were in reasonable agreement, but some additional work was still needed to fully understand the measured results. This project is documented and can be found in my first article[6] on the transmission line web site (www.t-linespeakers.org).

During the following four months, I spent a considerable amount of time working at understanding the final system measurements and improving the original MathCad model. The result was four separate MathCad models, covering different transmission line geometries, and a second article[7] on the transmission line web site. By July, the correlation between the calculated results, using these newer computer models and the final system measurements, had improved significantly for the Focal transmission line speaker system.

While these newer worksheets did a good job of predicting the response of transmission lines composed of straight constant cross-sectional area segments, when I started experimenting with tapered or expanding lines the results still did not appear to be correct. A second round of revisions took place that corrected a sign error in the derived equations, fixed a couple of typo's, and added a frequency dependent acoustic impedance at the terminus of the line. None of the improvements significantly impacted the results presented in the two articles mentioned above. These third generation worksheets were uploaded to the transmission line web site in September 2000 and have been available since then for others to download and use. The latest revision date for each worksheet is shown below in Table 1.

Table 1 : Worksheet Revision Dates

Worksheet Name	Revision Date
TL Closed End	9/02/00
TL Open End	9/19/00
TL Offset Driver	9/19/00
TL Sections	9/28/00

Correlating these third generation worksheets, before they were distributed, was a high priority. The first piece of data available was the measurements I had made of the test line and the final Focal transmission line speaker system. This data verified that the performance of a straight transmission line could be modeled accurately. To verify that tapered or expanding transmission line performance could also be simulated accurately, I reconfigured the worksheets to be able to calculate the responses of exponential horns. All of the plotted data for the exponential horn in Section 8.8 of Olsen's classic acoustics[8] text could be simulated very accurately by setting the damping coefficient equal to zero. Based on these results, I concluded that the worksheets were working correctly and I made them available for downloading.

Goals For My Next Project :

For my next project, I wanted to design and build either a tapered transmission line or a tapered quarter wavelength tube TQWT (really an expanding transmission line or sometimes referred to as a Voigt pipe). Both of these enclosure geometries would test the corrected equations in the MathCad worksheets. Although the calculations had been correlated to my satisfaction, the real verification of the equations would be to design, predict the performance, construct the enclosure, measure the performance, and then correlate the measurements for a completed speaker system. Until that had been done, there was always going to be nagging doubt in the back of my mind with respect to the capability of the MathCad worksheets to model general transmission line geometries. Verification of the MathCad transmission line worksheets became a primary goal for this project.

As a secondary goal, I also wanted to try a full range driver project. Some time ago, I discovered the Single Driver Website™ (http://melhuish.org/audio/). Having read the literature contained on the web site pages, the DIY project pages, and following the discussions on the forum for several months I became interested enough to want to try one of these types of drivers. If I took the total cost of a mid-bass driver, a tweeter, and the necessary crossover components required to build a respectable two way system and applied that amount to a quality full range driver would the result be something special? The simplicity of designing a system without any crossover between the driver and the amplifier was very appealing. Could a single high efficiency full range driver, in the right cabinet, cover the entire audio spectrum while at the same time produce superior imaging as claimed by the full range driver community? This was just too intriguing a challenge to pass up.

Driver Selection :

I started looking at the full range drivers in my local Radio Shack store. The Radio Shack drivers were constantly being discussed on the Single Driver Website™ forum. In particular, the 5 1/4″ RS 40-1354 driver was constructed from a paper cone with a small whizzer cone attached to the center where a dust cap is usually found in a typical mid-bass driver. The list price of approximately $15 was attractive but I was not all that impressed with the driver's construction quality. If I was going to spend several months designing and building a system, I could easily justify spending a little bit more for a better driver.

I decided to set my sights a little higher and started looking at the Fostex full range drivers. I looked at the Fostex FE-164 driver, the FE-167 driver, and FE-168 Sigma driver. All three of these six inch drivers appear to be very similar. I wouldn't be surprised if there were a lot of common parts shared by the three drivers. The biggest difference appears to be the price. All three drivers have impressive SPL response plots between 100 Hz and 20 kHz. I elected to go with the least expensive model, the FE-164 driver, keeping in mind the potential for upgrading later to the more expensive FE-168 Sigma driver.

I ordered two of the Fostex FE-164 drivers from the Fostex on-line Internet store (http://store.yahoo.com/fostex). Ordering was extremely simple and delivery was within one week. The drivers, including the screws and washers needed to mount the drivers and a rubber gasket to seal the opening, came packaged in individual double walled cardboard boxes. The quality of construction was excellent when compared to the Radio Shack RS 40-1354 drivers.

I connected the drivers to an old receiver and allowed music to play through them for 50 hours. The first test I ran was to determine the Thiele / Small parameters using Liberty Instrument's measurement program LAUD. Table 2 shows the results of these measurements along with the manufacturer's specifications. The plotted output is shown in Figure 1.

Table 2 : Measured Thiele / Small Parameters
of the Fostex FE-164 Full Range Driver

Property	Spec.	Average	Driver 1	Driver 2	Units
f_d	50.0	57.8	58.2	57.4	Hz
V_{ad}	32.2	28.8	28.8	28.9	liters
Q_{td}	0.31	0.35	0.35	0.35	
Q_{ed}	0.34	0.38	0.38	0.38	
Q_{md}	4.00	4.90	5.01	4.78	
R_e	7.2	7.1	6.9	7.2	ohm
S_d	132				cm^2
M_{md}	6.9	6.4	6.3	6.5	gm
Bl		6.58	6.54	6.63	N/amp
SPL/w/m	92	93.5	93.6	93.4	dB
X_{max}	1.0				mm

Figure 1 : Measured Impedance and Derived T/S Parameters

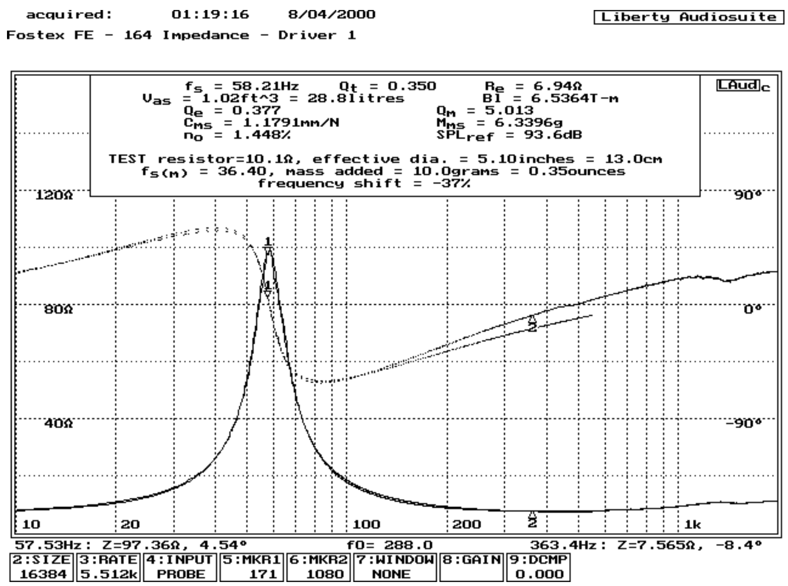

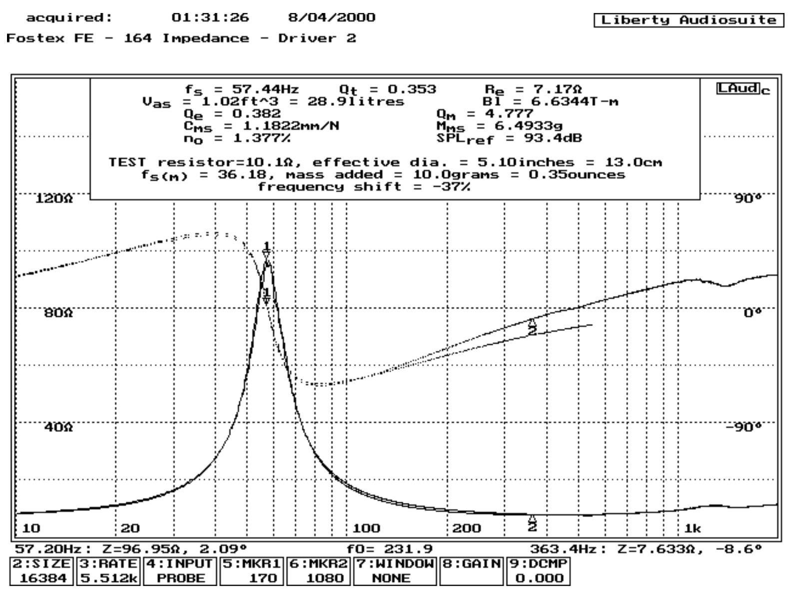

Behavior of Tapered, Straight, and Expanding Transmission Lines :

After making the corrections and improvements to the MathCad worksheets, my understanding of tapered and expanding transmission lines improved considerably. I began to see some real benefits for both tapered and expanding transmission lines. One thing I studied was the changes that occur, in the straight transmission line's quarter wavelength resonant frequencies, when a tapered or expanding geometry is introduced.

The following example illustrates the differences in the quarter wavelength resonant frequencies for a tapered, a straight, and an expanding transmission line. Assume that the three transmission lines all have the same length and the same internal volume and are modeled without any internal stuffing. The basic geometry is defined below for the straight transmission line designed for a 40 Hz quarter wavelength resonant frequency.

Area = (10 in) (10 in) = 100 in^2
= 0.065 m^2

Length = c / (4 x f)
= (342 m/sec) / (4 x 40 Hz)
= 84.15 in
= 2.14 m

Volume = Area x Length
= 8415.4 in^3
= 137.9 liters

Table 3 shows the area at the driven end of the transmission line S_0 and the area at the open end (terminus) of the transmission line S_L for the three different assumed geometries. Again, all three transmission lines have the same length and internal volume.

Table 3 : Cross-Sectional Area Definitions

Transmission Line Configuration	S_0 (in^2) at x = 0	S_L (in^2) at x = L
Tapered Line	150	50
Straight Line	100	100
Expanding Line	50	150

Figure 2 shows the magnitude of the air velocity at the terminus end of the transmission line assuming a 1 m/sec velocity at the driven end. This applied 1 m/sec air velocity is assumed to be uniform over the entire area S_0. As the frequency of the driven end increases from 1 Hz to 1000 Hz, thirteen separate resonant frequencies are excited. The sharp peaks in the plots in Figure 2 define the frequency of each resonance.

Looking in Figure 2 at the magnitude of ε for the frequencies below 10 Hz you can see that the value is different for each of the three transmission line geometries. The magnitude is equal to the ratio of the driven area S_0 over the terminus area S_L. This indicates that at very low frequencies, the volume of air moving into the line at x = 0 is equal to the volume of air moving out of the line at x = L. This relationship is derived as follows for frequencies below 10 Hz.

$$\varepsilon = u(L,t) / u(0,t)$$
$$= u(L,t) / (1 \text{ m/sec})$$

$$S_0 \times u(0,t) = S_L \times u(L,t)$$
$$S_0 \times (1 \text{ m/sec}) = S_L \times u(L,t)$$
$$S_0 / S_L = u(L,t) / (1 \text{ m/sec})$$

$$\varepsilon = S_0 / S_L$$

Also notice in Figure 2 that the resonant peaks above 100 Hz appear to occur at approximately the same frequencies. However it can also be seen in Figure 2, that the first resonance for each of the transmission lines occurs at a different frequency.

Table 4 summarizes the resonant frequencies of the first five modes for each of the three transmission lines. Also shown, in the second column of Table 4, are the ideal quarter wavelength frequencies that would be calculated based on a classical solution of the one-dimensional wave equation. The solution of the one-dimensional wave equation can be found in most undergraduate physics or acoustics textbooks. The problem being solved in these textbooks is typically a constant cross-section pipe with a boundary condition specified at each end. The boundary conditions used to solve the wave equation for an open ended transmission line are a sinusoidal velocity applied at the driven end S_0 and a zero pressure (or velocity maximum) defined at the open terminus end S_L.

Table 4 : Frequencies of the Quarter Wavelength Standing Waves

Mode Number (n)	Calculated n x c / (4 x L)	Tapered Line	Straight Line	Expanding Line
1	40	30	38	47
3	120	113	114	116
5	200	191	190	190
7	280	269	267	266
9	360	347	343	340
Units	(Hz)	(Hz)	(Hz)	(Hz)

Comparing the second and the fourth columns of Table 4, the MathCad model consistently calculates lower resonant frequencies then the classic textbook solution. This is due to the frequency dependent acoustic impedance specified at the terminus, in the MathCad model, instead of the zero pressure boundary condition assumed in the textbook solution. The acoustic impedance boundary condition makes the pipe appear to be slightly longer which leads to lower resonant frequencies. A similar situation occurs when sizing the length of a port in a bass reflex enclosure. The effective length of the port, used in most design calculations, is typically longer then the actual physical length of the port.

Also notice in Table 4, that the resonant frequencies above 100 Hz are approximately the same. As stated previously, when discussing Figure 2, the first mode occurs at different frequencies for each of the three transmission line geometries. For the tapered transmission line, the lowering of the first resonant frequency would lead to a shorter line for a 40 Hz design goal. For the expanding transmission line, the increase in the first resonant frequency would have the opposite effect of requiring a longer line for a 40 Hz design goal.

For most transmission lines, the cross-sectional area is usually held constant or tapered. Looking back at the work done by Bailey[(9)] and then by Bradbury[(10)], the sketches in Bailey's article would indicate that they were working with test results from tapered transmission lines. Suppose that the expected quarter wavelength resonant frequencies were calculated in the same manner as those shown in the second column in Table 4. Then recognize that the measured results were probably more typical of the resonant frequencies listed in the third column of Table 4. The tapered transmission line would have exhibited a lower resonant frequency for the first mode, when compared to a straight transmission line, but correlated closely with the higher frequency modes of the straight transmission line. Bradbury's theory contends that only the low frequency sound waves couple with the fibers, through a viscous damping coefficient, resulting in motion of the fibers and a reduction in the speed of sound due to the added moving fiber mass. This postulated reduction in the speed of sound would result in a lower resonant frequency for the first quarter wavelength mode as observed in the test data. At higher frequencies, the fibers are not coupled to the sound waves and do not move so the speed of sound is unchanged and the resonant frequencies are closer to the expected values. If the impact of the tapered geometry on the quarter wavelength frequencies was not included in the analysis of Bailey's test data, then I have to wonder if this oversight was the impetus for the moving fiber explanation derived by Bradbury.

Figure 2 : Magnitude of the Terminus Velocity Response for a 1 m/sec Driven Excitation

Terminus Velocity for a Tapered Transmission Line

Terminus Velocity for a Straight Transmission Line

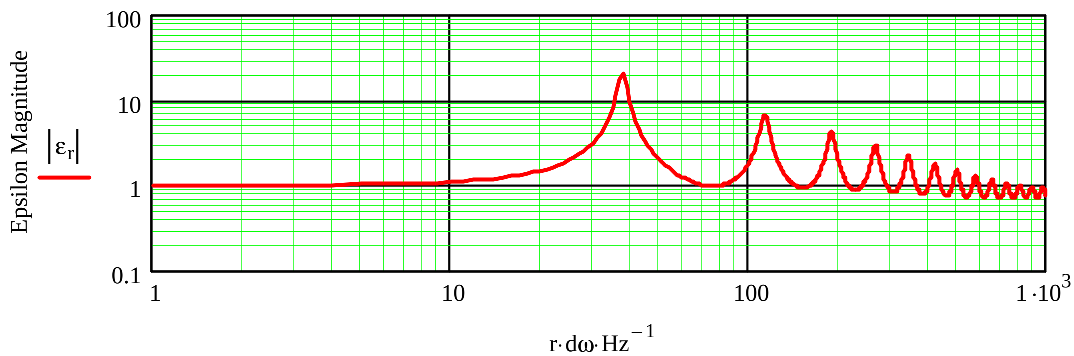

Terminus Velocity for an Expanding Transmission Line

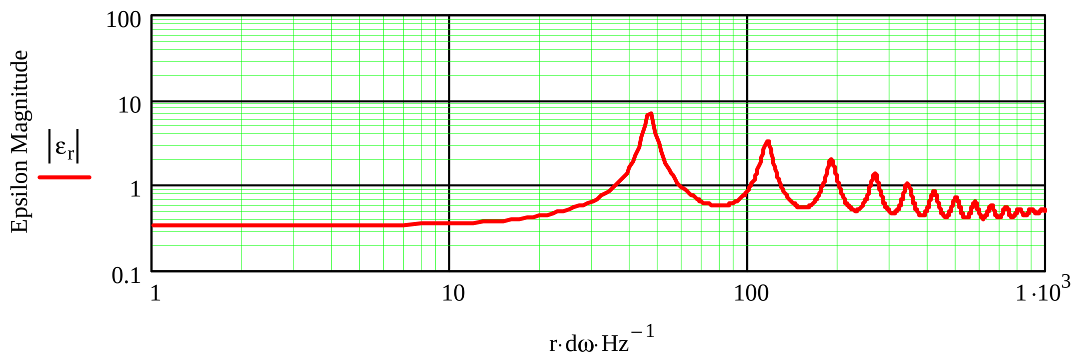

Original Design Options :

I looked at three different designs for the Fostex FE-164 drivers, a tapered transmission line, a folded TQWT, and a tall straight TQWT. For each design option I experimented with the cross-sectional area, the line length and taper rate, the position of the driver, and the location and density of the fiber stuffing material. One design goal was to keep the driver height between 30 and 40 inches so it would be compatible with a comfortable sitting position for listening. The results of these studies are shown in Figures 3, 4, and 5.

The same information is presented in each of the figures. At the top of the figure is a sketch of the enclosure with the critical dimensions shown in inches. Also in the sketches, is a shaded region indicating the location of Dacron Hollofil II stuffing. For each design, the density of the stuffing is defined in the figure’s title. Just below the sketches are two calculated SPL response plots. The upper SPL response is the sum of the driver and terminus SPL responses, which are shown in the lower plots. The appropriate phase angles have been accounted for during the summations. In the lower plot, the solid line represents the driver SPL response while the dashed line represents the terminus SPL response.

For each of the three design options, the resonant frequencies calculated using the MathCad worksheet were correlated against natural frequencies and mode shapes calculated using the ANSYS finite element program. The frequencies of the peaks calculated in the MathCad simulations matched the ANSYS natural frequencies so I knew that the line geometry had been correctly modeled in MathCad. The ANSYS results also indicated at what frequency the standing waves depart from being axial waves, along the length of the line, and became transverse waves. This was an indication of the upper frequency limit for which the MathCad results were accurate. For the geometries shown in Figures 3, 4, and 5 this upper frequency limit is reached at approximately 500 Hz.

Looking at the response plots shown in Figures 3 and 4, there is not much difference in the summed system response. Both designs start to roll-off between 50 and 60 Hz and exhibit a significant ripple above 200 Hz. This similarity in the two system responses is interesting considering that within approximately the same cabinet volume, the folded TQWT has a line length that is almost twice the tapered transmission line length.

The most interesting response plot is shown in Figure 5. Not only does the bass response extend down to 40 Hz, the ripple above 200 Hz is significantly reduced. There are several key features in this design that contribute to the extended bass output and almost flat frequency response. By eliminating the fold, reflections inside the cabinet that result from this discontinuity were eliminated. Also, mounting the driver at mid length significantly improved the smoothness of the system response. Moving the driver to a different location along the length introduces additional ripples into the midrange response.

The final detail that plays a major roll in the system response, shown in Figure 5, is the narrow shelf that forms the terminus geometry. The terminus in this design represents a significant restriction at the end the line. The air in the slot becomes an additional mass loading on the quarter wavelength standing waves. If the base of the cabinet was removed, and the terminus area increased to the maximum cross-section, the first mode of the straight TQWT would rise to 73 Hz. By inserting the shelf and creating an air mass in the slot, the first quarter wavelength mode drops from 73 Hz to 38 Hz. In addition, this mass loading also causes the roll-off of the terminus response above 100 Hz to be significantly faster compared to the tapered transmission line and the folded TQWT. These are the reasons that I refer to this design geometry as a mass loaded tapered quarter wavelength tube or expressed in abbreviated format a ML TQWT.

I learned one more important lesson while working on these three designs. Notice that the placement of the stuffing in all three cabinets leaves the final section of each cabinet empty. Viscous damping, due to the fiber stuffing, reaches a maximum value at the location of the maximum air velocity. For the first quarter wavelength standing wave, the maximum air velocity is at the terminus of the transmission line. This is the mode we want to retain and use to augment the driver’s fading bass output. The higher modes have several locations, along the length of the line, at which the velocity reaches a maximum. By placing the stuffing material in the first two thirds of the line, the higher modes are attacked with damping while the first mode is minimally damped. I have seen this stuffing scheme recommended but have never pursued it until recently. I have now also implemented this stuffing tweak on my Focal transmission line system, which has resulted in improved low frequency performance.

Figure 3 : Tapered Transmission Line Option (Stuffing Density = 0.4 lb/ft^3)

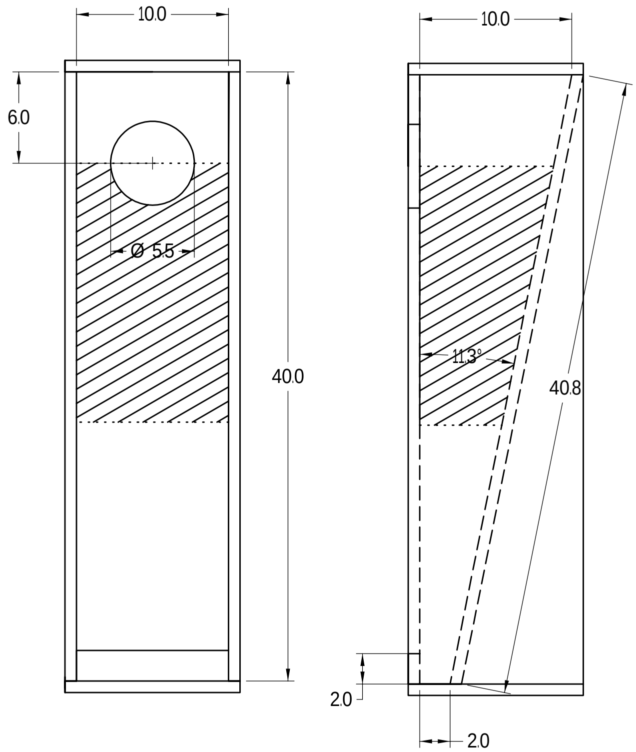

Far Field Tapered Transmission Line Sound Pressure Level Responses

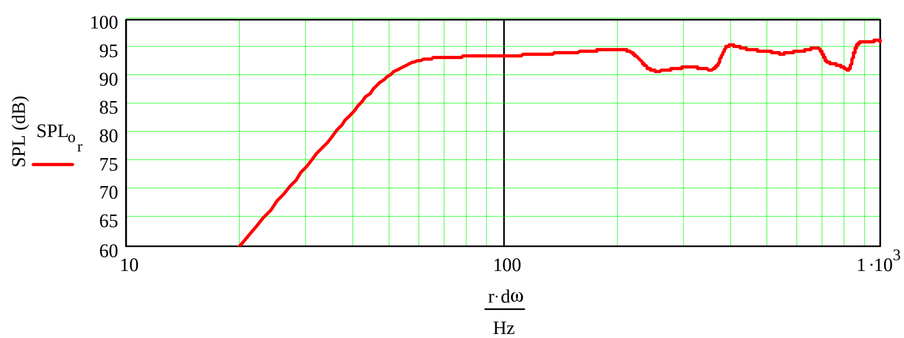

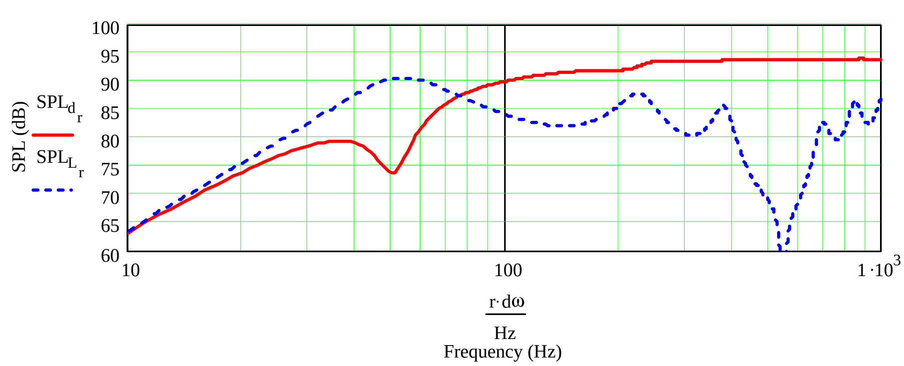

Figure 4 : Folded TQWT Option (Stuffing Density = 0.4 lb/ft^3)

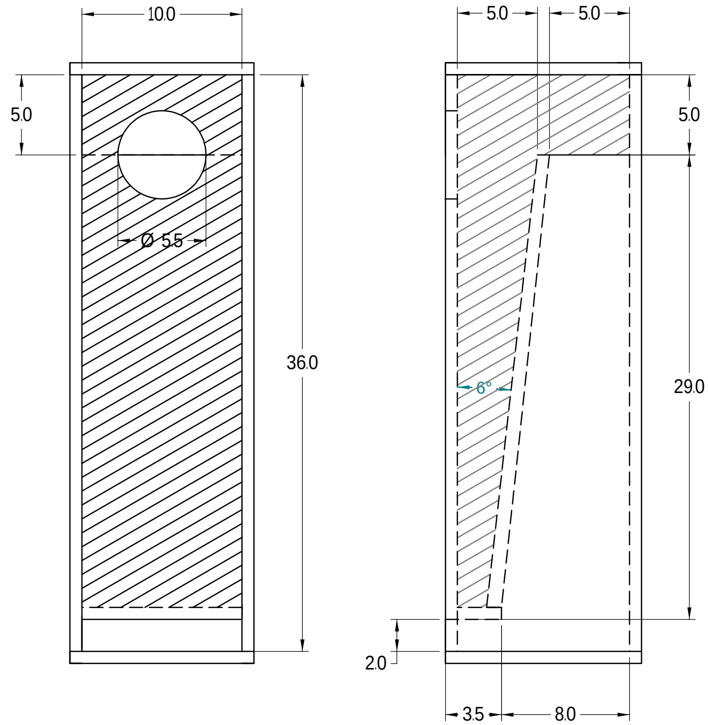

Far Field Folded TQWT Sound Pressure Level Responses

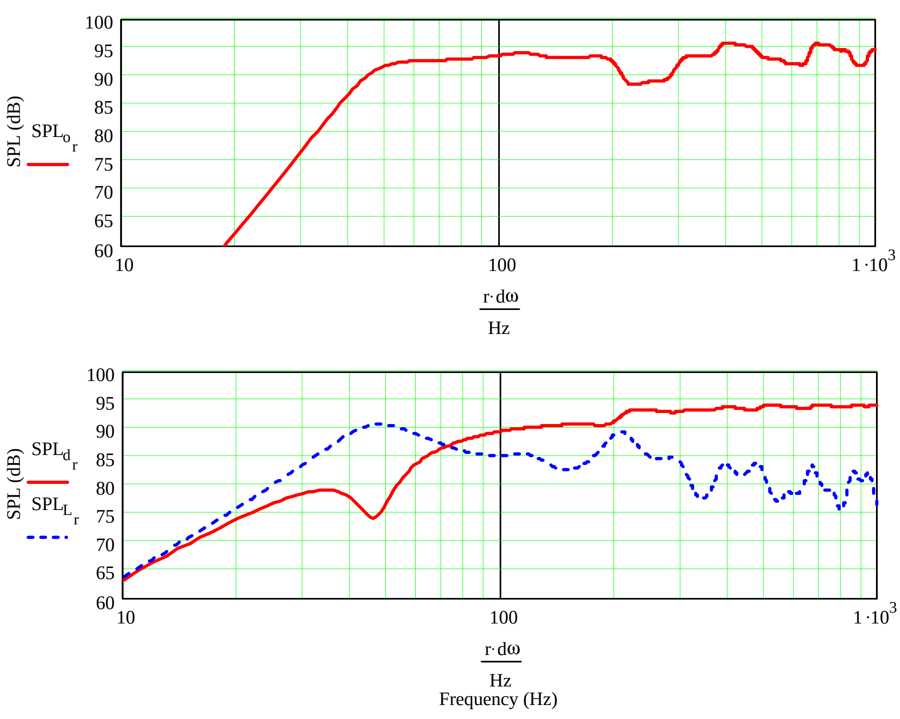

Figure 5 : Straight TQWT Option (Stuffing Density = 0.25 lb/ft^3)

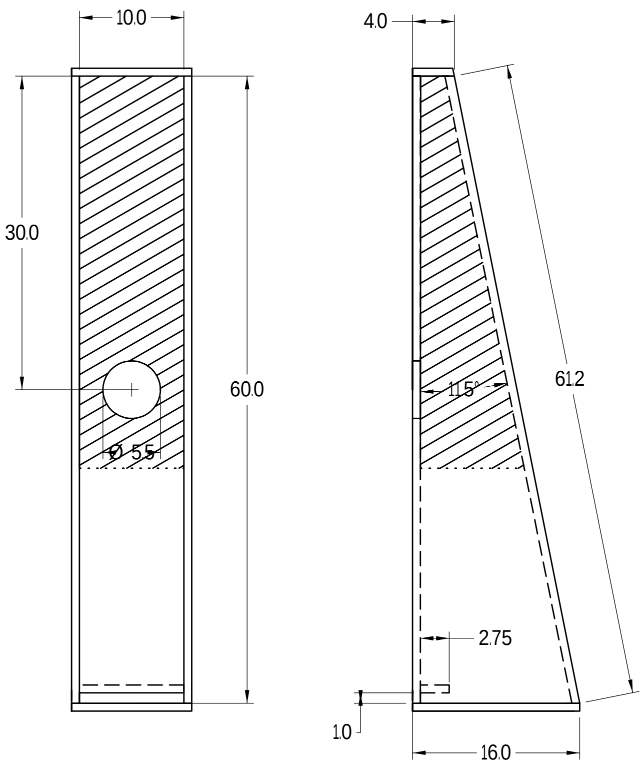

Far Field Straight TQWT Sound Pressure Level Responses

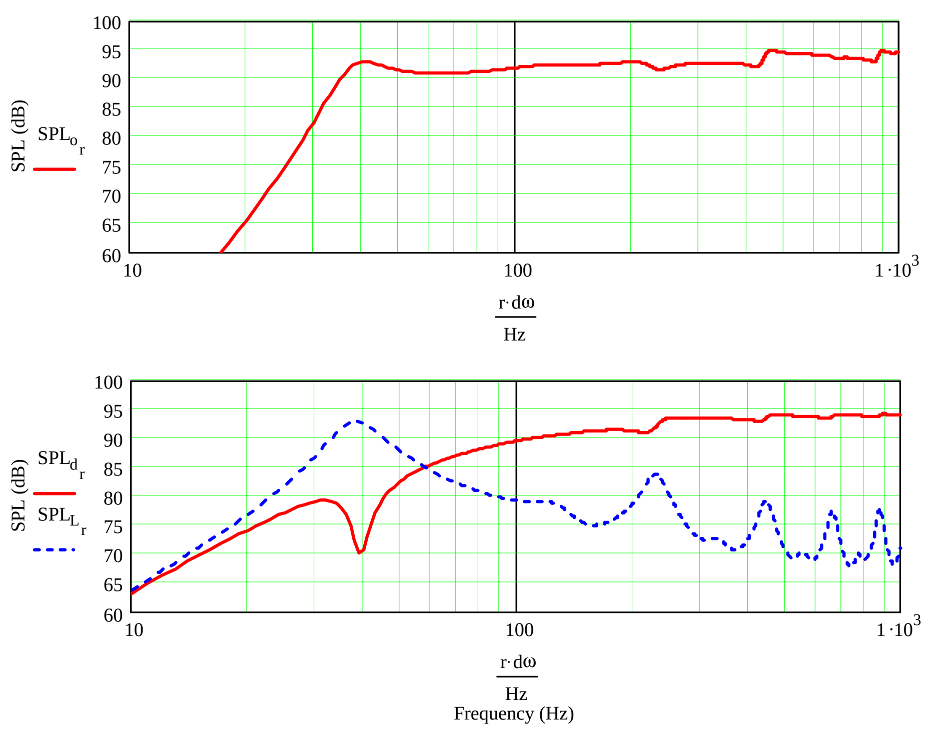

Comparing the ML TQWT Enclosure with a Large Bass Reflex Enclosure :

Several weeks ago, the first sketches of the ML TQWT enclosure and some preliminary SPL measurements were posted on the transmission line web site. Immediately, questions were raised concerning the claim that this was indeed a TQWT enclosure as opposed to a large bass reflex enclosure. My classification of this enclosure as a variant of a TQWT is rooted in the difference in the type of spring that the cabinet has created for the port mass. A classic vented box is composed of a uniformly compressed air spring that interacts with the port mass to form a low resonant frequency spring-mass system. In the ML TQWT, the spring is a quarter wavelength standing wave that interacts with the port mass to form a low resonant frequency spring-mass system. This is a slight difference that produces a lot of the same behavior in the driver and terminus SPL responses and in the electrical impedance. But there are some significant differences.

To try and illustrate the difference in the behavior of the air springs, I constructed two acoustic finite element models. The first model is representative of the ML TQWT geometry as shown in the sketch at the top of Figure 5. The second model is representative of a bass reflex cabinet that includes the same slot geometry and has an equal enclosure volume. These models do not include any damping effects associated with fiber stuffing. All natural frequencies and mode shapes are calculated for an empty enclosure.

The results of these analyses are included as Attachments 1 and 2. Each attachment contains six plots. The first plot shows the model geometry and the finite element mesh. Setting the pressure at the terminus equal to zero is the only boundary condition applied to the finite element model. The next five plots show the first five natural frequencies and mode shapes for each enclosure. Looking at each plot, the frequency is specified in the seventh line of the text block at the upper right and in the plot's title line. Also included in the text block is a legend that defines the pressure ranges associated with each color. Keep in mind that these pressure levels represent a normalized result and are intended only to show relative pressure distributions within the enclosure.

The first mode of each enclosure is shown in the color contour plot immediately following the plot of the finite element mesh. The ML TQWT's first mode occurs at 40 Hz. The pressure distribution in the enclosure exhibits a maximum pressure at the closed end that decreases in a quarter wavelength pattern as the terminus is approached. The bass reflex enclosure's first mode occurs at 43 Hz. The pressure is essentially constant everywhere in the enclosure. While the first mode frequencies are almost equal, the difference in the pressure distribution within each enclosure should be obvious.

All modes shown, for the ML TQWT, are quarter wavelength pressure distributions and are accurately predicted by the MathCad worksheets. Looking at the bottom plot in Figure 5, peaks are evident at each of these frequencies. Notice that the 3/4, 7/4, 11/4, and 15/4 peaks can barely be seen in the terminus response in Figure 5. This is due to the driver being located at the half height position in the enclosure. The 3/4 and 7/4 modes, as shown in Attachment 1, have a zero pressure value very close to the enclosure half height, which minimizes the excitation of these modes by the driver.

While the first mode shown for the bass reflex cabinet is what we expected to see, the next four modes are all standing waves that occur inside the enclosure. The frequencies of these modes can be verified by calculating the frequencies of the half sine waves with wavelengths equal to the basic enclosure dimensions. These modes will disturb the frequency response plots for the bass reflex enclosure. If the “TL Sections” worksheet is used to model the bass reflex enclosure, the impact of just the axial modes can be seen in the system frequency response. These results are shown in Figure 6 and can be compared to the response plots shown in Figure 5. It should also be noted that adding fiber stuffing to the enclosure attenuates these modes significantly.

Figure 6 : Bass Reflex SPL Response

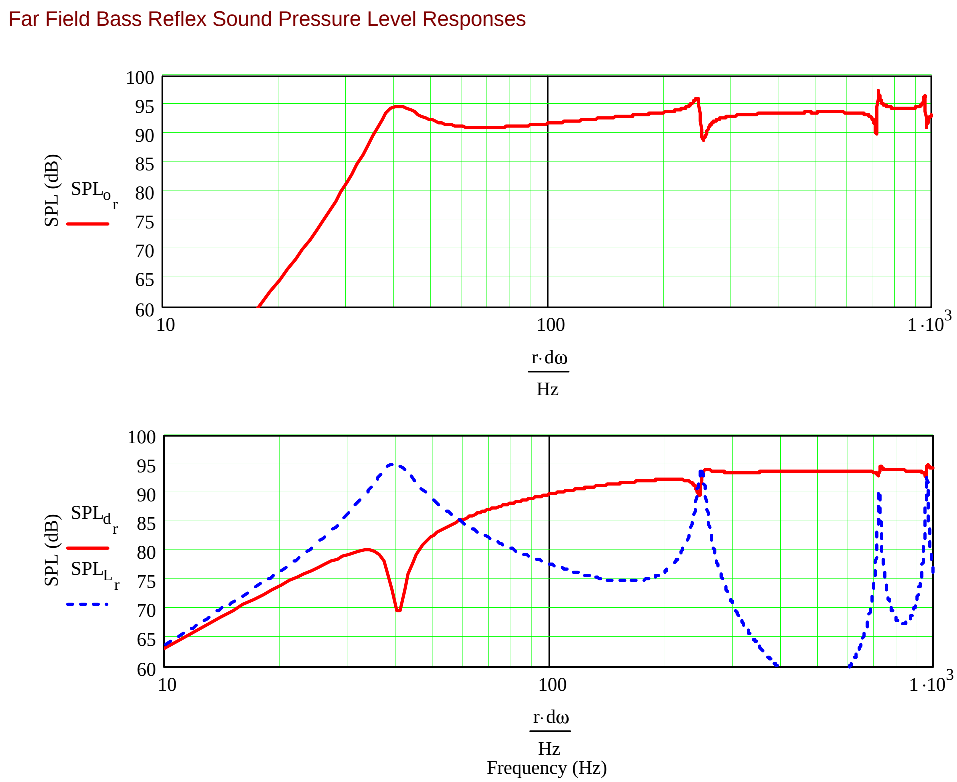

In summary, I consider the design shown in Figure 5 to be a variant of a TQWT that I have chosen to classify as a ML TQWT. I justify this position by showing, in Attachment 1, that the first five natural frequencies and mode shapes are clearly quarter wavelength in nature. All of these modes are accounted for in the MathCad worksheets. The design has been optimized to maximize the contribution of the first mode, to the system bass response, while minimizing the peaks and nulls usually associated with the higher modes of a TQWT. The design requires the terminus to be at one end of the cabinet and is sensitive to the placement of the driver along the length of the line and the tapered shape of the enclosure. The classic bass reflex design does not place any of these requirements on the enclosure shape and is reasonable insensitive to the placement of the driver and the port.

Final Design Optimization :

A few changes were made to the enclosure shown in Figure 5. I decided to move the driver to one of the tapered sides and then make a mirror image pair of enclosures. This was purely a cosmetic change. I also elected to use a port instead the original shelf design for the terminus. Using a port allows easy adjustment of the mass load by increasing or decreasing the port length. Finally, to add more stability to the cabinet, the bottom panel was cut larger by two inches in all directions and rubber feet were placed one inch in from the bottom panel corners. The final design configuration is illustrated in Figure 7.

A final simulation was run, based on the construction geometry shown in Figure 7, and is included as Attachment 3. Several of the resulting plots have been copied and included as Figures 8, 9, and 10.

Figure 7 : ML TQWT Final Design Drawing

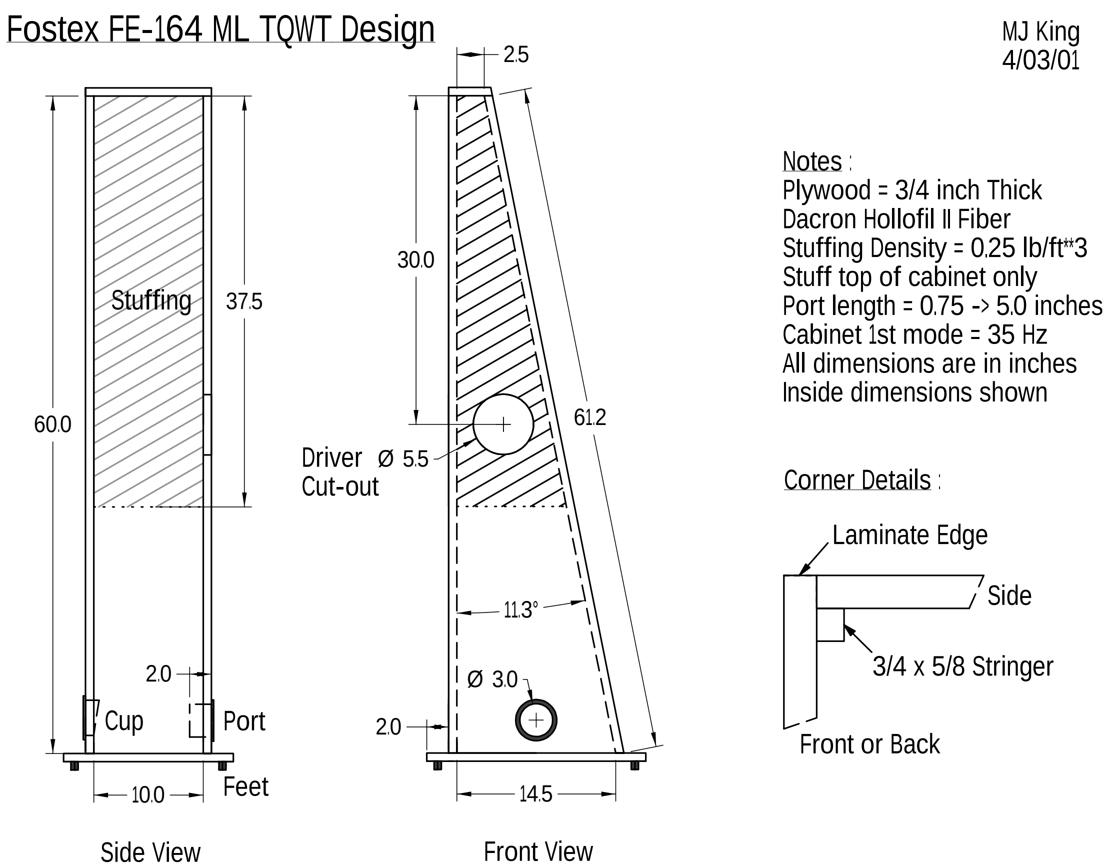

Figure 8 : Calculated System SPL Results for the ML TQWT
(solid line = transmission line, dashed line = infinite baffle)

Far Field Transmission Line System and Infinite Baffle Sound Pressure Level Responses

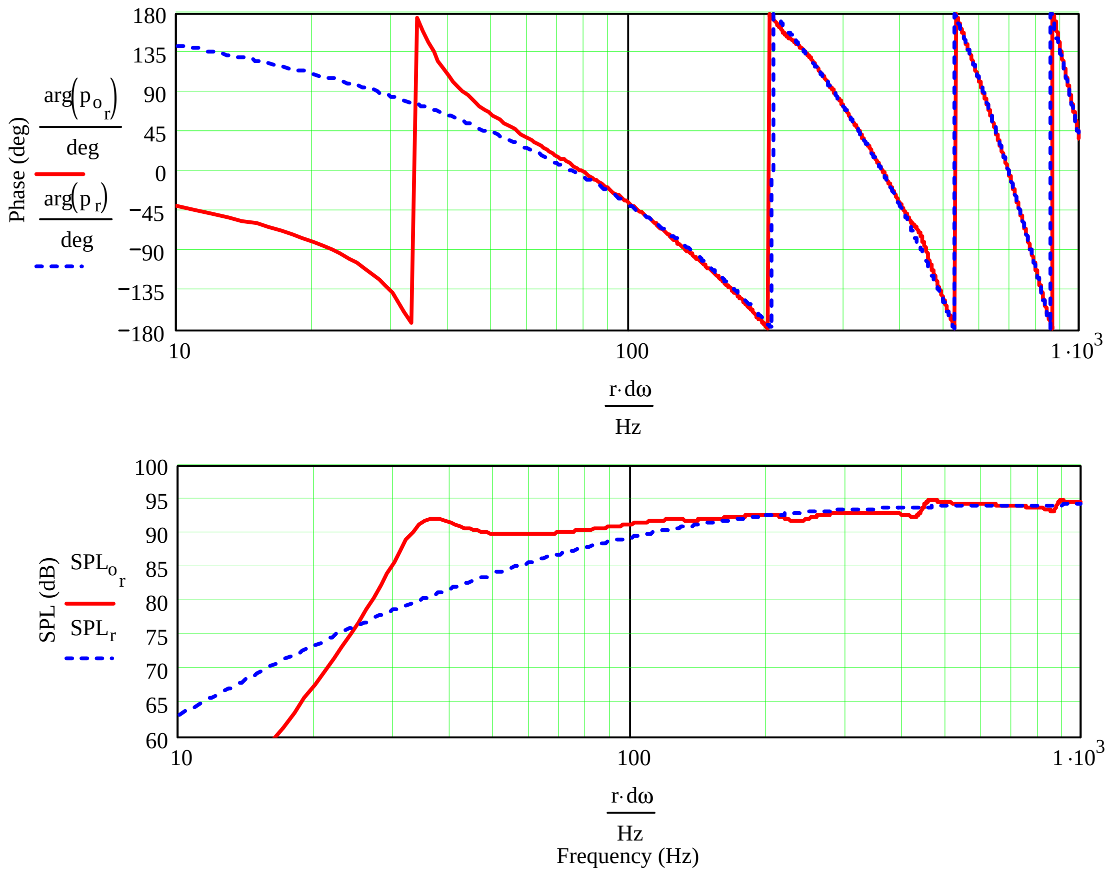

Figure 9 : Calculated Driver and Terminus SPL Results for the ML TQWT
(solid line = driver, dashed line = terminus)

Woofer and Terminus Far Field Sound Pressure Level Responses

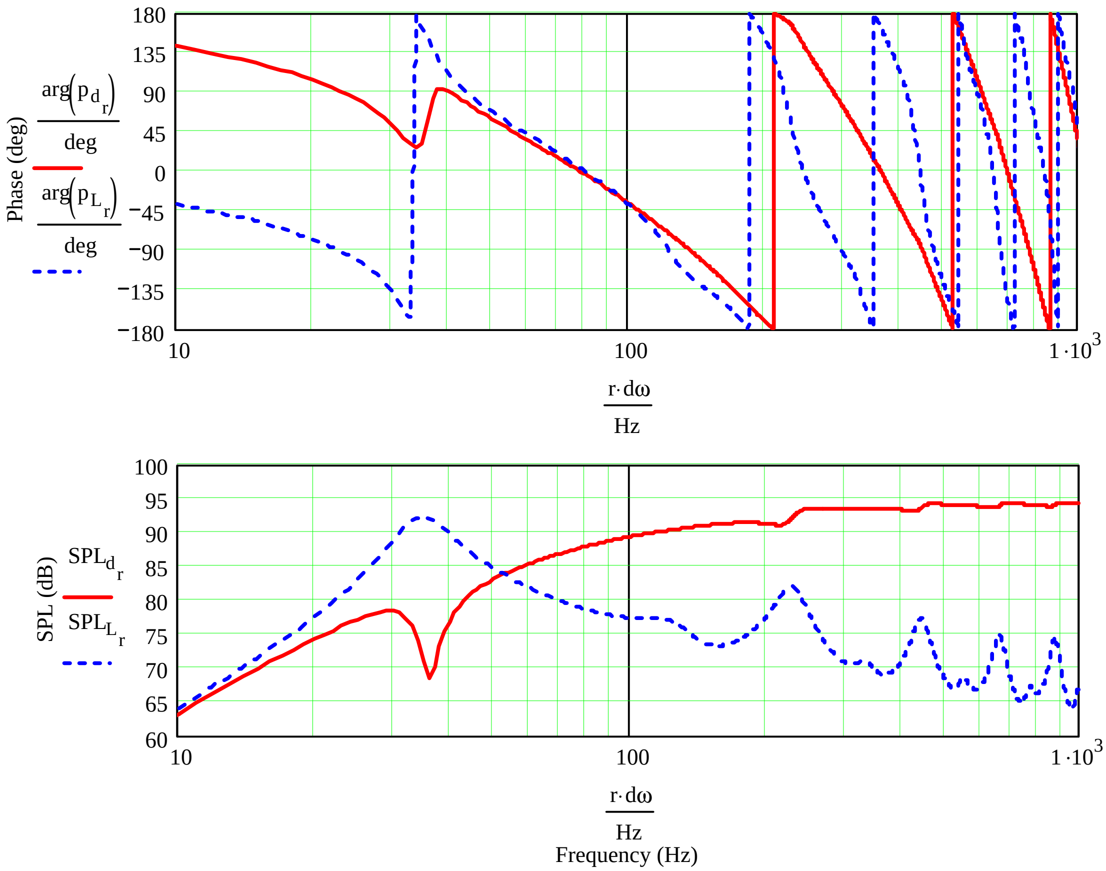

Figure 10 : Calculated Impedance Results for the ML TQWT
(solid line = transmission line, dashed line = infinite baffle)

Transmission Line System and Infinite Baffle Impedance

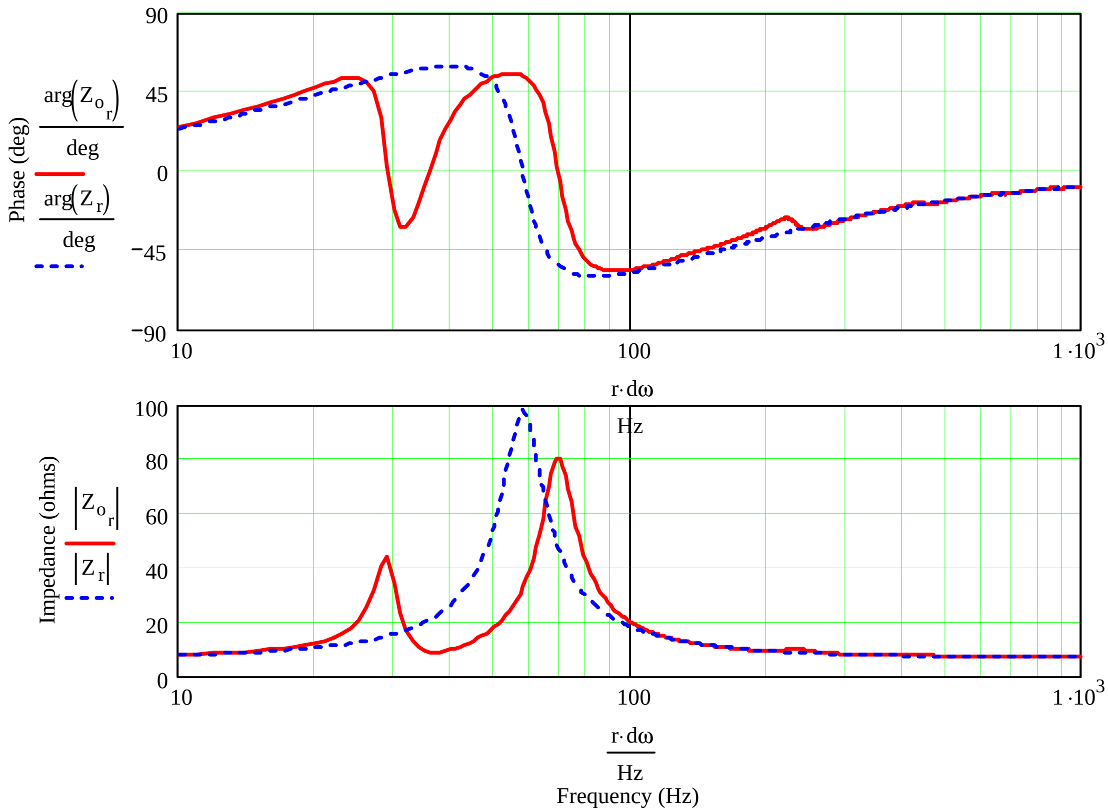

Construction Details :

Building the enclosure, shown in Figure 7, was fairly straightforward with just a couple of challenges. I am sure that there are many ways to build this design, I will only cover my approach briefly highlighting some of the important aspects. All of the parts were cut from two 3/4″ thick 4′ x 8′ sheets of birch veneer plywood. I used simple butt corner joints with an iron-on birch laminate applied to the exposed end grains.

I started with the first challenge, cutting the front and back panels. These are the large trapezoidal shapes. I used an eight-foot aluminum ruler and a circular saw to cut each one separately. By measuring twice, and using a new blade in the saw, I was able to produce four pieces that were very close in size. After cutting the four pieces, I made all of the required holes in the front and back panels and laminated the exposed end grains. I then glued long strips of plywood, 3/4″ x 5/8″ cross-section, along the inside surface of the front and back panels. Small nails were used to hold everything in place while the glue dried. These long stringers ran from the top of the cabinet to the bottom of the cabinet and were placed 3/4″ back from the edges. The stringers formed a backing strip used for attaching the sides of the enclosure during assembly.

I cut the sides to width using a table saw. A radial arm saw was used to trim the straight sides to the correct length. Then I started working on the angled cuts at the top and bottom of the slanted sides. To make the angled cuts, I set the radial arm saw at 11.5 degrees. I had to remember to make the top and bottom cuts parallel so they were flush with the top and bottom pieces of the cabinet.

After cutting the sides I attached them to the enclosure's front panels. Again I used glue with small nails to hold them in place while the glue dried. Details of the corner joints are shown in Figure 7. When attaching the sides I was very careful making sure everything aligned evenly at the top of the cabinet. I was not as concerned with the alignment at the bottom of the cabinet since my plan was to make the bottom removable. After the glue holding the front and sides was dry I slid the back into position, after applying glue along the joint, then clamped and nailed it in place. I used some light sanding to level out any high spots on the top and bottom surfaces. All joints were then sealed with silicon caulk.

The small top cap was custom fit to the top of each cabinet maintaining an 11.5 degree slope on the slanted side. Attaching the small cap presented the second challenge. I ended up applying a bead of silicon caulk around the perimeter and then nailing the top down with finishing nails. Any excess caulk, which squeezed out of the joint, was immediately wiped off.

Making a removable bottom was reasonably simple. I cut two rectangular pieces two inches oversized in all directions. Rubber feet were attached at each corner one inch from the edge. I then glued four blocks to the bottom of the front and back panels and used four long screws to secure the bottom to the cabinet. To assure an air tight seal, I placed 3/4″ wide rubber Weather-strip on the bottom panel in a rectangular shape to match the base of the enclosure. Tightening screws compressed this seal nicely. With a removable bottom, the wiring, stuffing, and port installation could now be completed.

Before adding the drivers, ports, stuffing, and connection cups I stained the cabinets with a Golden Pecan MinWax stain. For the first time, I used a MinWax wood preconditioner just prior to staining. The color came out very even without any blotching. Final finishing was accomplished with several coats of polyurethane.

To hold the stuffing in the top of the cabinet, I screwed four eyebolts into the front and back panels. Then I measured 150 gm (0.25 lb/ft^3) of Dacron Hollofil II stuffing and after teasing, wrapped it in a tapered cheese cloth sleeve. The ends of the sleeve were tied shut with string. The sleeve was inserted into the upper section of the cabinet and then another length of string was tied crisscrossed between the eyebolts to form a support.

The diameter of the hole for the port, in the front panel, was cut about 1/4″ oversized. A wrap of 3/16″ thick Weather-strip was applied to the outside of the port. The port was squeezed into the hole resulting in a snug and secure fit. I bought three pairs of ports that could be trimmed to different lengths and inserted into the enclosure in this manner.

Wiring the driver was easy. A length of speaker wire was soldered to the connection cup on the back panel and then threaded up through the open driver hole in the front panel. After double checking the polarity, the wire was soldered to the driver lugs. The driver was inserted and screwed into place using the gasket material supplied by Fostex. Finally a trim ring, to hold a removable black mesh grill, was added. These speakers were intended for my family room and needed the extra protection from accidental damage. The bottom of the cabinet was reattached and they were ready for action.

The final cost breakdown is shown below in Table 5. I did not include the glue, nails, screws, stain, polyurethane, connection cup, wire, stuffing, or Weather-strip since these were supplies that I had on hand. Pictures of the front and back of the completed speakers are shown in Figures 11 and 12 respectively.

Table 5 : Cost Breakdown

Item	Cost
2 x Fostex FE 164 drivers	$116.77
2 x sheets of 4′ x 8′ birch plywood and edge laminate	$100.39
2 x 3″ diameter ports from Parts Express	
2 x 8″ diameter grill screens from Parts Express	
8 x 1″ rubber feet from Parts Express	$ 28.79
Total	$245.95

Figure 11 : Front View of Finished Speakers

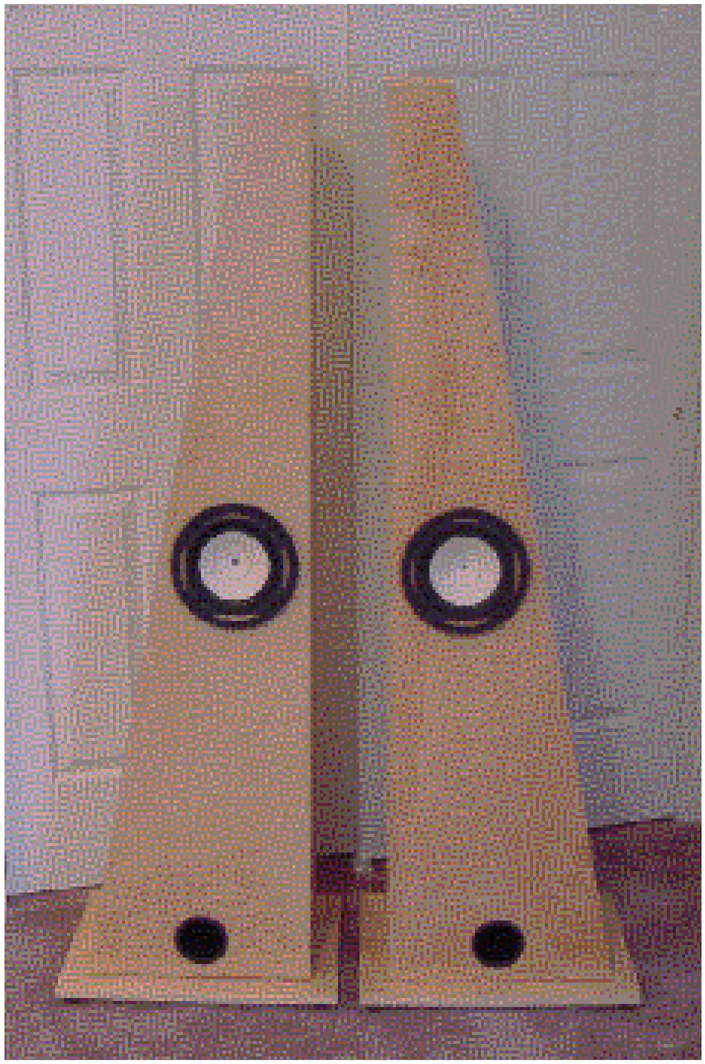

Figure 12 : Back View of Finished Speakers

Measurement Results and Correlation with the MathCad Simulation :

Once the speakers were completed, I measured the system electrical impedance and the near field acoustic SPL for the driver and the port. To try and isolate the speakers from the floor and the nearby walls, I laid them horizontally on a workbench pointing into the large open area of my basement. For the acoustic measurements, the microphone was positioned one inch from the front baffle and centered on the driver or the port. Both speakers were measured and the results are presented in Figures 13, 14, and 15. The response plots include all of the LAUD settings used during the measurements. Each measurement was made using ten averages without any filtering (windowing) being applied. There has been no “smoothing” applied to any of the measured data.

Combining the measured near field driver and terminus SPL responses, to derive the equivalent far field system SPL response, requires a correction due to the different diameters of the driver and the port. I have seen different formulas for this correction discussed in textbooks and on various Internet forums. The equations given have not been consistent and I became curious about which one was correct. To try and resolve this confusion, I derived my own set of equations for combining the output from two near-field measurements of different sized sources to determine the far-field system response. Attachment 4 contains a MathCad worksheet that calculates the correction that should be applied, for this test set-up, to the terminus response before summing with the driver response to determine the system response. Figure 16 presents the estimated system response.

To correlate the measured results against the MathCad predictions, I read the measurement data into MathCad and displayed the measurements and the predictions on the same plots. In general, the phase curves matched closely. However, while the shape of the magnitude curves was obviously correct, an offset was evident in both the driver and the terminus SPL response plots. Two adjustments were needed to be able to obtain the final comparison of these results.

First, the terminus measurement was approximately 5 dB higher for all frequencies compared to the calculation. Since these are all relative SPL results, the driver and terminus measurement data could be reduced 5 dB to bring the terminus magnitude curves in line. This first adjustment took care of the terminus data, but the measured driver response was now below the calculated driver response. To bring the driver measured response in line with the calculated response, 6 dB needed to be added back to the measured result. How can this second adjustment be justified?

Since the shape of the measured magnitude and phase plots matched the calculated plots so closely, I concluded that the MathCad model was fairly accurate in predicting the system behavior. Scaling the driver and terminus plot by an equal 5 dB is just a change in the reference level and does not change the relationship between them. To justify adding a constant 6 dB to the driver magnitude I can only present the following observations. The calculated results are the SPL responses exactly one inch from the driver and terminus acoustic sources. The measured results are the SPL responses approximately one inch from the speaker front baffle. The positions of the actual acoustic sources, for the driver and terminus, have not been accounted for in the measurement.

For the driver, the acoustic source probably resides further from the microphone then the one inch distance to the baffle (it is behind the front surface of the baffle). If the acoustic source for the terminus were assumed to be located just in front of the baffle, then the magnitude of the measurements are clearly biased towards the terminus. Using the worksheet in Attachment 4 to evaluate the change in SPL with distance from the driver, if the offset between the driver and terminus acoustic sources was between one and two inches the measured SPL level mismatch would be between 3 and 6 dB. I am assuming this error is 6 dB to bring the driver SPL curves closer together.

The final adjusted plots showing the correlation between the measured data and the calculated responses are shown in Figures 17, 18, 19, and 20. Clearly this last adjustment of the measured driver SPL response has not been proven rigorously beyond any doubt. However, since the correlation of the impedance and the terminus SPL response is very good I am not that uncomfortable making this final adjustment. Also recognize that the SPL level mismatch is not unique to the ML TQWT design. A similar situation would exist if the design were a simple ported box. Not accounting for the locations of the acoustic sources in the measurements is the cause of this response mismatch. For completeness, I have included the MathCad worksheet that shows the unadjusted curves and the final adjusted curves as Attachment 5. After reviewing the plotted data presented in Attachment 5, the readers can draw their own conclusions with respect to these adjustments.

Figure 13 : Measured Impedance Results for the ML TQWT Speaker

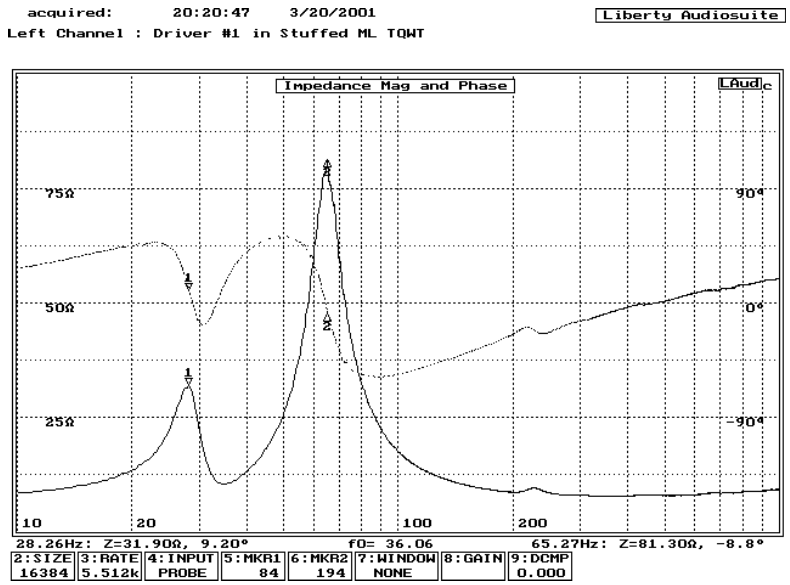

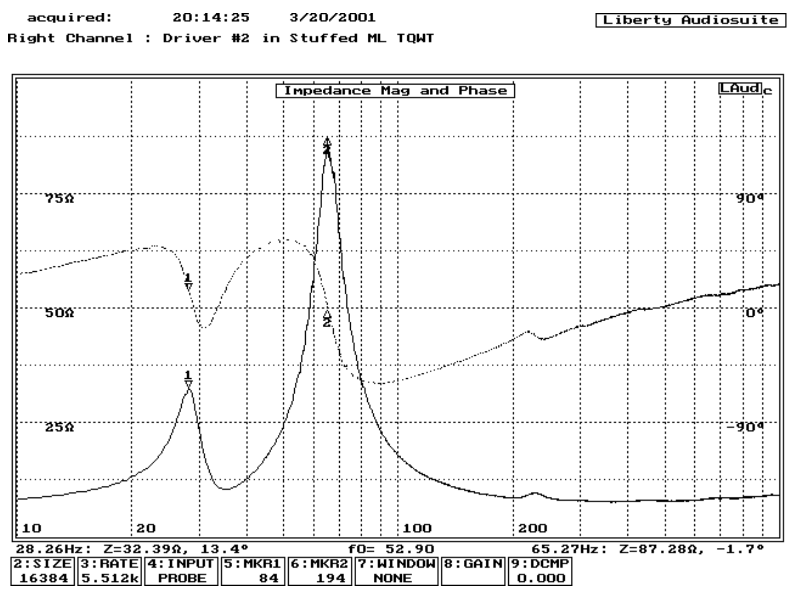

Figure 14 : Measured Driver SPL Response for the ML TQWT Speaker

acquired: 19:43:50 3/20/2001 Liberty Audiosuite
Left Channel : Driver #1 SPL in Stuffed ML TQWT (d = 1.0 inch)

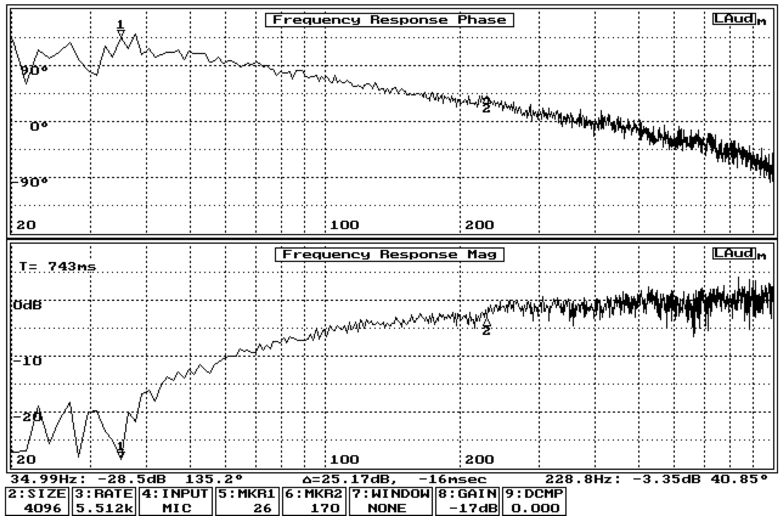

acquired: 20:09:11 3/20/2001 Liberty Audiosuite
Right Channel : Driver #2 SPL in Stuffed ML TQWT (d = 1.0 inch)

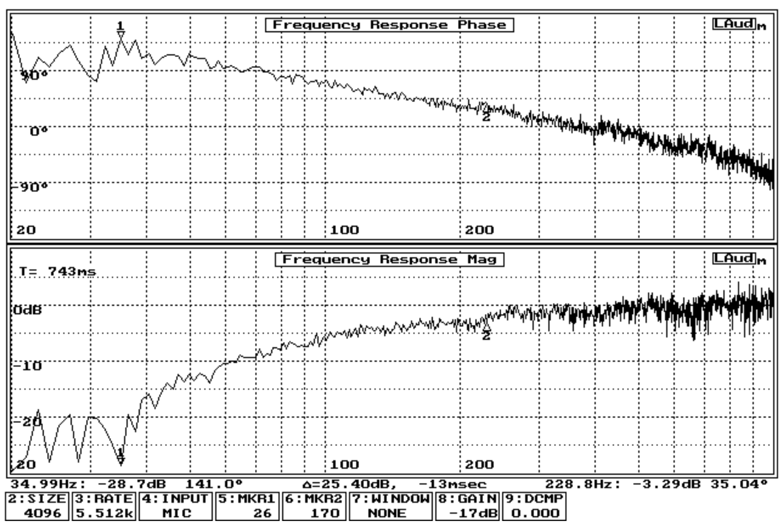

Figure 15 : Measured Terminus SPL Response for the ML TQWT Speaker

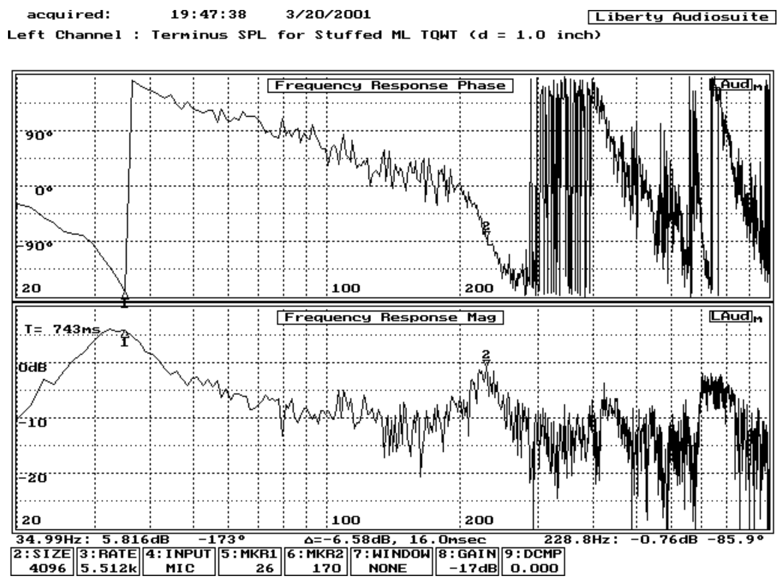

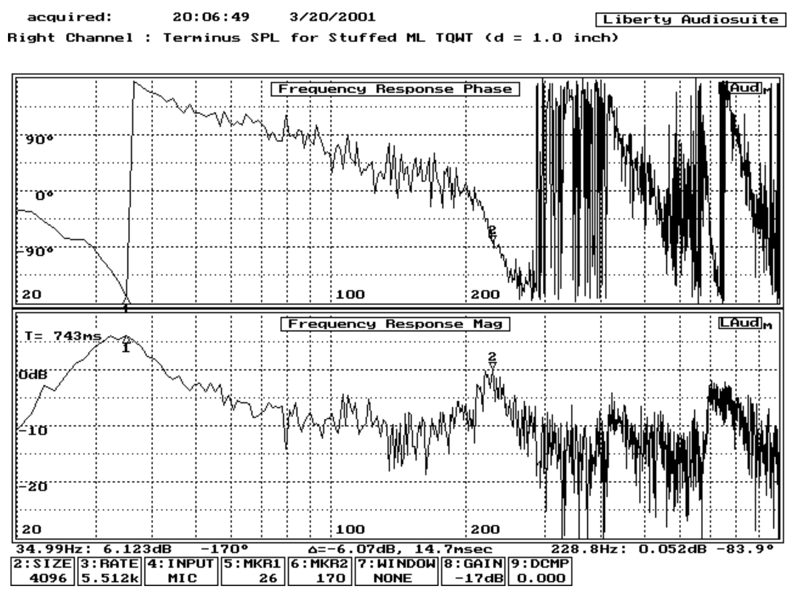

Figure 16 : Summed Driver and Terminus SPL Response for the ML TQWT Speaker

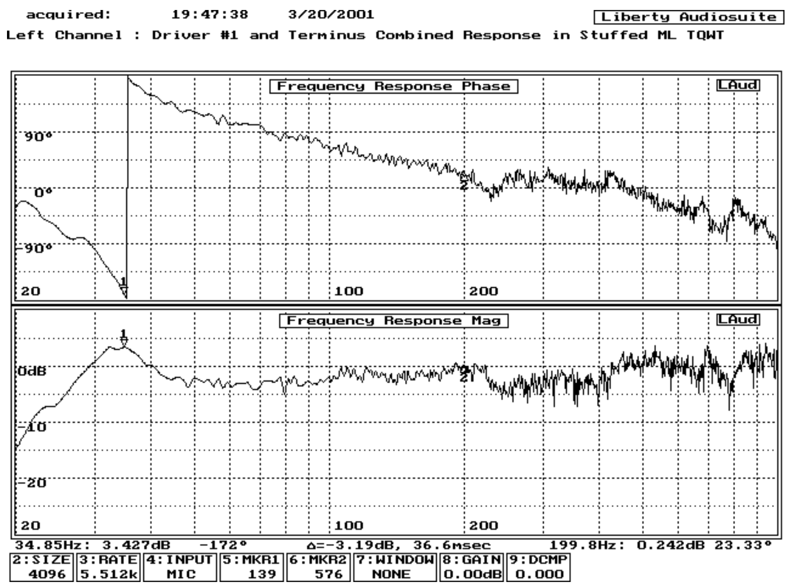

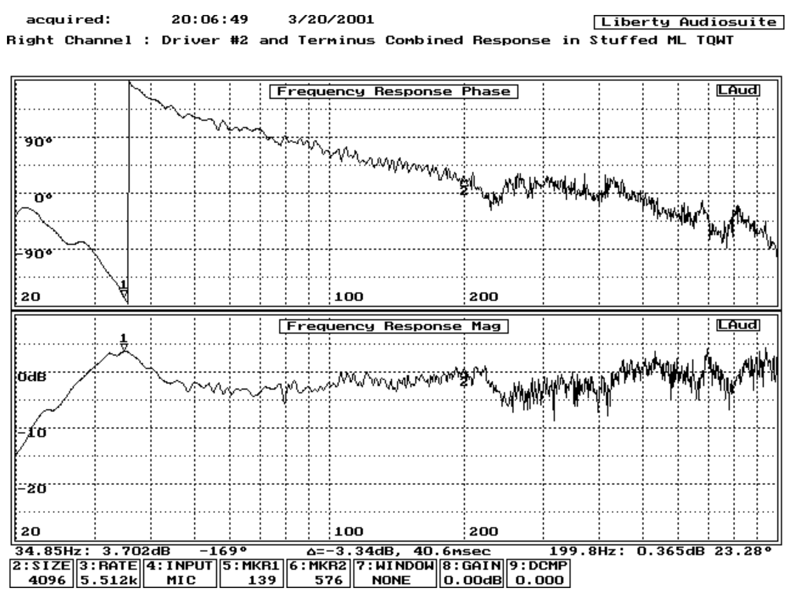

Figure 17 : Measured and Calculated Impedance Results for the ML TQWT Speaker
(solid line = calculated, dashed line = measured)

Calculated and Measured Impedance

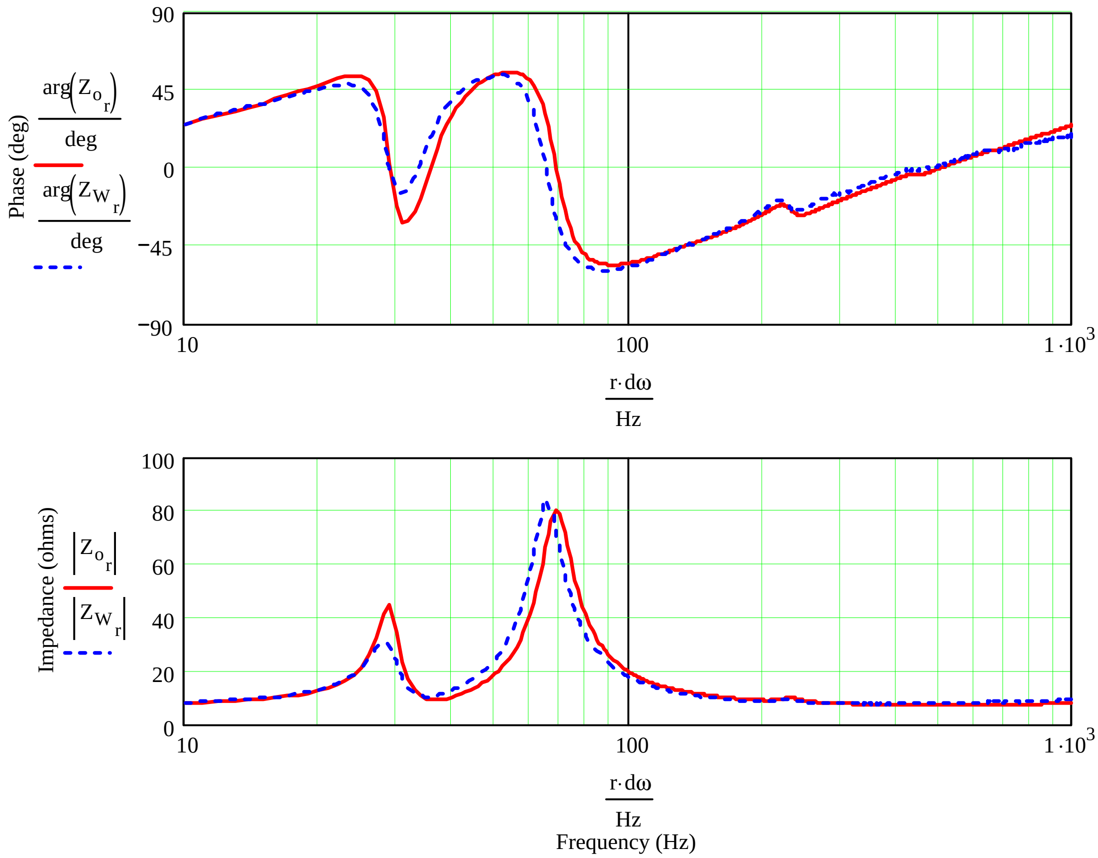

Figure 18 : Measured and Calculated Driver SPL Results for the ML TQWT Speaker
(solid line = calculated, dashed line = measured)

Driver Calculated and Measured Near Field Sound Pressure Level Response - After Adjustments

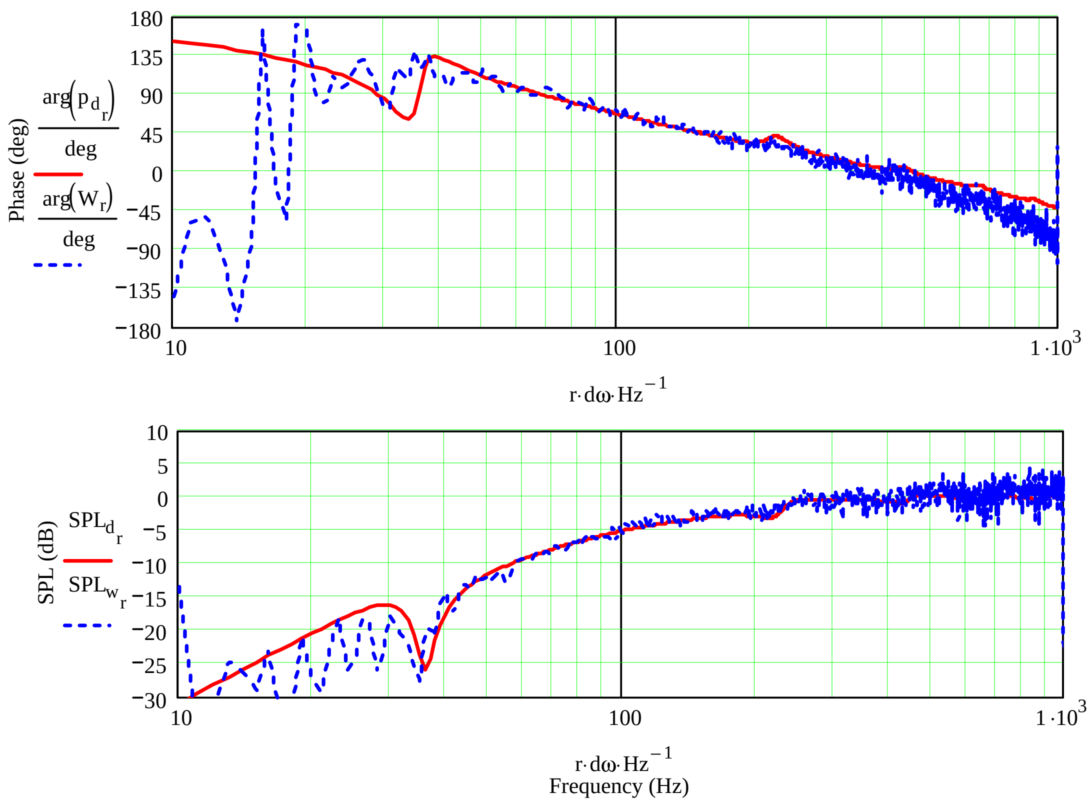

Figure 19 : Measured and Calculated Terminus SPL Results for the ML TQWT Speaker
(solid line = calculated, dashed line = measured)

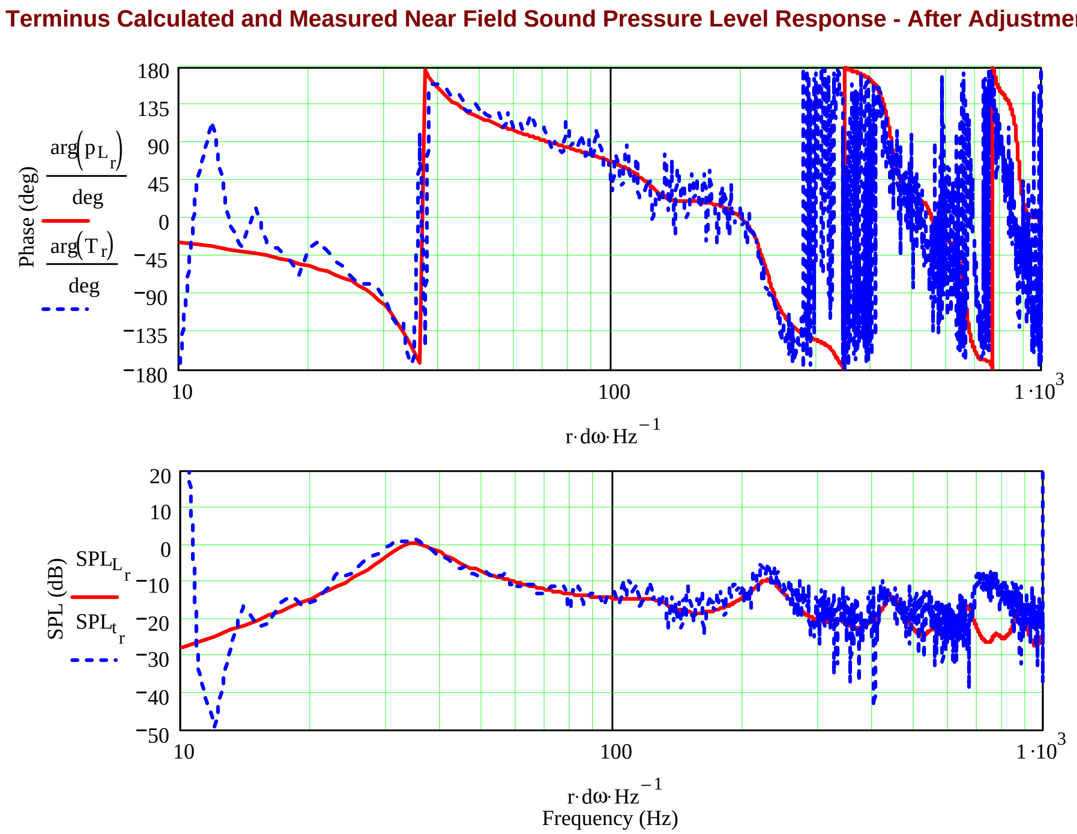

Figure 20 : Measured and Calculated System SPL Results for the ML TQWT Speaker
(solid line = calculated, dashed line = measured)

System Calculated and Measured Near Field Sound Pressure Level Response - After Adjustments

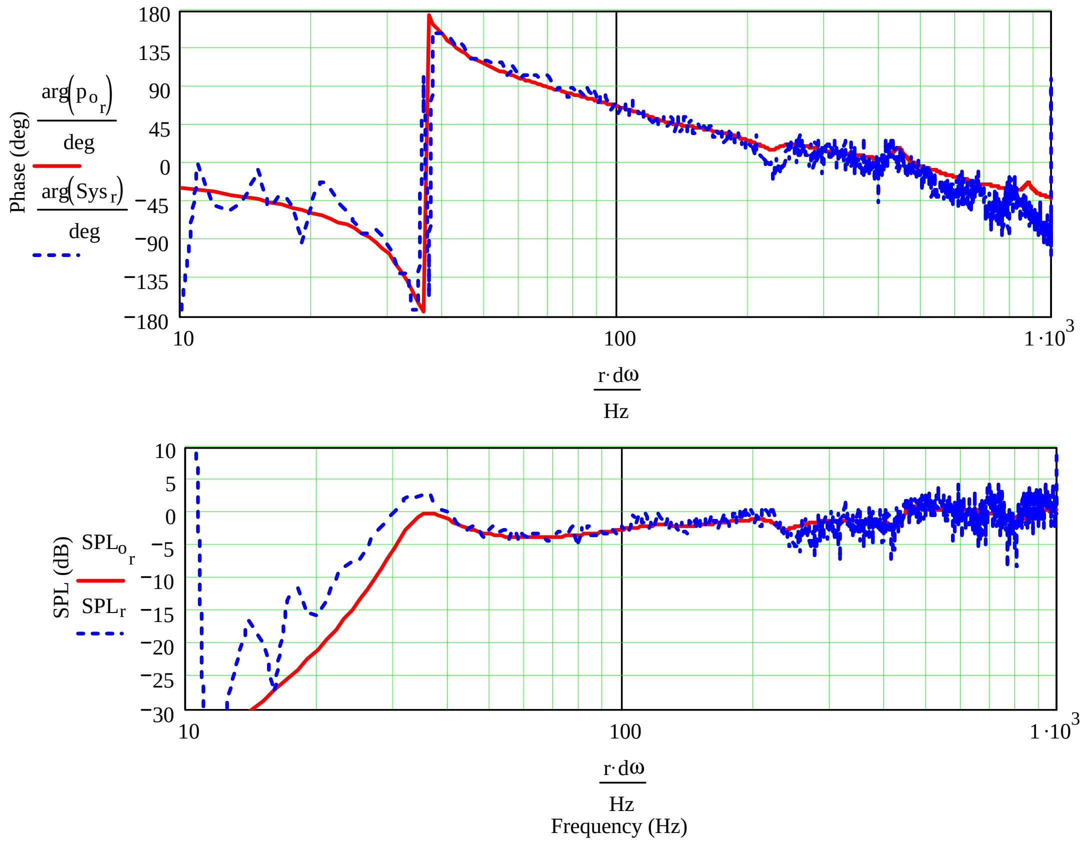

Conclusions :

In the introduction, I stated that I had two goals for this project. First, I wanted to test the MathCad models and see if a tapered geometry could be simulated accurately. Second, I wanted to try an inexpensive full-range driver and see what the potential benefits are for such a simple design. I will try and address each of these goals in the following paragraphs.

In my opinion, the MathCad models accurately predicted the performance of the ML TQWT design. While some might debate the adjustments I made to the LAUD measurements, the shape of the curves indicated that the model was simulating very closely the acoustics of the tapered line. If I were to go back and perform some additional detailed tests, to try and determine the exact acoustic source locations for both the driver and the terminus, I believe that my assumption would be confirmed. The MathCad transmission line simulations, if applied correctly, appear to be as accurate as the classic closed and vented box models based on the Thiele and Small papers. In fact, the MathCad models can be used to simulate closed and vented box enclosures with the additional feature of being able to including standing wave interactions in one of the basic box dimensions.

With respect to the benefits of using a full range driver, this was a very simple and inexpensive system to design and build. By eliminating the crossover, and only focusing on the enclosure and reinforcing the lower bass, the skill level required to design a successful system was greatly reduced. Lets face it, designing an enclosure is significantly less demanding when compared to designing and tweaking a good cross-over circuit that smoothly transitions between two (if not three) drivers. With the computer tools available to most hobbyists, designing an enclosure can be done quickly and with some degree of confidence that the result will perform as predicted. Without an acoustic measurement system, and some sophisticated optimization software, designing a crossover using textbook equations is somewhat of a hit or miss proposition. Summing the cost of a mid-bass driver, a tweeter, and the required crossover components and then applying this total towards purchasing a single full range driver results in a very interesting trade-off if you are faced with a $200 to $500 budget. A quality full range driver can significantly reduce the difficulty and probably the cost associated with designing a high performance speaker system.

After breaking in the Fostex FE-164 drivers, I mounted them in a baffle and measured the frequency response from 20 Hz to 20 kHz. This measurement showed that the manufacturer’s on-axis response curve was representative of the two units I received. The SPL response extended out to approximately 18 kHz before it started to roll-off slightly. With the ML TQWT enclosure adding bass extension down to 35 Hz, the on-axis system SPL frequency response is very impressive. While I am very happy with the performance of the Fostex FE-164 drivers, I am still considering upgrading to the even higher performance Fostex FE-168 Sigma drivers for the ML TQWT enclosure.

I was pleasantly surprised when I first listened to the finished speaker system. The bass went very low in frequency but it was not the type of bass output that you can feel and hear. After all, these are only six inch drivers, with a limited X_{max}, so the amount of air being moved is not tremendous. Imaging and detail were also very impressive. I am still tweaking the speaker position in my listening room, and adjusting the port length, to try and optimize the final performance.

Comparing the Fostex ML TQWT system to my Focal TL system (at more than twice the price) yields a few subtle differences but not as dramatic as I expected. I think that the Focal TL system response is smoother across the entire spectrum but not by much. I have not found any glaring weakness in the Fostex ML TQWT's and have really enjoyed listening to them. On the other hand, a lot of the big advantages that are claimed by the full range driver enthusiasts are not evident to me. Imaging is not noticeably better than the Focal two-way TL system I built just over a year ago. I think the biggest advantages that a full range driver system has over a multi-driver (plus crossover) system are the ease of design and construction, and the potential cost trade-off.

I have been contacted by a number of people since the first design sketches and system SPL measurements of the ML TQWT were posted on the Transmission Line Website (www.t-linespeakers.org). There have been questions concerning the classification of the design as a variant of a TQWT as opposed to being a strangely shaped vented box. I have tried to outline my position on the classification of the design and have enjoyed the discussions. There has also been significant interest from some people about possibly building a pair of ML TQWT's. I have tried to answer the questions they have asked and I hope to hear their opinions of the design if they do build this project. I would be particularly interested in any tweaks that are made to the design that lead to an improvement of the final system performance.

References :

1) Loudspeakers in Vented Boxes Parts I and II by A. N. Thiele; Loudspeakers an Anthology, Volume 1 through 25 of the Journal of the Audio Engineering Society, pages 181-205.

2) Direct Radiator Loudspeaker System Analysis by R. H. Small; Loudspeakers an Anthology, Volume 1 through 25 of the Journal of the Audio Engineering Society, pages 271-284.

3) Closed-Box Loudspeaker Systems Parts I and II by R. H. Small; Loudspeakers an Anthology, Volume 1 through 25 of the Journal of the Audio Engineering Society, pages 285-303.

4) Vented-Box Loudspeaker Systems Parts I, II, III, and IV by R. H. Small; Loudspeakers an Anthology, Volume 1 through 25 of the Journal of the Audio Engineering Society, pages 316-343.

5) MathCad 2000 Professional by Mathsoft Inc., www.mathsoft.com.

6) Derivation and Correlation of a Viscous Damping Model Used in the Design of a Transmission Line Loudspeaker by Martin J. King, 3/4/00, available at www.t-linespeakers.org.

7) Upgraded MathCad Computer Models for the Design of Transmission Line Loudspeakers by Martin J. King, 7/6/00, available at www.t-linespeakers.org.

8) Applied Acoustics (2nd edition) by H. F. Olsen and F. Massa, published by P. Blakiston's Son & Co. Inc, 1939.

9) A Non-Resonant Loudspeaker Enclosure Design by A. R. Bailey, Wireless World, October 1965.

10) The Use of Fibrous Material in Loudspeaker Enclosures by L. J. S. Bradbury; Loudspeakers an Anthology, Volume 1 through 25 of the Journal of the Audio Engineering Society, pages 404-412.

Attachment 1 : Natural Frequencies and Mode Shapes for the ML TQWT Enclosure

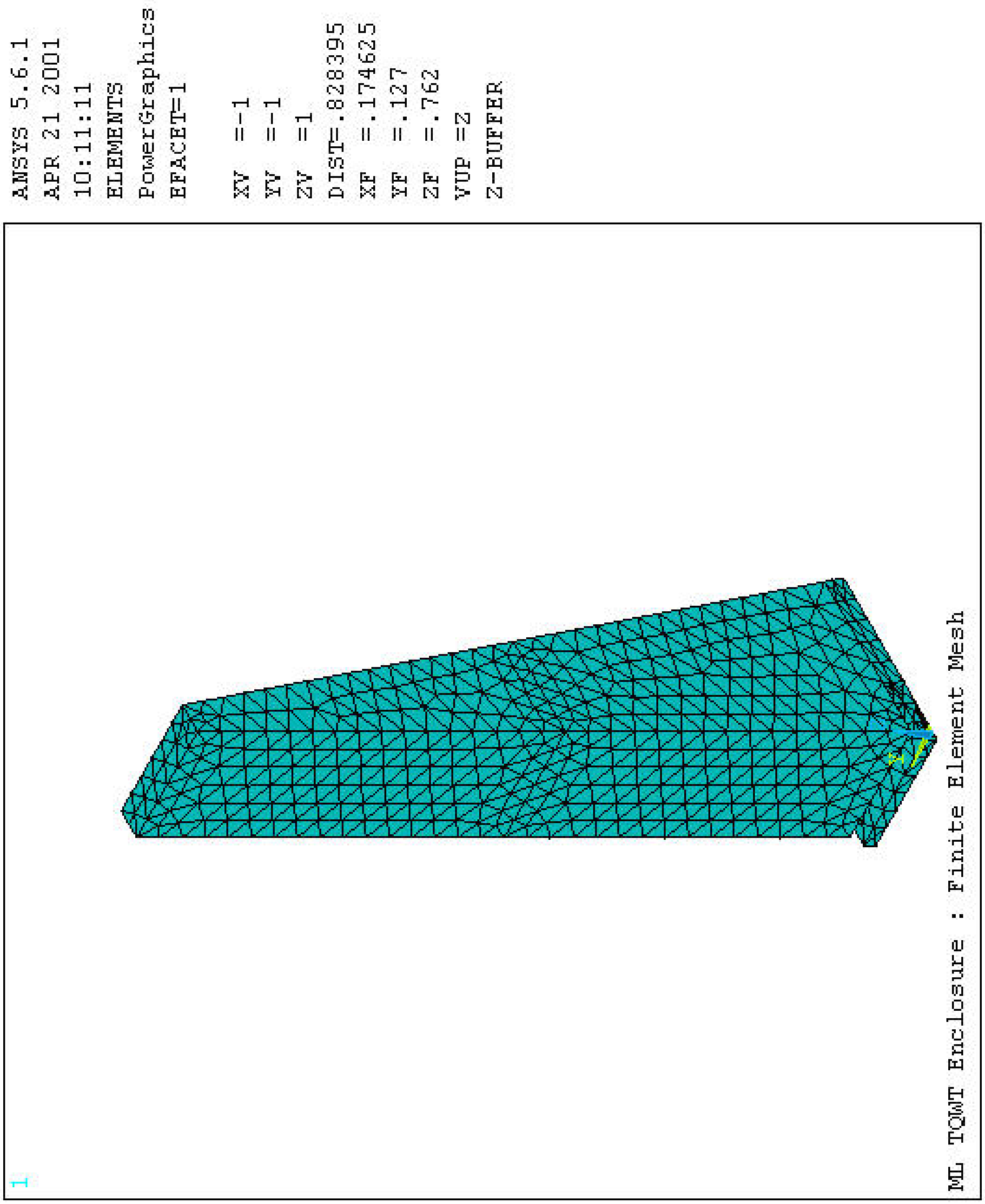
ANSYS 5.6.1
APR 21 2001
10:11:11
ELEMENTS
PowerGraphics
EFACET=1
XV =-1
YV =-1
ZV =1
DIST=.828395
XF =.174625
YF =.127
ZF =.762
VUP =Z
Z-BUFFER
ML TQWT Enclosure : Finite Element Mesh

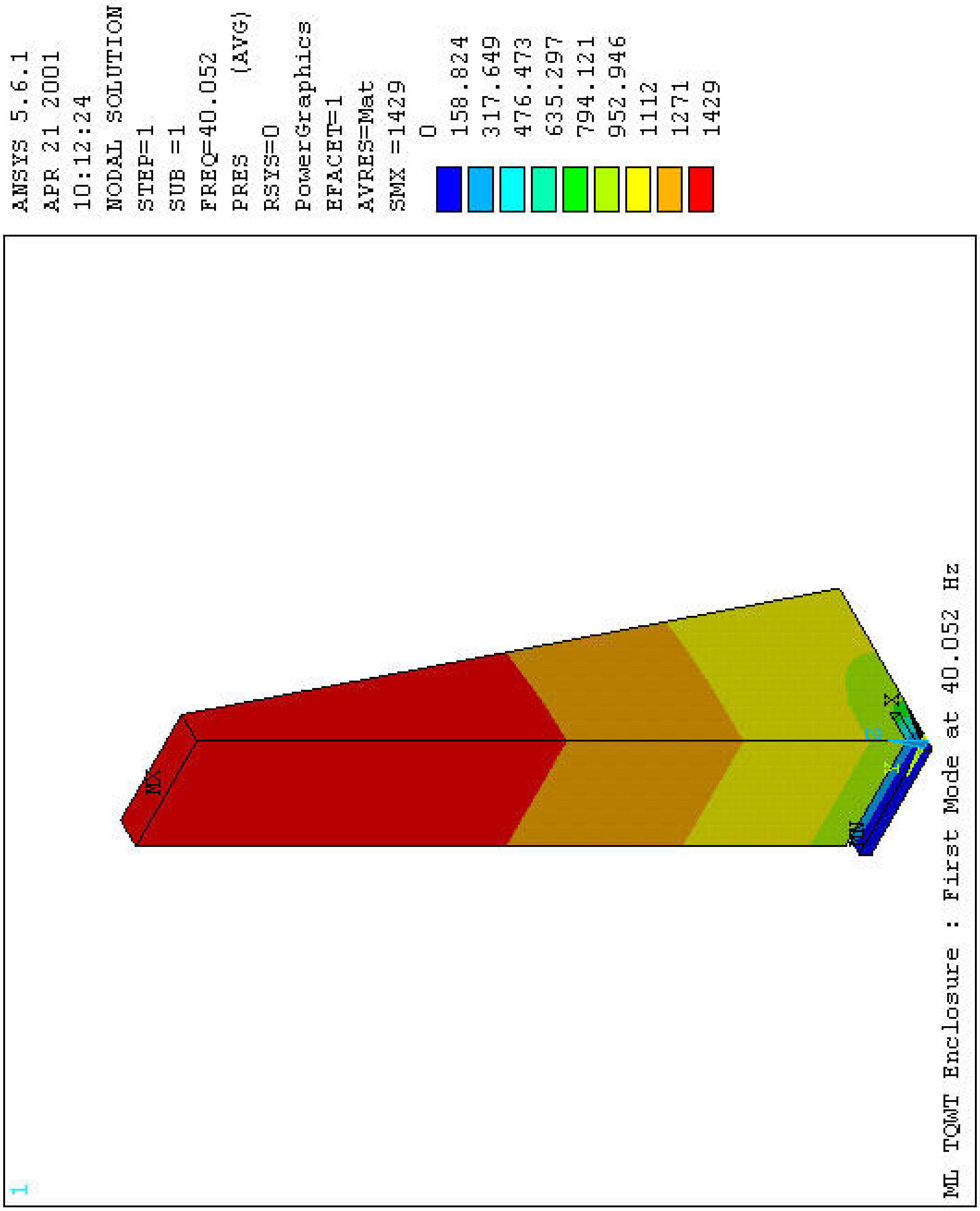
ANSYS 5.6.1
APR 21 2001
10:12:24
NODAL SOLUTION
STEP=1
SUB =1
FREQ=40.052
PRES (AVG)
RSYS=0
PowerGraphics
EFACET=1
AVRES=Mat
SMX =1429
0
158.824
317.649
476.473
635.297
794.121
952.946
1112
1271
1429
MX
MN
ML TQWT Enclosure : First Mode at 40.052 Hz

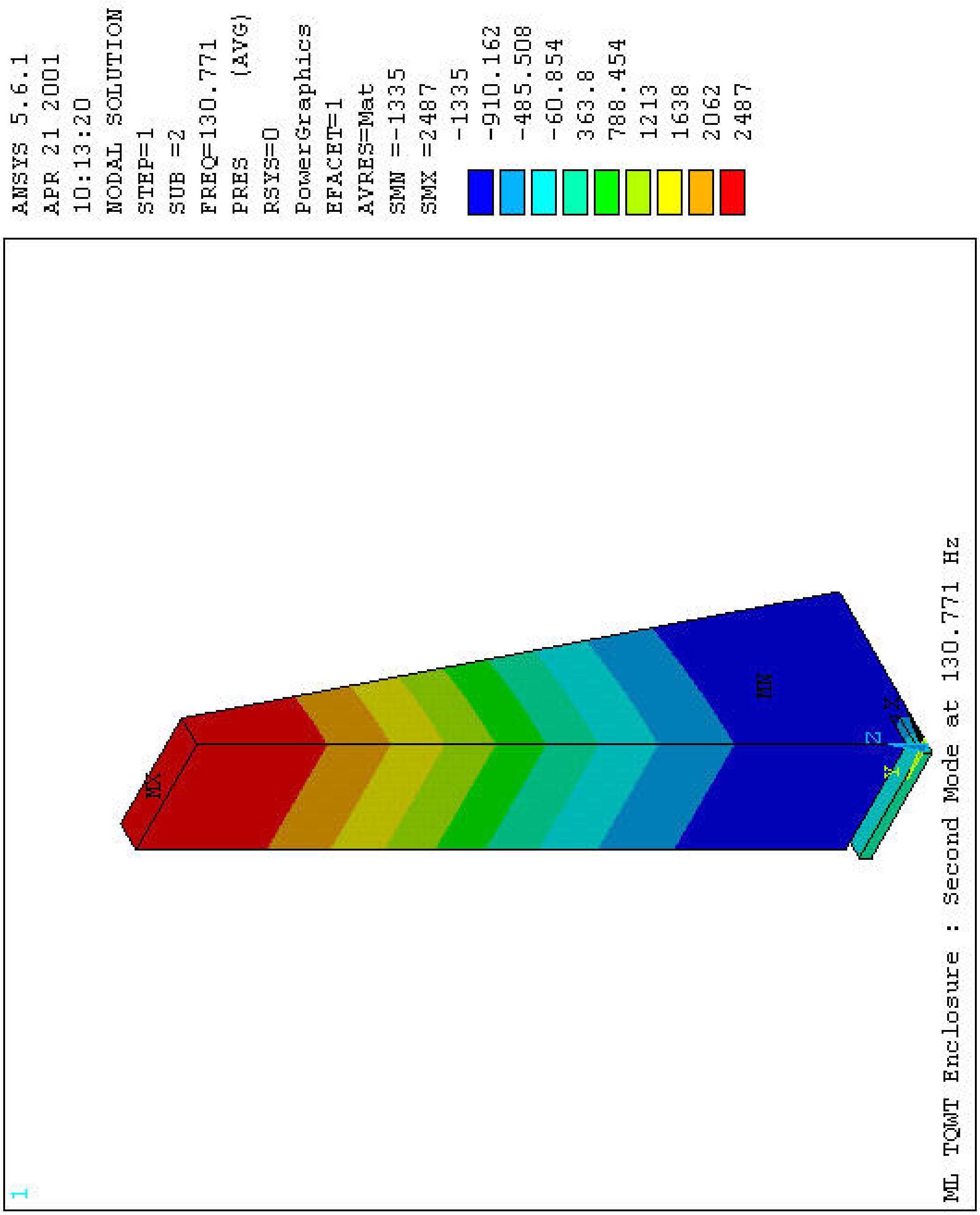
ANSYS 5.6.1
APR 21 2001
10:13:20
NODAL SOLUTION
STEP=1
SUB =2
FREQ=130.771
PRES (AVG)
RSYS=0
PowerGraphics
EFACET=1
AVRES=Mat
SMN =-1335
SMX =2487
-1335
-910.162
-485.508
-60.854
363.8
788.454
1213
1638
2062
2487
MX
MN
ML TQWT Enclosure : Second Mode at 130.771 Hz

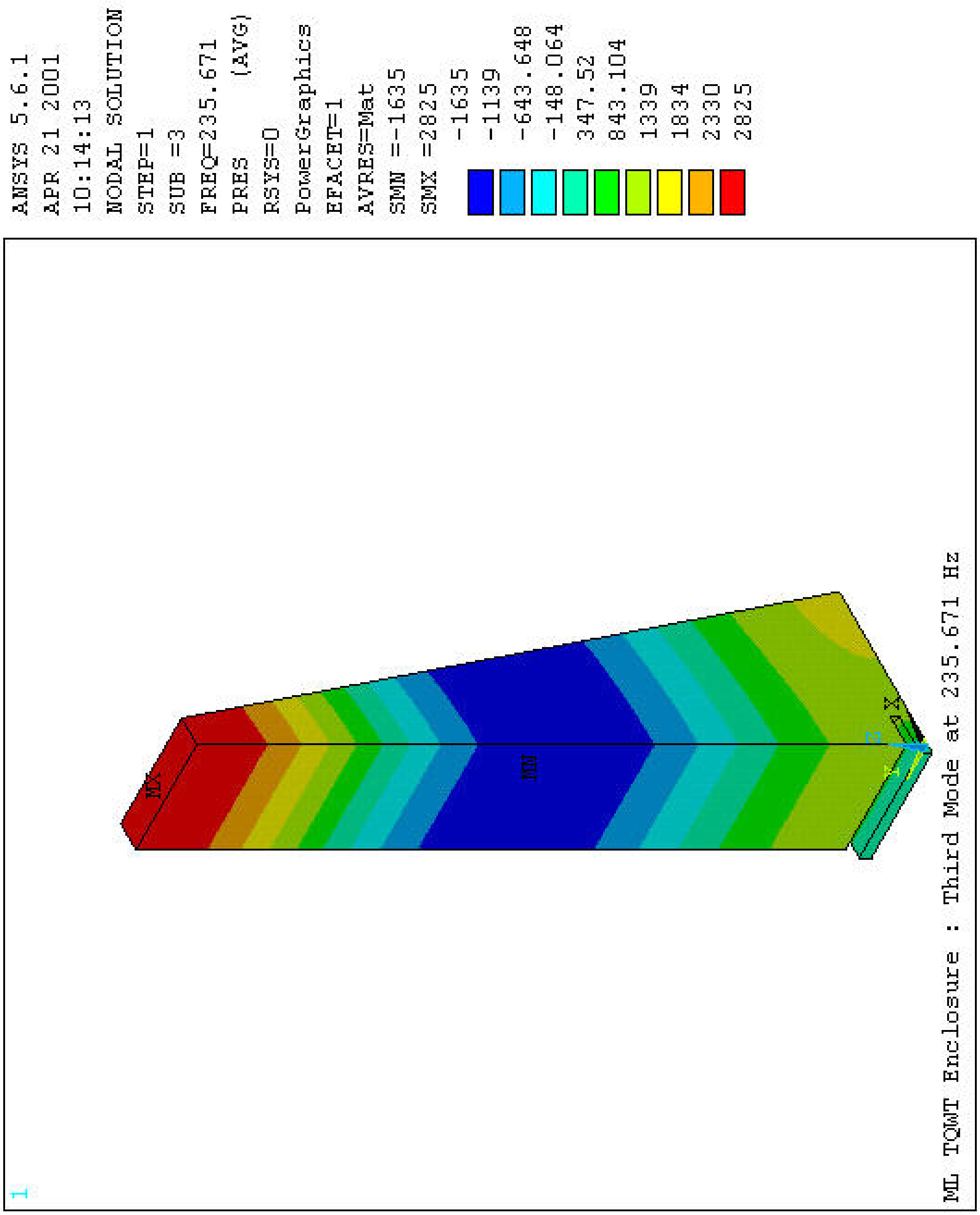
ANSYS 5.6.1
APR 21 2001
10:14:13
NODAL SOLUTION
STEP=1
SUB =3
FREQ=235.671
PRES (AVG)
RSYS=0
PowerGraphics
EFACET=1
AVRES=Mat
SMN =-1635
SMX =2825
-1635
-1139
-643.648
-148.064
347.52
843.104
1339
1834
2330
2825
MX
MN
ML TQWT Enclosure : Third Mode at 235.671 Hz

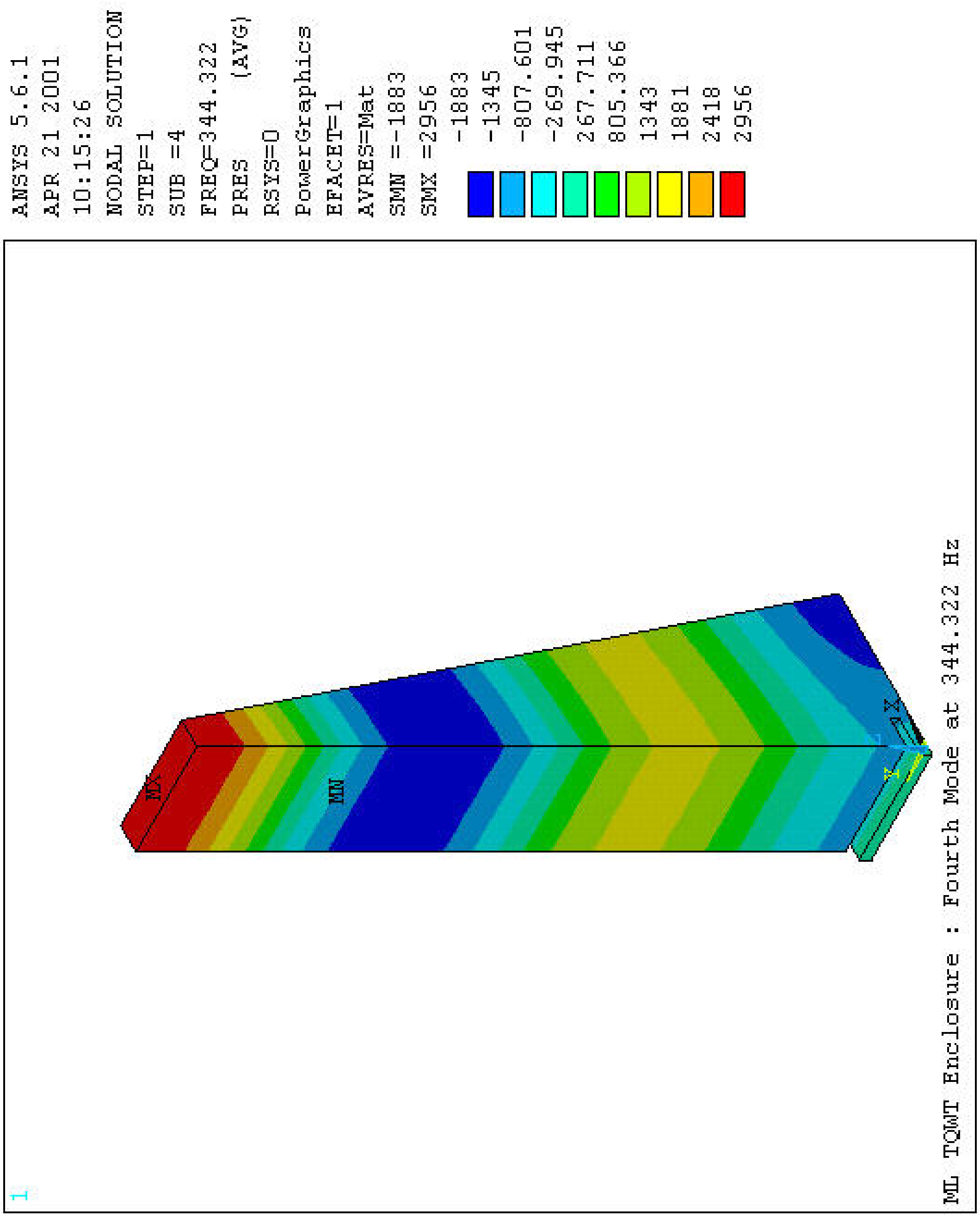
ANSYS 5.6.1
APR 21 2001
10:15:26
NODAL SOLUTION
STEP=1
SUB =4
FREQ=344.322
PRES (AVG)
RSYS=0
PowerGraphics
EFACET=1
AVRES=Mat
SMN =-1883
SMX =2956
-1883
-1345
-807.601
-269.945
267.711
805.366
1343
1881
2418
2956
MX
MN
ML TQWT Enclosure : Fourth Mode at 344.322 Hz

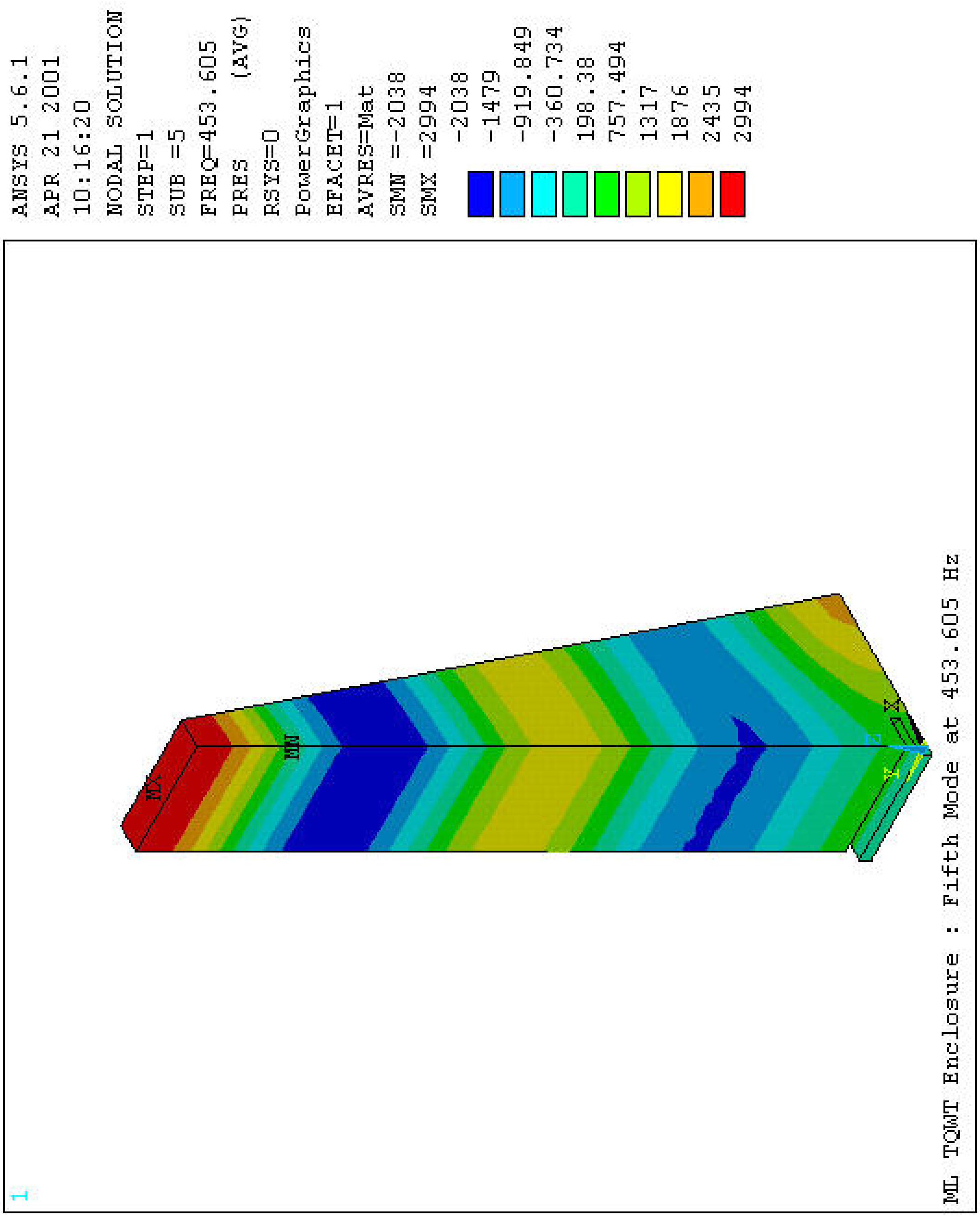
ANSYS 5.6.1
APR 21 2001
10:16:20
NODAL SOLUTION
STEP=1
SUB =5
FREQ=453.605
PRES (AVG)
RSYS=0
PowerGraphics
EFACET=1
AVRES=Mat
SMN =-2038
SMX =2994
-2038
-1479
-919.849
-360.734
198.38
757.494
1317
1876
2435
2994
MX
MN
ML TQWT Enclosure : Fifth Mode at 453.605 Hz

Attachment 2 : Natural Frequencies and Mode Shapes for the Bass Reflex Enclosure

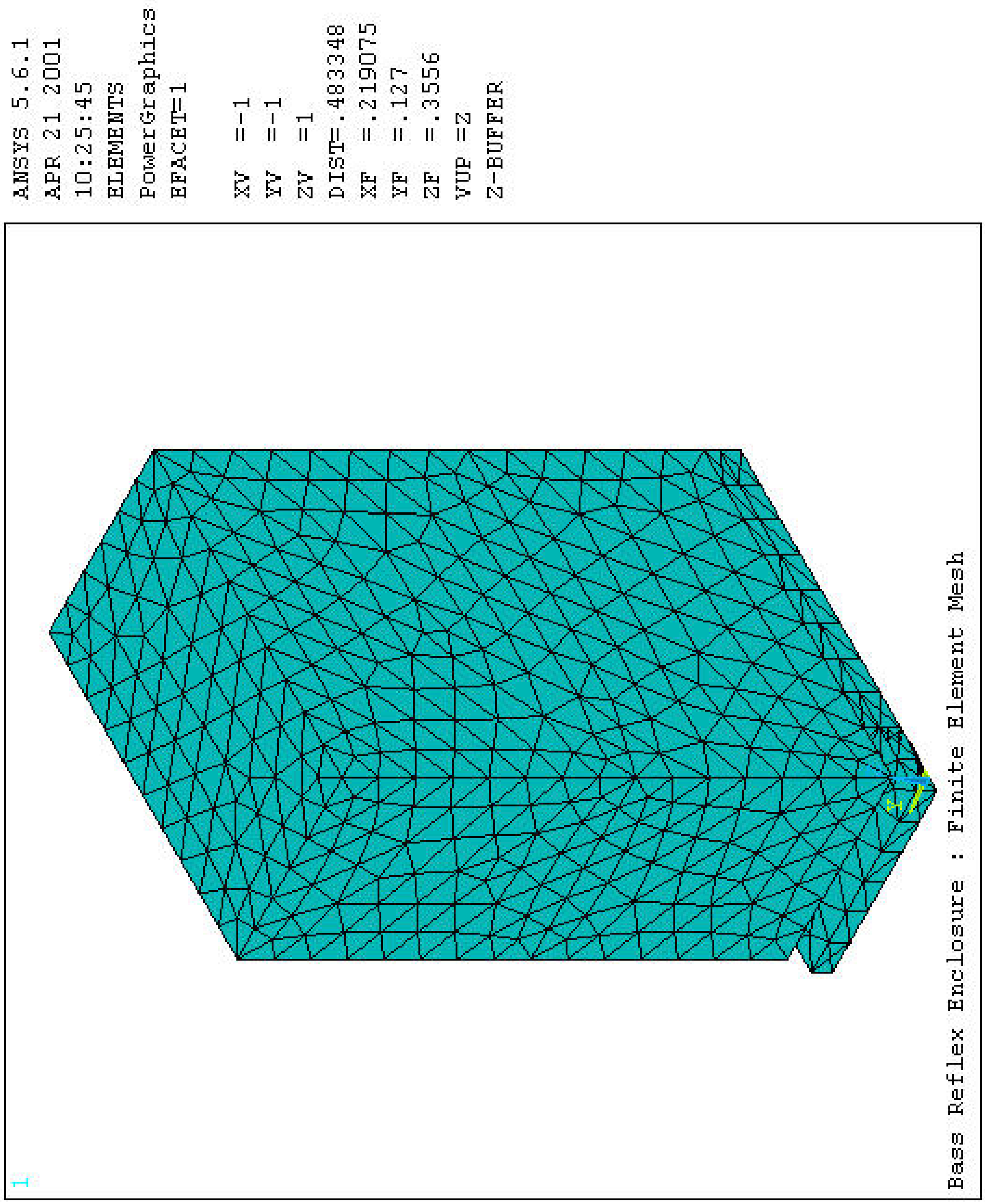
ANSYS 5.6.1
APR 21 2001
10:25:45
ELEMENTS
PowerGraphics
EFACET=1
XV =-1
YV =-1
ZV =1
DIST=.483348
XF =.219075
YF =.127
ZF =.3556
VUP =Z
Z-BUFFER
Bass Reflex Enclosure : Finite Element Mesh

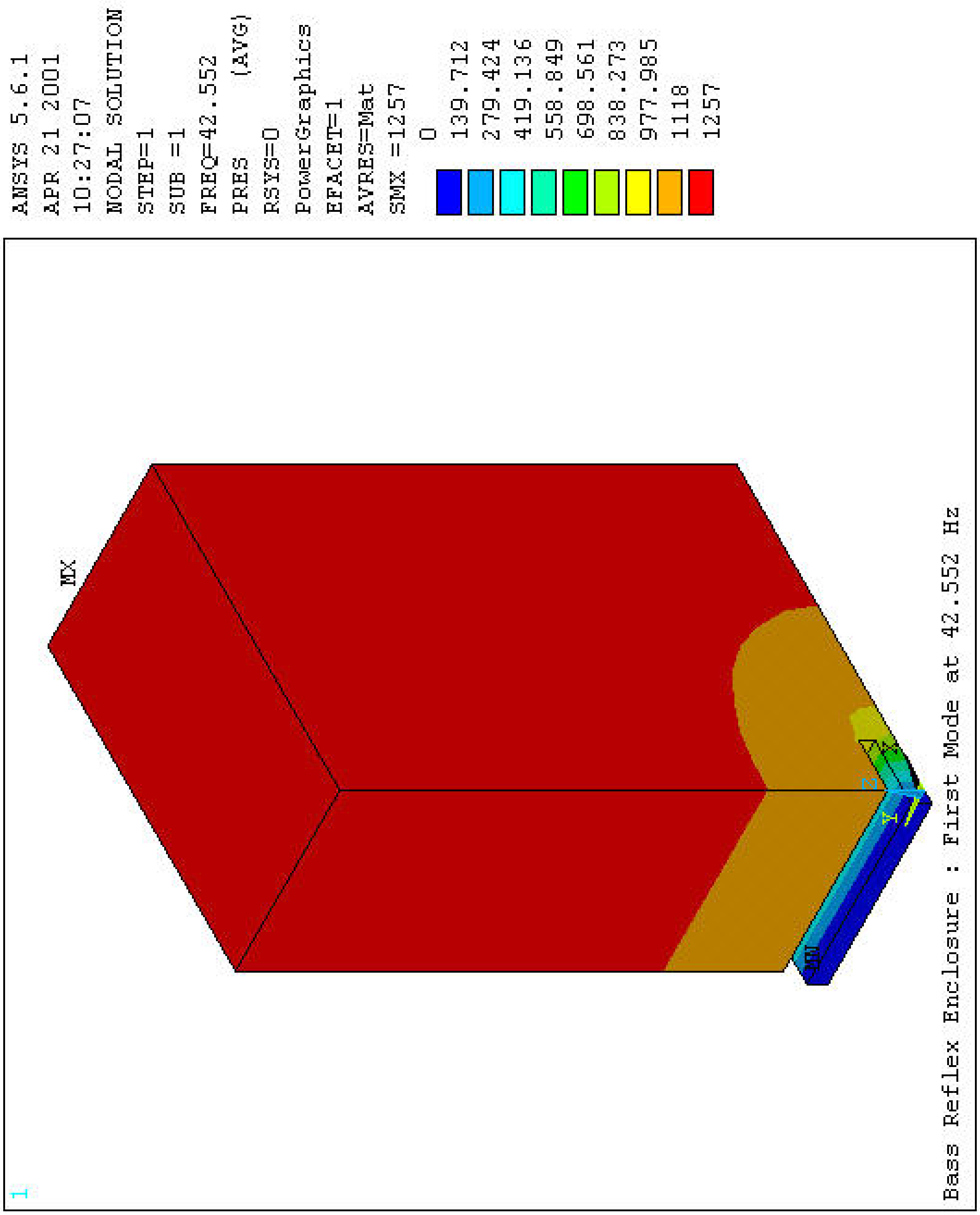
ANSYS 5.6.1
APR 21 2001
10:27:07
NODAL SOLUTION
STEP=1
SUB =1
FREQ=42.552
PRES (AVG)
RSYS=0
PowerGraphics
EFACET=1
AVRES=Mat
SMX =1257
0
139.712
279.424
419.136
558.849
698.561
838.273
977.985
1118
1257
MX
MN
1
Bass Reflex Enclosure : First Mode at 42.552 Hz

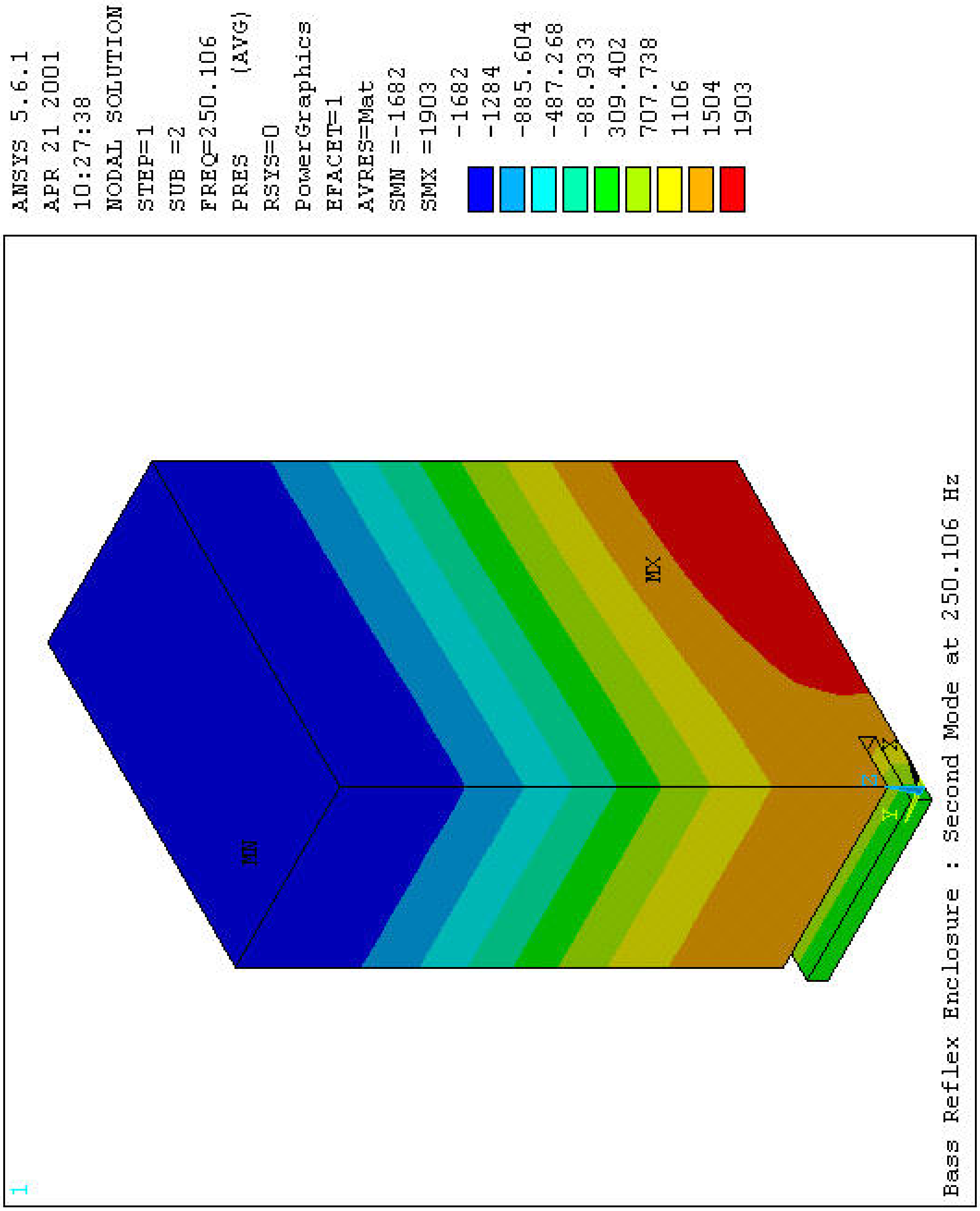
ANSYS 5.6.1
APR 21 2001
10:27:38
NODAL SOLUTION
STEP=1
SUB =2
FREQ=250.106
PRES (AVG)
RSYS=0
PowerGraphics
EFACET=1
AVRES=Mat
SMN =-1682
SMX =1903
-1682
-1284
-885.604
-487.268
-88.933
309.402
707.738
1106
1504
1903
MN
MX
Bass Reflex Enclosure : Second Mode at 250.106 Hz

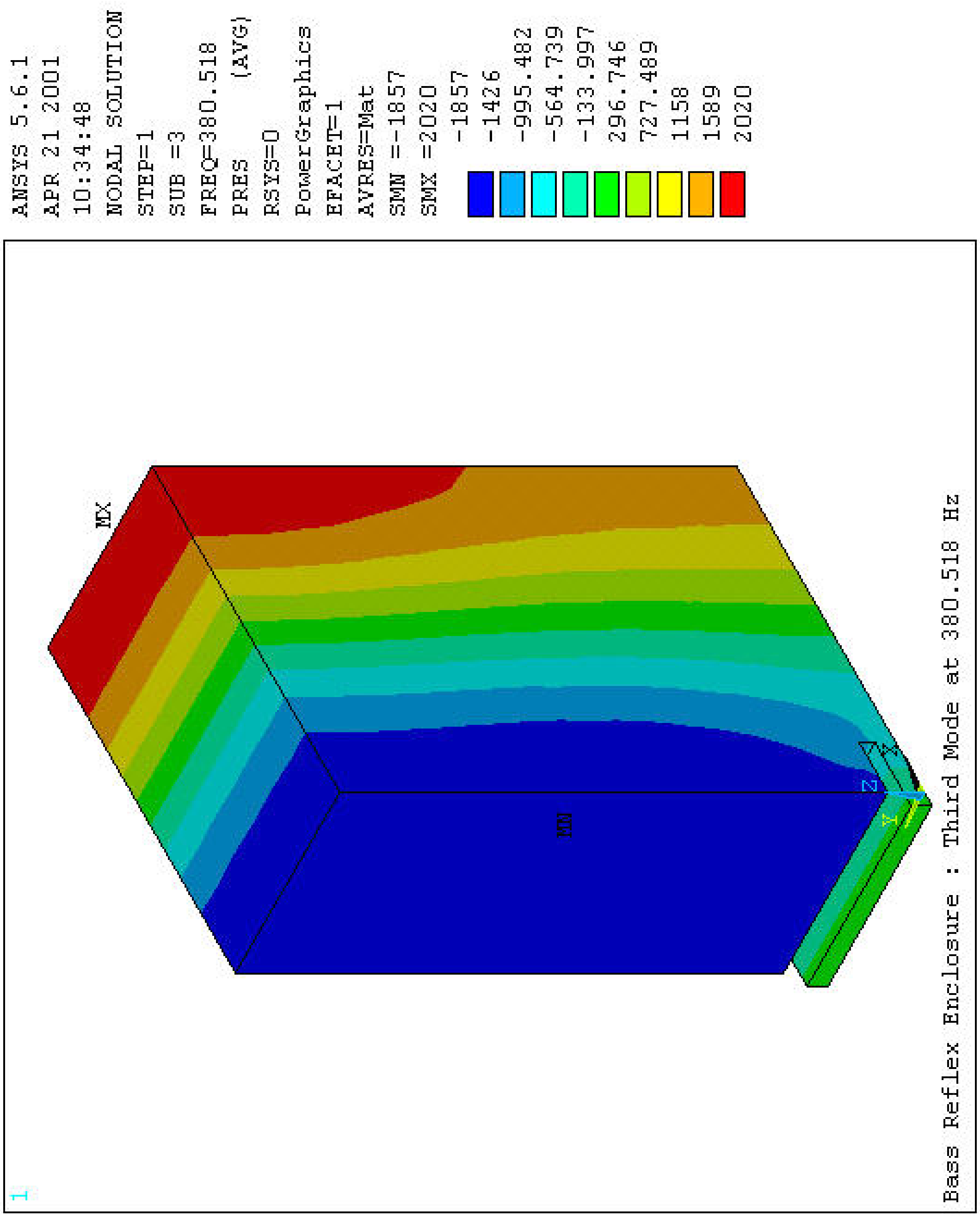
ANSYS 5.6.1
APR 21 2001
10:34:48
NODAL SOLUTION
STEP=1
SUB =3
FREQ=380.518
PRES (AVG)
RSYS=0
PowerGraphics
EFACET=1
AVRES=Mat
SMN =-1857
SMX =2020
-1857
-1426
-995.482
-564.739
-133.997
296.746
727.489
1158
1589
2020
MX
MN
Bass Reflex Enclosure : Third Mode at 380.518 Hz

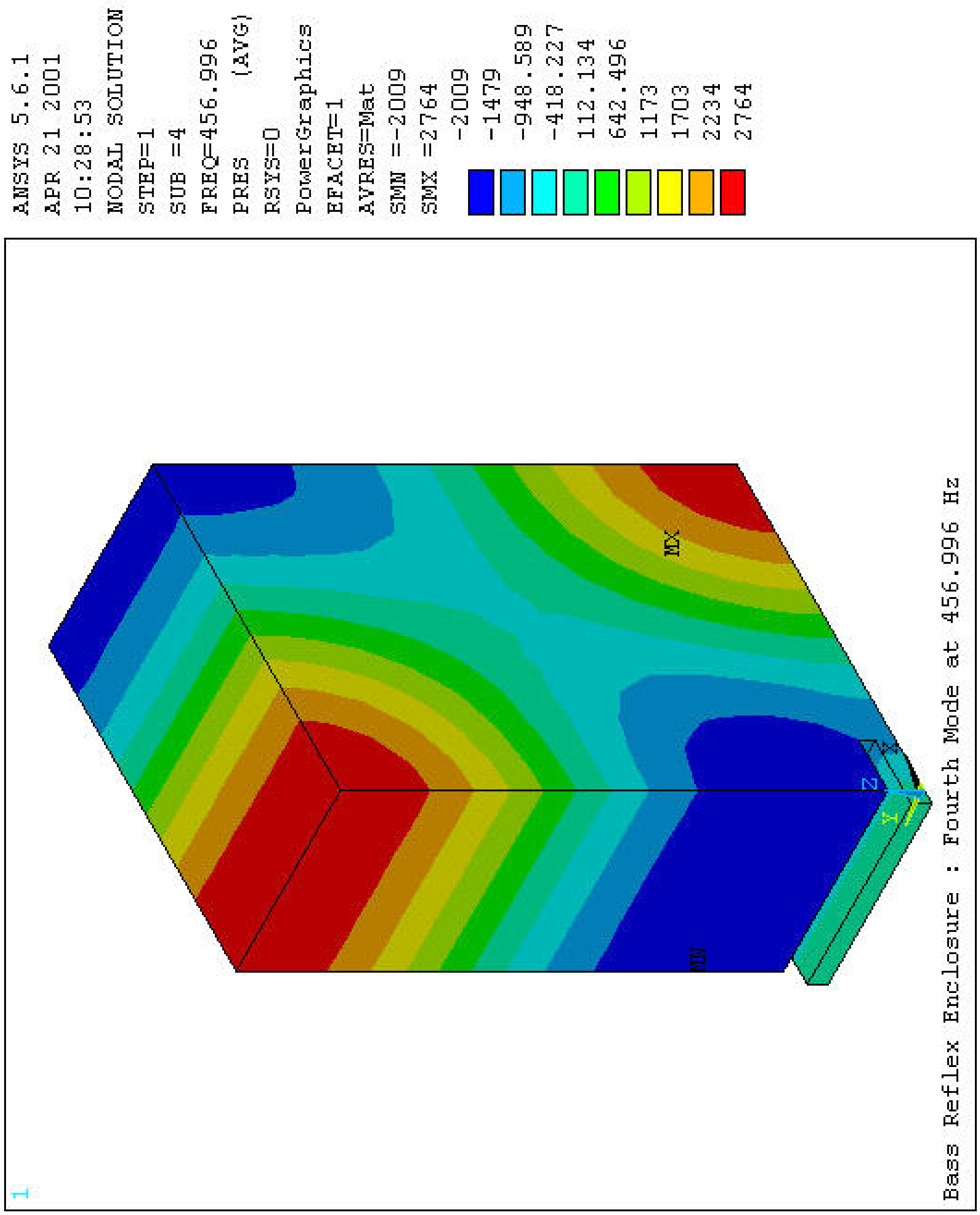
ANSYS 5.6.1
APR 21 2001
10:28:53
NODAL SOLUTION
STEP=1
SUB =4
FREQ=456.996
PRES (AVG)
RSYS=0
PowerGraphics
EFACET=1
AVRES=Mat
SMN =-2009
SMX =2764
-2009
-1479
-948.589
-418.227
112.134
642.496
1173
1703
2234
2764
MX
MN
Bass Reflex Enclosure : Fourth Mode at 456.996 Hz

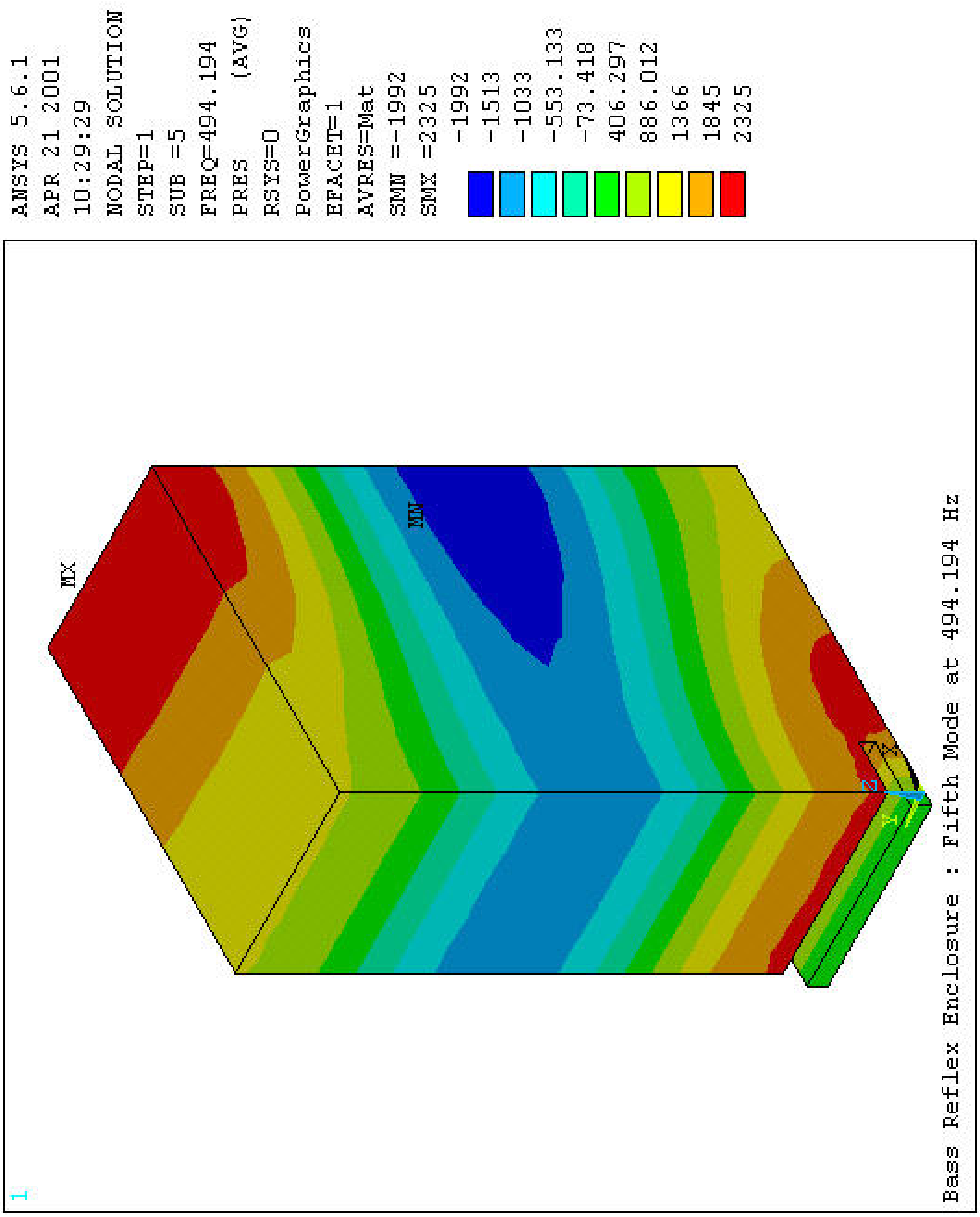
ANSYS 5.6.1
APR 21 2001
10:29:29
NODAL SOLUTION
STEP=1
SUB =5
FREQ=494.194
PRES (AVG)
RSYS=0
PowerGraphics
EFACET=1
AVRES=Mat
SMN =-1992
SMX =2325
-1992
-1513
-1033
-553.133
-73.418
406.297
886.012
1366
1845
2325
MX
MN
Bass Reflex Enclosure : Fifth Mode at 494.194 Hz

Attachment 3 : Final ML TQWT MathCad Model Simulation

3/23/01

Reference : Upgraded MathCad Computer Models for the Design of Transmission Line Loudspeakers

by Martin J. King
40 Dorsman Dr.
Clifton Park, NY 12065
e-mail MJKing57@aol.com

Worksheet down loaded from http://www.t-linespeakers.org/

Unit and Constant Definition

$cycle := 2 \cdot \pi \cdot rad$

$Hz := cycle \cdot sec^{-1}$

Air Density : $\rho := 1.21 \cdot kg \cdot m^{-3}$

Speed of Sound : $c := 342 \cdot m \cdot sec^{-1}$

User Input (Edit This Section and Input all of the Parameters for the System to be Analyzed)

Driver Thiele / Small Parameters : Fostex FE-164 Properties

$f_d := 57.83\,Hz$ $V_d := 28.85\,liter$

$R_e := 7.06\,\Omega$ $Q_{ed} := 0.380$

$L_{vc} := 0 \cdot mH$ $Q_{md} := 4.895$

$Bl := 6.58 \cdot \dfrac{newton}{amp}$ $Q_{td} := \left(\dfrac{1}{Q_{ed}} + \dfrac{1}{Q_{md}}\right)^{-1}$

$S_d := 132 \cdot cm^2$ $Q_{td} = 0.353$

Transmission Line Definition (0 lb/ft^3 < D < 1 lb/ft^3)

Closed End of Transmission Line

$x_0 := 30 \cdot in$ (length)

$D_0 := 0.25\,lb \cdot ft^{-3}$ (stuffing density)

$S_{0,0} := S_0 + TR \cdot x_0$ (driver end)

$S_{0,1} := S_0$ (closed end)

Expansion Definition (actual geometry)

$L := 60 \cdot in$

$S_0 := 10 \cdot in \cdot 2.5 \cdot in - 4 \cdot 0.75 \cdot in \cdot 0.625 \cdot in$

$S_L := 10 \cdot in \cdot 14.5 \cdot in - 4 \cdot 0.75 \cdot in \cdot 0.625 \cdot in$

$TR := (S_L - S_0) \cdot L^{-1}$

$S_0 = 23.125\,in^2$

$S_L = 143.125\,in^2$

$\dfrac{S_0}{S_d} = 1.130$

$\dfrac{S_L}{S_d} = 6.995$

Open End of Transmission Line

Section Length	Initial Area	Final Area	Stuffing Density
$x_1 := 0.25 \cdot (L - x_0)$	$S_{1,0} := S_{0,0}$	$S_{1,1} := S_{1,0} + TR \cdot x_1$	$D_1 := 0.25 \cdot lb \cdot ft^{-3}$
$x_2 := x_1 + 0.25 \cdot (L - x_0)$	$S_{2,0} := S_{1,1}$	$S_{2,1} := S_{2,0} + TR \cdot (x_2 - x_1)$	$D_2 := 0.0 \cdot lb \cdot ft^{-3}$
$x_3 := x_2 + 0.25 \cdot (L - x_0)$	$S_{3,0} := S_{2,1}$	$S_{3,1} := S_{3,0} + TR \cdot (x_3 - x_2)$	$D_3 := 0.0 \cdot lb \cdot ft^{-3}$
$x_4 := x_3 + 0.25 \cdot (L - x_0)$	$S_{4,0} := S_{3,1}$	$S_{4,1} := S_{4,0} + TR \cdot (x_4 - x_3)$	$D_4 := 0.0 \cdot lb \cdot ft^{-3}$
$x_5 := x_4 + 2 \cdot in + 0.6 \cdot 1.5 \cdot in$	$S_{5,0} := \pi \cdot (1.5 \cdot in)^2$	$S_{5,1} := \pi \cdot (1.5 \cdot in)^2$	$D_5 := 0.0 \cdot lb \cdot ft^{-3}$

Total Transmission Line Length

$$x_0 + x_5 = 62.900 in$$

Set-up Counters for Numerical Analysis

$N := 2^{11}$ $\quad N = 2048$

Time Domain

$n := 0, 1 .. N - 1$

$T_{max} := 1 \cdot sec$ $\quad dt := T_{max} \cdot N^{-1}$

Frequency Domain

$r := 1, 2 .. 0.5 \cdot N$ $\quad s := 0, 1 .. 0.5 \cdot N$

$d\omega := cycle \cdot T_{max}^{-1}$ $\quad d\omega = 1.0 Hz$

Calculate Acoustic Circuit Elements From Driver Thiele / Small Parameters

$$C_{ad} := \frac{V_d}{\rho \cdot c^2} \qquad C_{ad} = 2.038 \times 10^{-7} \frac{m^5}{newton}$$

$$M_{ad} := \frac{1}{f_d^2 \cdot C_{ad}} \qquad M_{ad} = 37.156 \frac{kg}{m^4}$$

$$R_{ad} := \frac{Bl^2}{S_d^2} \cdot \left(\frac{Q_{ed}}{R_e \cdot Q_{md}} \right) \qquad R_{ad} = 2.732 \times 10^3 \frac{newton \cdot sec}{m^5}$$

$$R_{atd_s} := R_{ad} + \frac{Bl^2}{S_d^2 \cdot (R_e + j \cdot s \cdot d\omega \cdot L_{vc})} \qquad \left| R_{atd_0} \right| = 3.793 \times 10^4 \frac{newton \cdot sec}{m^5}$$

Individual Section Lengths

$L_0 := x_0$

$n := 2 .. 5$

$L_1 := x_1$

$L_n := x_n - x_{n-1}$

Acoustic Impedance Calculation for the Transmission Line

$n := 0..5$

Exponential Line Coefficient

$$\gamma_n := \frac{\ln\left[S_{n,1}\cdot\left(S_{n,0}\right)^{-1}\right]}{L_n}$$

Viscous Damping Coefficient

$$\lambda_{tube} := 50\cdot\frac{newton\cdot sec}{m^4}$$

$$\lambda_{fiber_n} := D_n\cdot\frac{ft^3}{lb}\cdot 1570\cdot\frac{newton\cdot sec}{m^4}$$

$$order_n := 2 - \frac{1}{0.2}\cdot\left(D_n\cdot\frac{ft^3}{lb} - 0.2\right)\cdot\Phi\left(D_n\cdot\frac{ft^3}{lb} - 0.2\right) + \frac{1}{0.2}\cdot\left(D_n\cdot\frac{ft^3}{lb} - 0.4\right)\cdot\Phi\left(D_n\cdot\frac{ft^3}{lb} - 0.4\right)$$

$$\lambda_{n,r} := \left(\lambda_{tube} + \lambda_{fiber_n}\right)\cdot\left(\frac{r\cdot d\omega}{50\cdot Hz}\right)^{order_n}\cdot\left[1 + \left(\frac{r\cdot d\omega}{50\cdot Hz}\right)^{order_n}\right]^{-1}$$

$$\theta_{n,r} := \frac{1}{2}\cdot\left(\operatorname{atan}\left(\frac{-\lambda_{n,r}}{r\cdot d\omega\cdot\rho}\right)\right)$$

$$\alpha_{n,r} := \left[1 + \left(\frac{\lambda_{n,r}}{r\cdot d\omega\cdot\rho}\right)^2\right]^{\frac{1}{4}}\cdot\cos\left(\theta_{n,r}\right) \qquad \beta_{n,r} := \left[1 + \left(\frac{\lambda_{n,r}}{r\cdot d\omega\cdot\rho}\right)^2\right]^{\frac{1}{4}}\cdot\sin\left(\theta_{n,r}\right)$$

Terminus Impedance : Piston in an Infinite Baffle Impedance Model

$$a_L := \sqrt{\frac{S_{5,1}}{\pi}}$$

$$J_1(x) := \sum_{k=0}^{25}\left[\frac{(-1)^k\cdot\left(\frac{x}{2}\right)^{2\cdot k+1}}{k!\cdot\Gamma(k+2)}\right]$$

$$H_1(x) := \sum_{k=0}^{25}\left[\frac{(-1)^k\cdot\left(\frac{x}{2}\right)^{2\cdot k+2}}{\Gamma\left(k+\frac{3}{2}\right)\cdot\Gamma\left(k+\frac{5}{2}\right)}\right]$$

$$Z_{mouth_r} := \frac{\rho\cdot c}{S_{5,1}}\cdot\left[\left(1 - \frac{2\cdot J_1\left(2\cdot\frac{r\cdot d\omega}{c}\cdot a_L\right)}{2\cdot\frac{r\cdot d\omega}{c}\cdot a_L}\right) + j\cdot\frac{2\cdot H_1\left(2\cdot\frac{r\cdot d\omega}{c}\cdot a_L\right)}{2\cdot\frac{r\cdot d\omega}{c}\cdot a_L}\right]$$

Speed of Sound

$$D_{points} := (0.000\ \ 0.191\ \ 0.382\ \ 0.573\ \ 1) \qquad c_{points} := (342\ \ 335\ \ 325\ \ 320\ \ 319)$$

$$smooth := cspline\left(D_{points}{}^{T}, c_{points}{}^{T}\right)$$

$$c_{fiber_n} := interp\left(smooth, D_{points}{}^{T}, c_{points}{}^{T}, D_n \cdot \frac{ft^3}{lb}\right) \cdot \frac{m}{sec}$$

Exponents

$$A_n := -\frac{1}{2} \cdot \gamma_n$$

$$B_{n,r} := \frac{1}{2} \cdot \frac{\sqrt{-\left(2 \cdot \alpha_{n,r} \cdot r \cdot d\omega + j \cdot 2 \cdot \beta_{n,r} \cdot r \cdot d\omega - c_{fiber_n} \cdot \gamma_n\right) \cdot \left(2 \cdot \alpha_{n,r} \cdot r \cdot d\omega + j \cdot 2 \cdot \beta_{n,r} \cdot r \cdot d\omega + c_{fiber_n} \cdot \gamma_n\right)}}{c_{fiber_n}}$$

Acoustic Impedance Calculation for the Closed End of the Transmission Line

$$N_{closed_r} := -A_0 \cdot \left[\exp\left[\left(-A_0 - B_{0,r}\right) \cdot x_0\right] - \exp\left[\left(-A_0 + B_{0,r}\right) \cdot x_0\right]\right] \dots$$
$$+ B_{0,r} \cdot \left[\exp\left[\left(-A_0 - B_{0,r}\right) \cdot x_0\right] + \exp\left[\left(-A_0 + B_{0,r}\right) \cdot x_0\right]\right]$$

$$D_{closed_r} := \exp\left[\left(-A_0 - B_{0,r}\right) \cdot x_0\right] - \exp\left[\left(-A_0 + B_{0,r}\right) \cdot x_0\right]$$

$$Z_{ac_r} := j \cdot \frac{\rho \cdot \left(c_{fiber_0}\right)^2}{r \cdot d\omega \cdot S_{0,0}} \cdot \frac{N_{closed_r}}{D_{closed_r}}$$

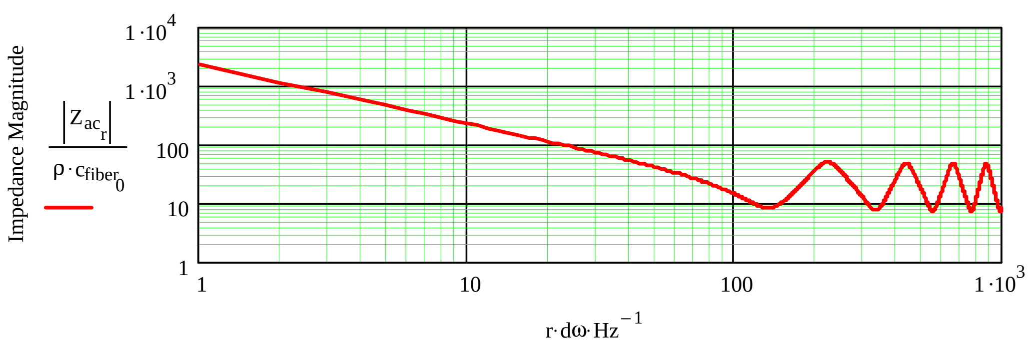

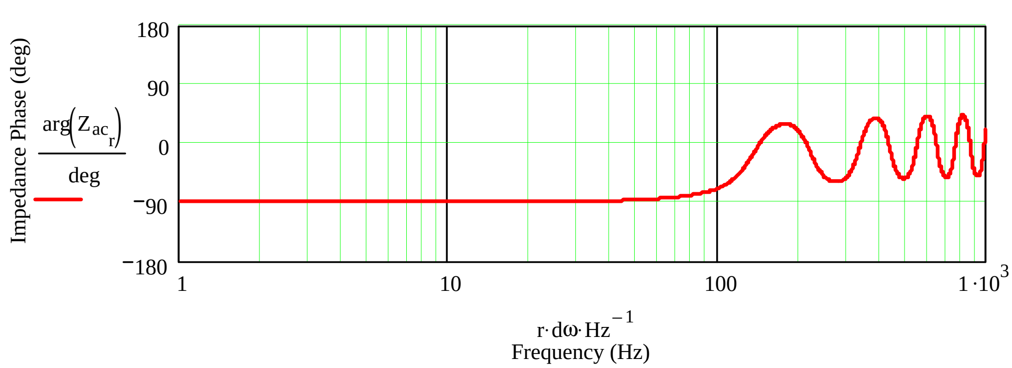

Acoustic Impedance Calculation for the Open End Transmission Line

Equation 0 :

$$c00_r := S_{1,0} \cdot m^{-2} \qquad c01_r := S_{1,0} \cdot m^{-2}$$

Equation 1 :

$$c10_r := S_{1,1} \cdot \exp\left[\left(-A_1 - B_{1,r}\right) \cdot x_1\right] \cdot m^{-2} \qquad c11_r := S_{1,1} \cdot \exp\left[\left(-A_1 + B_{1,r}\right) \cdot x_1\right] \cdot m^{-2}$$

$$c12_r := S_{2,0} \cdot \exp\left[\left(-A_2 - B_{2,r}\right) \cdot x_1\right] \cdot m^{-2} \qquad c13_r := S_{2,0} \cdot \exp\left[\left(-A_2 + B_{2,r}\right) \cdot x_1\right] \cdot m^{-2}$$

Equation 2 :

$$c20_r := \frac{-\rho \cdot \left(c_{fiber_1}\right)^2}{j \cdot r \cdot d\omega} \cdot \left(-A_1 - B_{1,r}\right) \cdot \exp\left[\left(-A_1 - B_{1,r}\right) \cdot x_1\right] \cdot \left(sec \cdot m^{-1} \cdot Pa\right)^{-1}$$

$$c21_r := \frac{-\rho \cdot \left(c_{fiber_1}\right)^2}{j \cdot r \cdot d\omega} \cdot \left(-A_1 + B_{1,r}\right) \cdot \exp\left[\left(-A_1 + B_{1,r}\right) \cdot x_1\right] \cdot \left(sec \cdot m^{-1} \cdot Pa\right)^{-1}$$

$$c22_r := \frac{-\rho \cdot \left(c_{fiber_2}\right)^2}{j \cdot r \cdot d\omega} \cdot \left(-A_2 - B_{2,r}\right) \cdot \exp\left[\left(-A_2 - B_{2,r}\right) \cdot x_1\right] \cdot \left(sec \cdot m^{-1} \cdot Pa\right)^{-1}$$

$$c23_r := \frac{-\rho \cdot \left(c_{fiber_2}\right)^2}{j \cdot r \cdot d\omega} \cdot \left(-A_2 + B_{2,r}\right) \cdot \exp\left[\left(-A_2 + B_{2,r}\right) \cdot x_1\right] \cdot \left(sec \cdot m^{-1} \cdot Pa\right)^{-1}$$

Equation 3 :

$$c32_r := S_{2,1} \cdot \exp\left[\left(-A_2 - B_{2,r}\right) \cdot x_2\right] \cdot m^{-2} \qquad c33_r := S_{2,1} \cdot \exp\left[\left(-A_2 + B_{2,r}\right) \cdot x_2\right] \cdot m^{-2}$$

$$c34_r := S_{3,0} \cdot \exp\left[\left(-A_3 - B_{3,r}\right) \cdot x_2\right] \cdot m^{-2} \qquad c35_r := S_{3,0} \cdot \exp\left[\left(-A_3 + B_{3,r}\right) \cdot x_2\right] \cdot m^{-2}$$

Equation 4 :

$$c42_r := \frac{-\rho \cdot \left(c_{fiber_2}\right)^2}{j \cdot r \cdot d\omega} \cdot \left(-A_2 - B_{2,r}\right) \cdot \exp\left[\left(-A_2 - B_{2,r}\right) \cdot x_2\right] \cdot \left(sec \cdot m^{-1} \cdot Pa\right)^{-1}$$

$$c43_r := \frac{-\rho \cdot \left(c_{fiber_2}\right)^2}{j \cdot r \cdot d\omega} \cdot \left(-A_2 + B_{2,r}\right) \cdot \exp\left[\left(-A_2 + B_{2,r}\right) \cdot x_2\right] \cdot \left(sec \cdot m^{-1} \cdot Pa\right)^{-1}$$

$$c44_r := \frac{-\rho \cdot \left(c_{fiber_3}\right)^2}{j \cdot r \cdot d\omega} \cdot \left(-A_3 - B_{3,r}\right) \cdot \exp\left[\left(-A_3 - B_{3,r}\right) \cdot x_2\right] \cdot \left(sec \cdot m^{-1} \cdot Pa\right)^{-1}$$

$$c45_r := \frac{-\rho \cdot \left(c_{fiber_3}\right)^2}{j \cdot r \cdot d\omega} \cdot \left(-A_3 + B_{3,r}\right) \cdot \exp\left[\left(-A_3 + B_{3,r}\right) \cdot x_2\right] \cdot \left(sec \cdot m^{-1} \cdot Pa\right)^{-1}$$

Equation 5 :

$$c54_r := S_{3,1} \cdot \exp\left[\left(-A_3 - B_{3,r}\right) \cdot x_3\right] \cdot m^{-2} \qquad c55_r := S_{3,1} \cdot \exp\left[\left(-A_3 + B_{3,r}\right) \cdot x_3\right] \cdot m^{-2}$$

$$c56_r := S_{4,0} \cdot \exp\left[\left(-A_4 - B_{4,r}\right) \cdot x_3\right] \cdot m^{-2} \qquad c57_r := S_{4,0} \cdot \exp\left[\left(-A_4 + B_{4,r}\right) \cdot x_3\right] \cdot m^{-2}$$

Equation 6 :

$$c64_r := \frac{-\rho \cdot \left(c_{fiber_3}\right)^2}{j \cdot r \cdot d\omega} \cdot \left(-A_3 - B_{3,r}\right) \cdot \exp\left[\left(-A_3 - B_{3,r}\right) \cdot x_3\right] \cdot \left(sec \cdot m^{-1} \cdot Pa\right)^{-1}$$

$$c65_r := \frac{-\rho \cdot \left(c_{fiber_3}\right)^2}{j \cdot r \cdot d\omega} \cdot \left(-A_3 + B_{3,r}\right) \cdot \exp\left[\left(-A_3 + B_{3,r}\right) \cdot x_3\right] \cdot \left(sec \cdot m^{-1} \cdot Pa\right)^{-1}$$

$$c66_r := \frac{-\rho \cdot \left(c_{fiber_4}\right)^2}{j \cdot r \cdot d\omega} \cdot \left(-A_4 - B_{4,r}\right) \cdot \exp\left[\left(-A_4 - B_{4,r}\right) \cdot x_3\right] \cdot \left(sec \cdot m^{-1} \cdot Pa\right)^{-1}$$

$$c67_r := \frac{-\rho \cdot \left(c_{fiber_4}\right)^2}{j \cdot r \cdot d\omega} \cdot \left(-A_4 + B_{4,r}\right) \cdot \exp\left[\left(-A_4 + B_{4,r}\right) \cdot x_3\right] \cdot \left(sec \cdot m^{-1} \cdot Pa\right)^{-1}$$

Equation 7 :

$$c76_r := S_{4,1} \cdot \exp\left[\left(-A_4 - B_{4,r}\right) \cdot x_4\right] \cdot m^{-2} \qquad c77_r := S_{4,1} \cdot \exp\left[\left(-A_4 + B_{4,r}\right) \cdot x_4\right] \cdot m^{-2}$$

$$c78_r := S_{5,0} \cdot \exp\left[\left(-A_5 - B_{5,r}\right) \cdot x_4\right] \cdot m^{-2} \qquad c79_r := S_{5,0} \cdot \exp\left[\left(-A_5 + B_{5,r}\right) \cdot x_4\right] \cdot m^{-2}$$

Equation 8 :

$$c86_r := \frac{-\rho \cdot \left(c_{fiber_4}\right)^2}{j \cdot r \cdot d\omega} \cdot \left(-A_4 - B_{4,r}\right) \cdot \exp\left[\left(-A_4 - B_{4,r}\right) \cdot x_4\right] \cdot \left(sec \cdot m^{-1} \cdot Pa\right)^{-1}$$

$$c87_r := \frac{-\rho \cdot \left(c_{fiber_4}\right)^2}{j \cdot r \cdot d\omega} \cdot \left(-A_4 + B_{4,r}\right) \cdot \exp\left[\left(-A_4 + B_{4,r}\right) \cdot x_4\right] \cdot \left(sec \cdot m^{-1} \cdot Pa\right)^{-1}$$

$$c88_r := \frac{-\rho \cdot \left(c_{fiber_5}\right)^2}{j \cdot r \cdot d\omega} \cdot \left(-A_5 - B_{5,r}\right) \cdot \exp\left[\left(-A_5 - B_{5,r}\right) \cdot x_4\right] \cdot \left(sec \cdot m^{-1} \cdot Pa\right)^{-1}$$

$$c89_r := \frac{-\rho \cdot \left(c_{fiber_5}\right)^2}{j \cdot r \cdot d\omega} \cdot \left(-A_5 + B_{5,r}\right) \cdot \exp\left[\left(-A_5 + B_{5,r}\right) \cdot x_4\right] \cdot \left(sec \cdot m^{-1} \cdot Pa\right)^{-1}$$

Equation 9 :

$$c98_r := \left[\frac{-\rho \cdot \left(c_{fiber_5}\right)^2}{j \cdot r \cdot d\omega} \cdot \left(-A_5 - B_{5,r}\right) - Z_{mouth_r} \cdot S_{5,1}\right] \cdot \exp\left[\left(-A_5 - B_{5,r}\right) \cdot x_5\right] \cdot \left(sec \cdot m^{-1} \cdot Pa\right)^{-1}$$

$$c99_r := \left[\frac{-\rho \cdot \left(c_{fiber_5}\right)^2}{j \cdot r \cdot d\omega} \cdot \left(-A_5 + B_{5,r}\right) - Z_{mouth_r} \cdot S_{5,1}\right] \cdot \exp\left[\left(-A_5 + B_{5,r}\right) \cdot x_5\right] \cdot \left(sec \cdot m^{-1} \cdot Pa\right)^{-1}$$

Solving for the Coefficients

$$\begin{pmatrix} C11_r \\ C12_r \\ C21_r \\ C22_r \\ C31_r \\ C32_r \\ C41_r \\ C42_r \\ C51_r \\ C52_r \end{pmatrix} := \begin{pmatrix} c00_r & c01_r & 0 & 0 & 0 & 0 & 0 & 0 & 0 & 0 \\ c10_r & c11_r & -c12_r & -c13_r & 0 & 0 & 0 & 0 & 0 & 0 \\ c20_r & c21_r & -c22_r & -c23_r & 0 & 0 & 0 & 0 & 0 & 0 \\ 0 & 0 & c32_r & c33_r & -c34_r & -c35_r & 0 & 0 & 0 & 0 \\ 0 & 0 & c42_r & c43_r & -c44_r & -c45_r & 0 & 0 & 0 & 0 \\ 0 & 0 & 0 & 0 & c54_r & c55_r & -c56_r & -c57_r & 0 & 0 \\ 0 & 0 & 0 & 0 & c64_r & c65_r & -c66_r & -c67_r & 0 & 0 \\ 0 & 0 & 0 & 0 & 0 & 0 & c76_r & c77_r & -c78_r & -c79_r \\ 0 & 0 & 0 & 0 & 0 & 0 & c86_r & c87_r & -c88_r & -c89_r \\ 0 & 0 & 0 & 0 & 0 & 0 & 0 & 0 & c98_r & c99_r \end{pmatrix}^{-1} \cdot \begin{pmatrix} S_d \cdot m^{-2} \cdot 1 \\ 0 \\ 0 \\ 0 \\ 0 \\ 0 \\ 0 \\ 0 \\ 0 \\ 0 \end{pmatrix} \cdot \frac{m}{sec}$$

Acoustic Impedance Calculation for the Open Ended Transmission Line

$$p0_r := \frac{-\rho \cdot \left(c_{fiber_1}\right)^2}{j \cdot r \cdot d\omega} \cdot \left[C11_r \cdot \left(-A_1 - B_{1,r}\right) + C12_r \cdot \left(-A_1 + B_{1,r}\right) \right]$$

$$U_0 := S_d \cdot 1 \cdot \frac{m}{sec}$$

$$Z_{ao_r} := \frac{p0_r}{U_0}$$

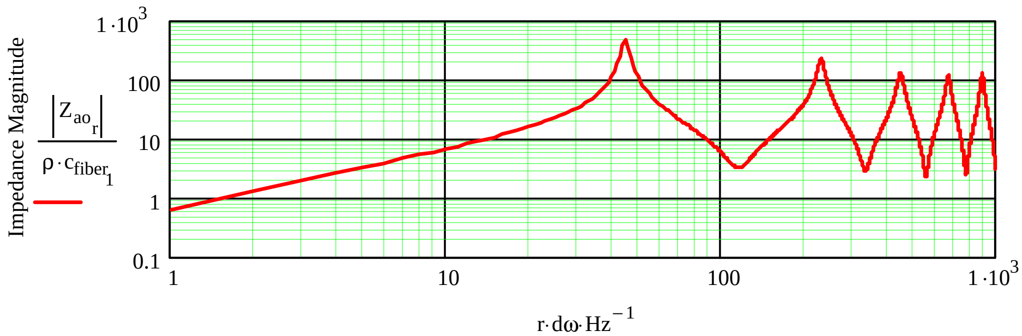

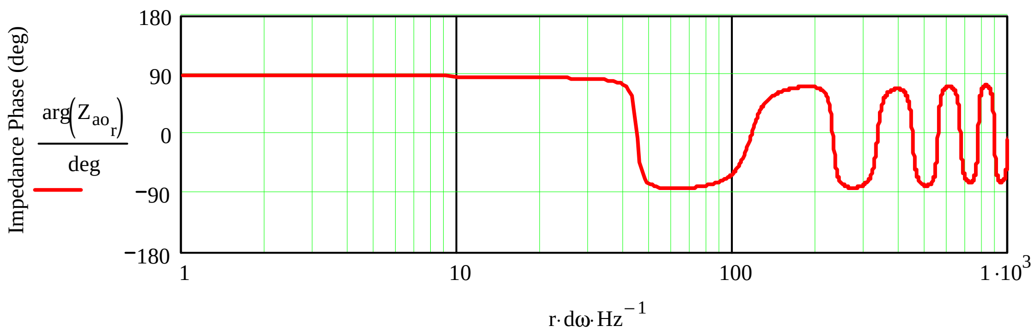

Velocity at the Terminus of the Transmission Line for a 1 m/sec Driver Excitation

$$\varepsilon_r := \frac{\frac{S_{1,0}}{S_{1,1}} \cdot \frac{S_{2,0}}{S_{2,1}} \cdot \frac{S_{3,0}}{S_{3,1}} \cdot \frac{S_{4,0}}{S_{4,1}} \cdot \frac{S_{5,0}}{S_{5,1}} \cdot \left[C51_r \cdot \exp\left[\left(-A_5 - B_{5,r}\right) \cdot \left(x_5\right)\right] + C52_r \cdot \exp\left[\left(-A_5 + B_{5,r}\right) \cdot \left(x_5\right)\right] \right]}{\left(S_d \cdot 1 \cdot m \cdot sec^{-1}\right) \cdot \left(S_{1,0}\right)^{-1}}$$

Resulting Acoustic Impedance for the Transmission Line

$$Zal_r := \left(\frac{1}{Zac_r} + \frac{1}{Zao_r}\right)^{-1}$$

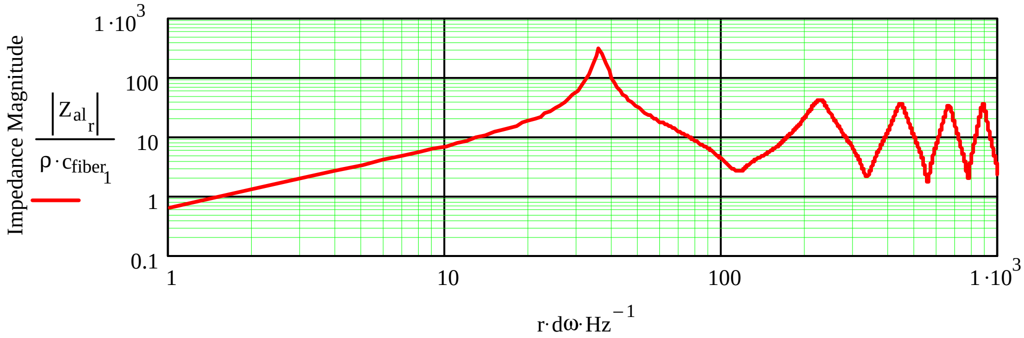

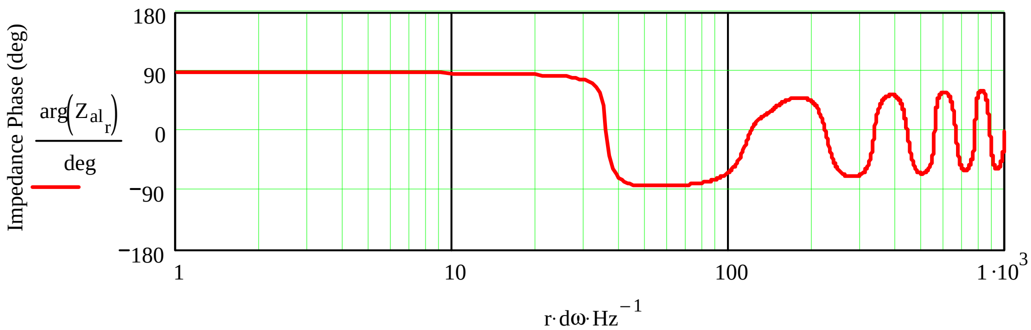

Velocity at the Terminus of the Transmission Line for a 1 m/sec Driver Excitation

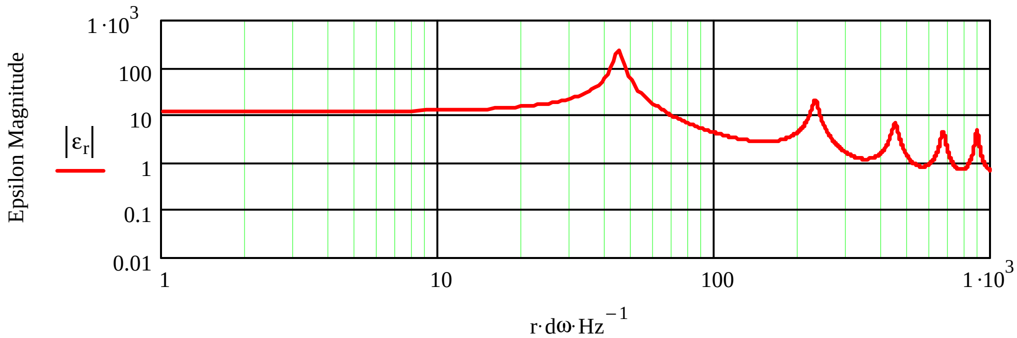

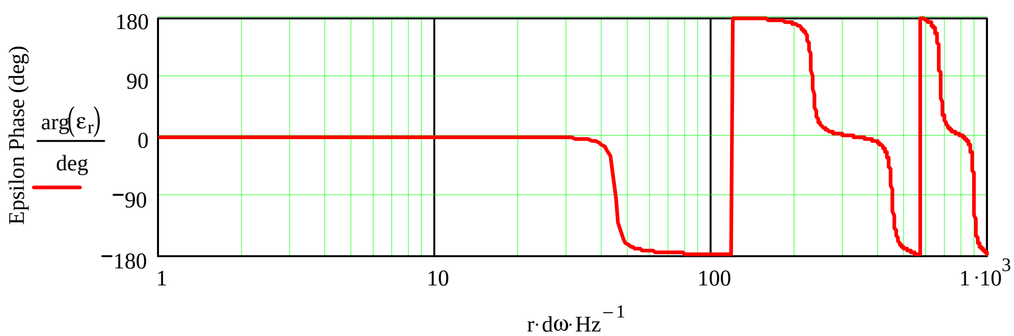

Driver Radius : $a_d := \sqrt{\frac{S_d}{\pi}}$

Terminus Radius : $a_L := \sqrt{\frac{S_{5,1}}{\pi}}$

Response Radius : $radius := 1 \cdot m$

Calculate the System Response for a Voltage that Produces a 1 Watt Input into an 8 Ohm Driver.

$p_g := \frac{2.8284 volt \cdot Bl}{S_d \cdot (R_e)}$ and $k_r := \frac{r \cdot d\omega}{c}$ $\qquad \frac{(2.8284 volt)^2}{8 \cdot \Omega} = 1.000 watt$ (RMS)

Driver ("d" subscript)

$$Ud_r := \frac{p_g}{\left(\frac{1}{j \cdot r \cdot d\omega \cdot C_{ad}} + R_{atd_r} + j \cdot r \cdot d\omega \cdot M_{ad} + Z_{al_r}\right)} \qquad Ud_0 := 0 \cdot m^3 \cdot sec^{-1}$$

$$pd_r := \rho \cdot c \cdot \frac{Ud_r}{S_d} \cdot \left(\exp(-j \cdot k_r radius) - \exp\left(-j \cdot k_r \cdot \sqrt{radius^2 + a_d^2}\right)\right) \qquad SPLd_r := 20 \cdot \log\left(\frac{|pd_r|}{2 \cdot 10^{-5} \cdot Pa}\right)$$

Terminus ("L" subscript)

$$UL_r := -\varepsilon_r \cdot \frac{S_{5,1}}{S_{1,0}} \cdot \frac{Zal_r}{Zao_r} \cdot Ud_r \qquad UL_0 := 0 \cdot m^3 \cdot sec^{-1}$$

$$pL_r := \rho \cdot c \cdot \frac{UL_r}{S_{5,1}} \cdot \left(\exp(-j \cdot k_r radius) - \exp\left(-j \cdot k_r \cdot \sqrt{radius^2 + a_L^2}\right)\right) \qquad SPLL_r := 20 \cdot \log\left(\frac{|pL_r|}{2 \cdot 10^{-5} \cdot Pa}\right)$$

System ("o" subscript)

$$Uo_s := Ud_s + UL_s$$

$$po_r := pd_r + pL_r \qquad SPLo_r := 20 \cdot \log\left(\frac{|po_r|}{2 \cdot 10^{-5} \cdot Pa}\right)$$

Acoustic Response of the Driver in an Infinite Baffle

Driver (no subscript)

$$U_r := \frac{p_g}{\left(\frac{1}{j \cdot r \cdot d\omega \cdot C_{ad}} + R_{atd_r} + j \cdot r \cdot d\omega \cdot M_{ad}\right)} \qquad U_0 := 0 \cdot m^3 \cdot sec^{-1}$$

$$p_r := \rho \cdot c \cdot \frac{U_r}{S_d} \cdot \left(\exp(-j \cdot k_r radius) - \exp\left(-j \cdot k_r \cdot \sqrt{radius^2 + a_d^2}\right)\right) \qquad SPL_r := 20 \cdot \log\left(\frac{|p_r|}{2 \cdot 10^{-5} \cdot Pa}\right)$$

Far Field Transmission Line System and Infinite Baffle Sound Pressure Level Responses

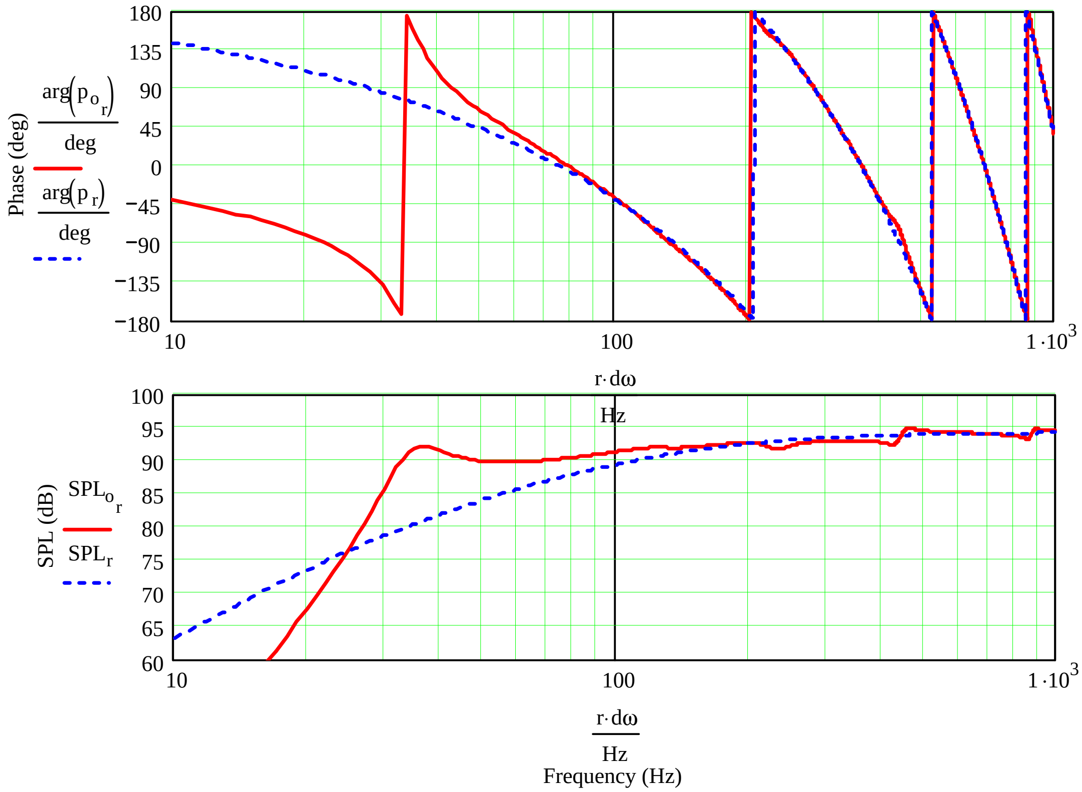

Woofer and Terminus Far Field Sound Pressure Level Responses

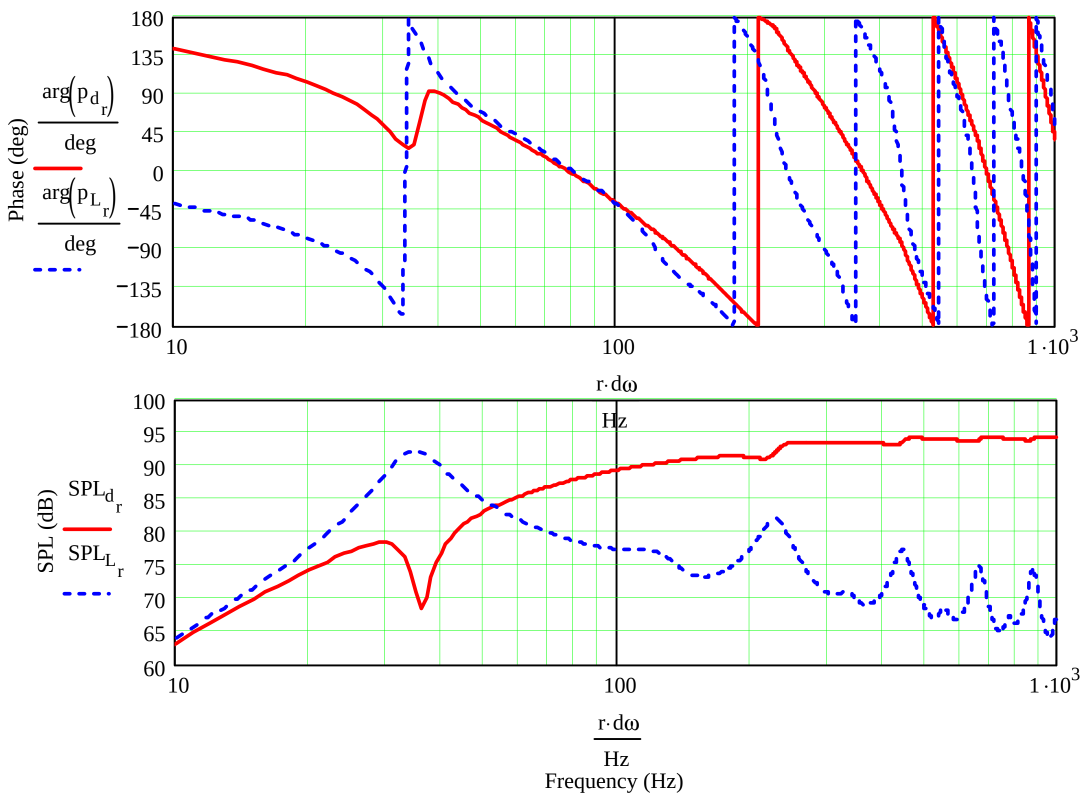

Transmission Line System and Infinite Baffle Impedance

$L_{ced} := C_{ad} \cdot Bl^2 \cdot S_d^{-2}$ $\qquad L_{ced} = 50.654\,\mathrm{mH}$

$C_{med} := M_{ad} \cdot Bl^{-2} \cdot S_d^{2}$ $\qquad C_{med} = 149.528\,\mu\mathrm{F}$

$R_{ed} := \dfrac{R_e \cdot Q_{md}}{Q_{ed}}$ $\qquad R_{ed} = 90.944\,\Omega$

$$Z_{el_r} := \frac{Bl^2}{S_d^{\,2} \cdot Z_{ac_r}} + \frac{Bl^2}{S_d^{\,2} \cdot Z_{ao_r}}$$

Impedance Calculation for the Transmission Line System and the Driver in an Infinite Baffle

$$Z_{o_r} := R_e + j \cdot r \cdot d\omega \cdot L_{vc} + \left(\frac{1}{j \cdot r \cdot d\omega \cdot L_{ced}} + j \cdot r \cdot d\omega \cdot C_{med} + \frac{1}{R_{ed}} + \frac{1}{Z_{el_r}} \right)^{-1}$$

$$Z_r := R_e + j \cdot r \cdot d\omega \cdot L_{vc} + \left(\frac{1}{j \cdot r \cdot d\omega \cdot L_{ced}} + j \cdot r \cdot d\omega \cdot C_{med} + \frac{1}{R_{ed}} \right)^{-1}$$

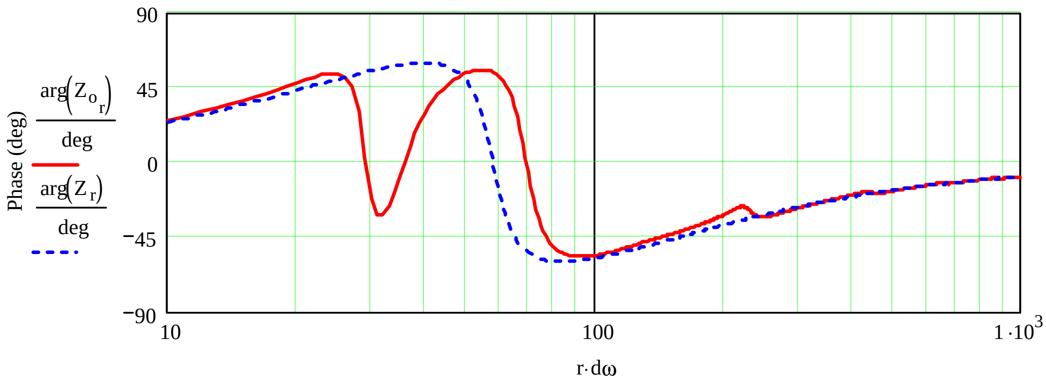

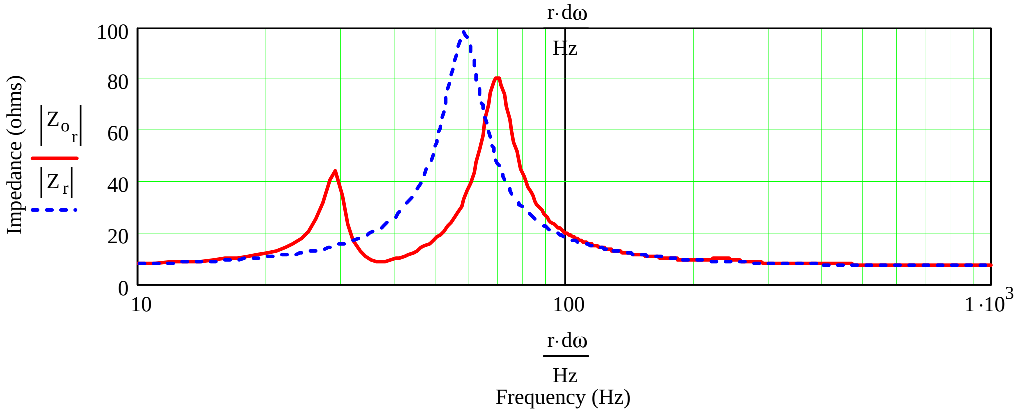

Woofer Displacement

$$x_{d_r} := \frac{U_{d_r}}{j \cdot r \cdot d\omega \cdot S_d}$$

$$x_r := \frac{U_r}{j \cdot r \cdot d\omega \cdot S_d}$$

$x_d(\omega) = U_d(\omega) / (j\ \omega\ S_d)$

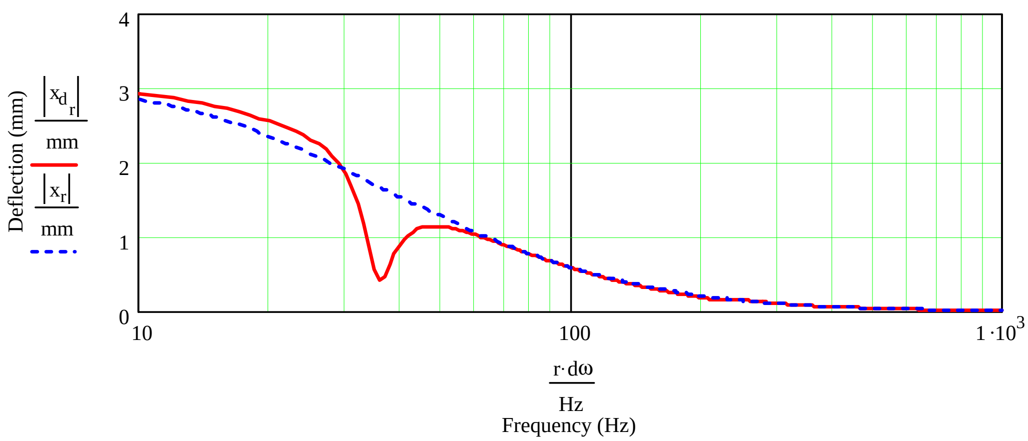

System Time Response for an Impulse Input

Results shifted by +/- 1000 Pa for easier visualization.

$n := 0, 1 .. N - 1$

$p_{driver} := IFFT(p_d) + 1000 \cdot Pa$

$p_{terminus} := IFFT(p_L) - 1000 \cdot Pa$

Time delay between pulses.

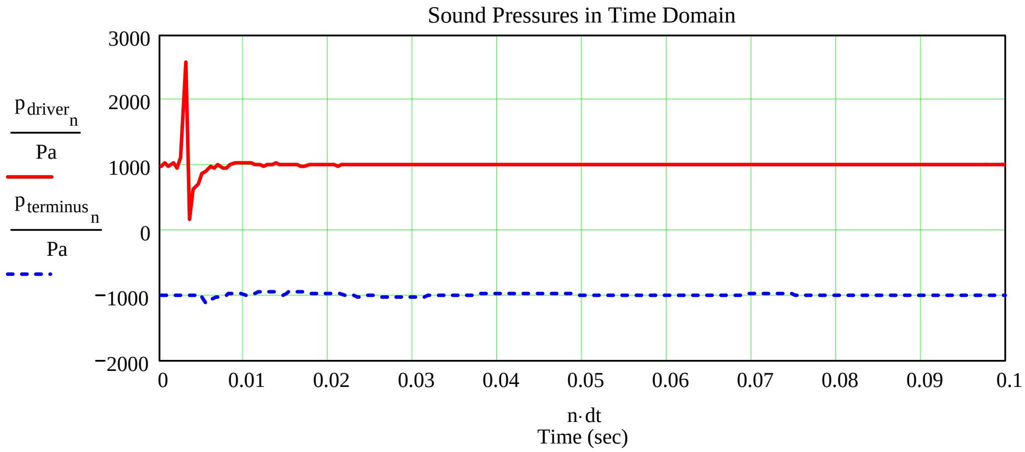

$p_{summed} := IFFT(p_o)$

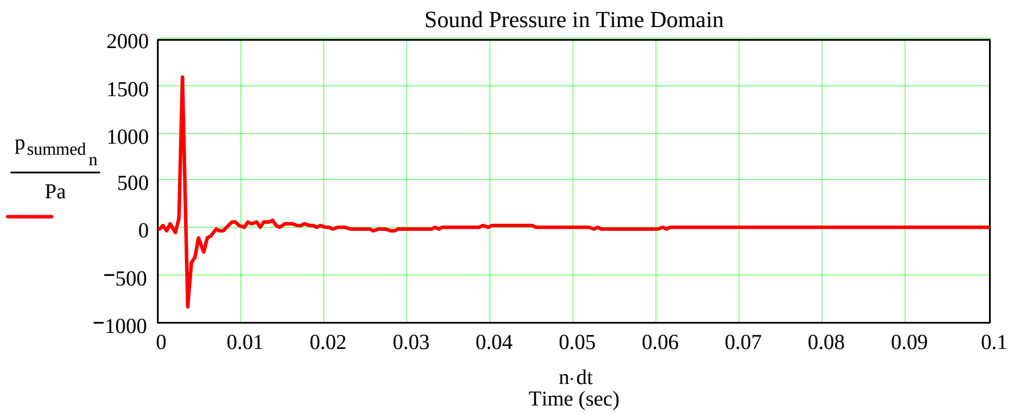

Attachment 4 : Near-Field to Far-Field SPL Correction Factor Calculation

Near Field / Far Field Correction

Unit and Constant Definition

$\text{cycle} := 2 \cdot \pi \cdot \text{rad}$

$\text{Hz} := \text{cycle} \cdot \text{sec}^{-1}$

Air Density : $\rho := 1.21 \cdot \text{kg} \cdot \text{m}^{-3}$

Speed of Sound : $c := 342 \cdot \text{m} \cdot \text{sec}^{-1}$

Frequency

$\omega := 35 \cdot \text{Hz}$

Near Field Microphone Distance

$r := 1.0 \cdot \text{in}$

SPL to Pressure Conversion

$SPL_{far} := 95$ dB at 1 watt input and 1 m distance

$$p_{far} := 2 \cdot 10^{-5} \cdot \text{Pa} \cdot 10^{\left(\frac{SPL_{far}}{20}\right)}$$

$p_{far} = 1.1247\text{Pa}$

On Axis Far Field Response of Fostex FE-164 Modeled as a Piston

$S_d := 132 \cdot \text{cm}^2$ $\quad a_d := \sqrt{\pi^{-1} \cdot S_d}$ $\quad a_d = 2.552\text{in}$

$$u_d := \frac{p_{far}}{2 \cdot \rho \cdot c \cdot \sin\left[\frac{1}{2} \cdot \frac{\omega}{c} \cdot 1 \cdot \text{m} \cdot \left[\sqrt{1 + \left(\frac{a_d}{1 \cdot \text{m}}\right)^2} - 1\right]\right]}$$

$u_d = 2.014\text{m}\,\text{sec}^{-1}$

$S_d \cdot u_d = 0.027\text{m}^3\,\text{sec}^{-1}$

On Axis Near Field Response

$$p_{near} := 2 \cdot \rho \cdot c \cdot u_d \cdot \sin\left[\frac{1}{2} \cdot \frac{\omega}{c} \cdot r \cdot \left[\sqrt{1 + \left(\frac{a_d}{r}\right)^2} - 1\right]\right] \qquad p_{near} = 23.697\text{Pa}$$

$$SPL_d := 20 \cdot \log\left(\frac{p_{near}}{2 \cdot 10^{-5} \cdot \text{Pa}}\right)$$

$SPL_d = 121.473$ dB

On Axis Far Field Response of the Port Modeled as a Piston

$r_p := 1.5 \cdot in$

$$u_p := \frac{p_{far}}{2 \cdot \rho \cdot c \cdot \sin\left[\frac{1}{2} \cdot \frac{\omega}{c} \cdot 1 \cdot m \cdot \left[\sqrt{1 + \left(\frac{r_p}{1 \cdot m}\right)^2} - 1\right]\right]}$$

$u_p = 5.826 m sec^{-1}$

$\pi \cdot (r_p)^2 \cdot u_p = 0.027 m^3 sec^{-1}$ (checks w/ driver calc.)

On Axis Near Field Response

$$p_{near} := 2 \cdot \rho \cdot c \cdot u_p \cdot \sin\left[\frac{1}{2} \cdot \frac{\omega}{c} \cdot r \cdot \left[\sqrt{1 + \left(\frac{r_p}{r}\right)^2} - 1\right]\right]$$

$p_{near} = 31.608 Pa$

$$SPL_p := 20 \cdot \log\left(\frac{p_{near}}{2 \cdot 10^{-5} \cdot Pa}\right)$$

$SPL_p = 123.975$ dB

Correction Formulas and Calculated Correction Results

Area Correction Formula

$$\Delta dB := 20 \cdot \log\left[\left[\pi \cdot (r_p)^2\right] \cdot (S_d)^{-1}\right]$$

$\Delta dB = -9.231$ dB

Radius Correction Formula

$$\Delta dB := 20 \cdot \log\left[(r_p) \cdot (a_d)^{-1}\right]$$

$\Delta dB = -4.616$ dB

Actual Required Correction

$SPL_d - SPL_p = -2.502$ dB

Attachment 5 : Correlation of the Measured Data and the MathCad Calculations

Processing the LAUD Measurements and Correlating with the MathCad Near Field Calculations

No Adjustments made to LAUD Data.
Size Correction of -2.502 dB Applied to Terminus Data.

Import Measured Impedance Data

$r := 10, 11 .. 1000$

$Data := 0 \quad f := 0 \quad Temp := 0$

$Data := READPRN("Imped.prn")$

$k_{max} := rows(Data) \qquad k := 0, 1 .. k_{max} - 3$

$f_k := Data_{k,0}$

$Temp_k := Data_{k,1}$

$smooth := cspline(f, Temp) \qquad Mag(r) := interp\left(smooth, f, Temp, \frac{r \cdot d\omega}{Hz}\right) \qquad M_r := Mag(r)$

$Temp_k := Data_{k,2}$

$smooth := cspline(f, Temp) \qquad Phase(r) := interp\left(smooth, f, Temp, \frac{r \cdot d\omega}{Hz}\right) \qquad P_r := Phase(r)$

$ZW_r := \left[\left(M_r \cdot ohm\right) \cdot exp\left(j \cdot P_r \cdot deg\right)\right]$

Import Driver Measured Data

$Data := 0 \quad f := 0 \quad Temp := 0$

$Data := READPRN("Driver.prn")$

$k_{max} := rows(Data) \qquad k := 0, 1 .. k_{max} - 3$

$f_k := Data_{k,0}$

$Temp_k := Data_{k,1}$

$smooth := cspline(f, Temp) \qquad Mag(r) := interp\left(smooth, f, Temp, \frac{r \cdot d\omega}{Hz}\right) \qquad M_r := 2 \cdot 10^{-5} \cdot 10^{\frac{Mag(r)}{20}}$

$Temp_k := Data_{k,2}$

$smooth := cspline(f, Temp) \qquad Phase(r) := interp\left(smooth, f, Temp, \frac{r \cdot d\omega}{Hz}\right) \qquad P_r := Phase(r)$

$W_r := \left(M_r \cdot Pa\right) \cdot exp\left(j \cdot P_r \cdot deg\right) \qquad SPL_{W_r} := 20 \cdot log\left(\frac{\left|W_r\right|}{2 \cdot 10^{-5} \cdot Pa}\right)$

Import Terminus Measured Data

$Data := 0 \quad f := 0 \quad Temp := 0$

$Data := READPRN("Terminus.prn")$

$k_{max} := rows(Data) \qquad k := 0, 1 .. k_{max} - 3$

$f_k := Data_{k,0}$

$Temp_k := Data_{k,1}$

$smooth := cspline(f, Temp) \qquad Mag(r) := interp\left(smooth, f, Temp, \frac{r \cdot d\omega}{Hz}\right) \qquad M_r := 2 \cdot 10^{-5} \cdot 10^{\frac{Mag(r)}{20}}$

$Temp_k := Data_{k,2}$

$smooth := cspline(f, Temp) \qquad Phase(r) := interp\left(smooth, f, Temp, \frac{r \cdot d\omega}{Hz}\right) \qquad P_r := Phase(r)$

$T_r := \left(M_r \cdot Pa\right) \cdot exp\left(j \cdot P_r \cdot deg\right) \qquad SPL_{t_r} := 20 \cdot log\left(\frac{\left|T_r\right|}{2 \cdot 10^{-5} \cdot Pa}\right)$

Driver Calculated and Measured Near Field Sound Pressure Level Response - As Measured Data

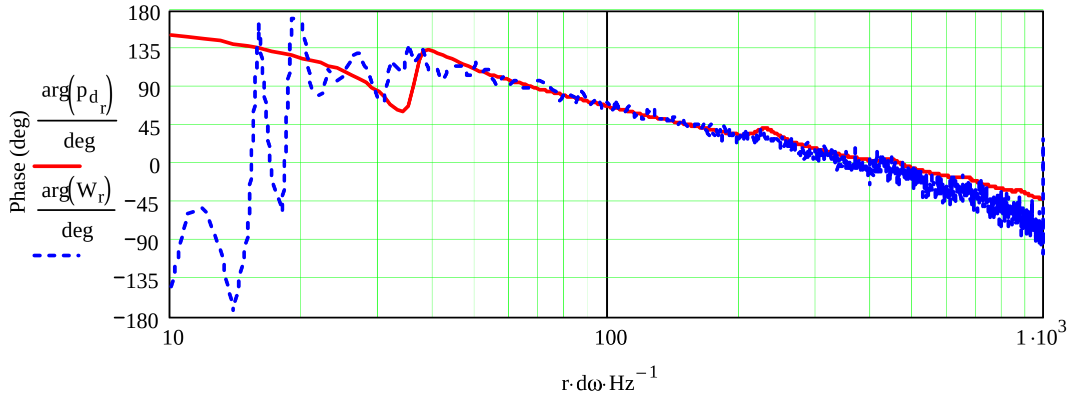

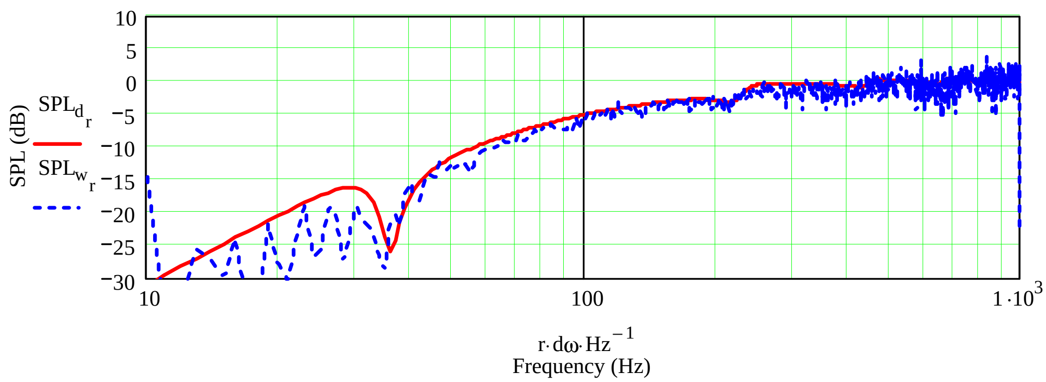

Terminus Calculated and Measured Near Field Sound Pressure Level Response - As Measured Data

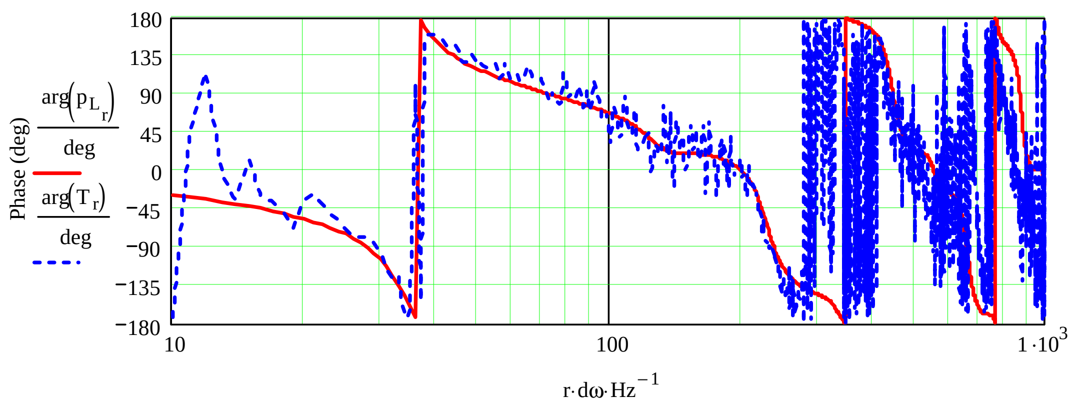

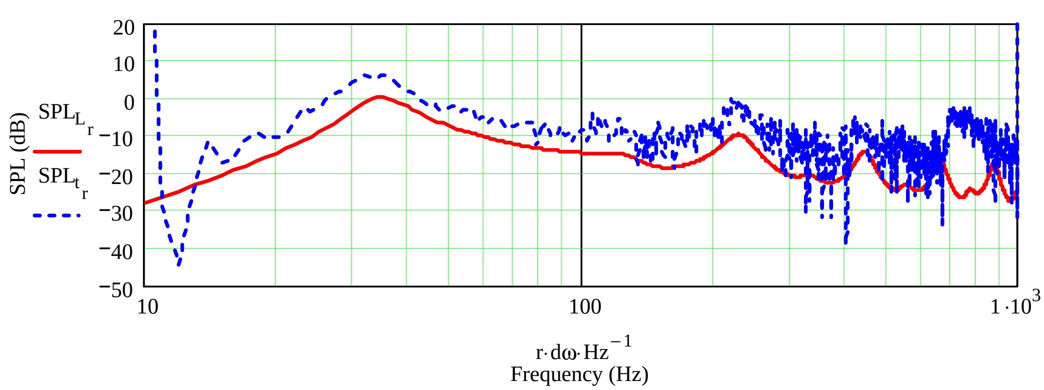

System Measured Data : LAUD Summation w/ 2.502 dB Size Correction

$\text{Data} := 0 \quad f := 0 \quad \text{Temp} := 0$

$\text{Data} := \text{READPRN}(\text{"System.prn"})$

$k_{max} := \text{rows}(\text{Data}) \qquad k := 0, 1 .. k_{max} - 3$

$f_k := \text{Data}_{k,0}$

$\text{Temp}_k := \text{Data}_{k,1}$

$\text{smooth} := \text{cspline}(f, \text{Temp}) \qquad \text{Mag}(r) := \text{interp}\left(\text{smooth}, f, \text{Temp}, \frac{r \cdot d\omega}{Hz}\right) \qquad M_r := 2 \cdot 10^{-5} \cdot 10^{\frac{\text{Mag}(r)}{20}}$

$\text{Temp}_k := \text{Data}_{k,2}$

$\text{smooth} := \text{cspline}(f, \text{Temp}) \qquad \text{Phase}(r) := \text{interp}\left(\text{smooth}, f, \text{Temp}, \frac{r \cdot d\omega}{Hz}\right) \qquad P_r := \text{Phase}(r)$

$\text{Sys}_r := (M_r \cdot Pa) \cdot \exp(j \cdot P_r \cdot \deg) \qquad \text{SPLs}_r := 20 \cdot \log\left(\frac{|\text{Sys}_r|}{2 \cdot 10^{-5} \cdot Pa}\right)$

System Calculated and Measured Near Field Sound Pressure Level Response

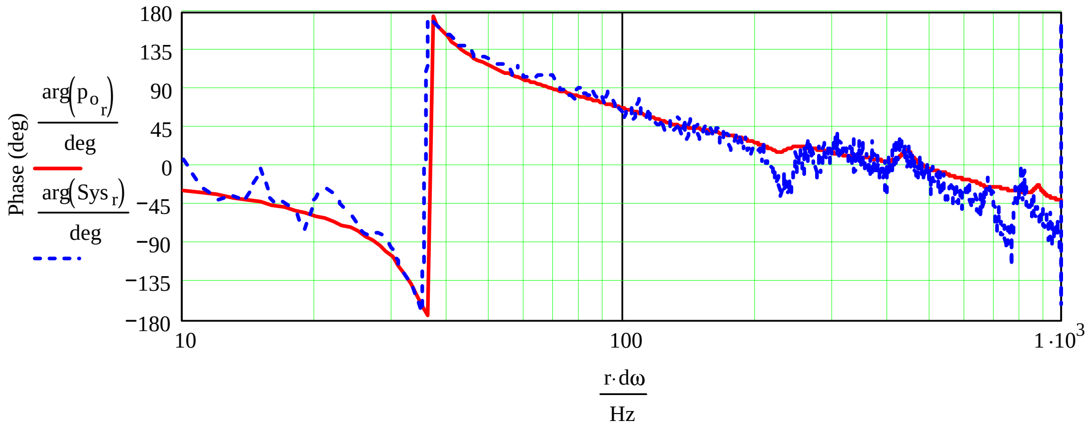

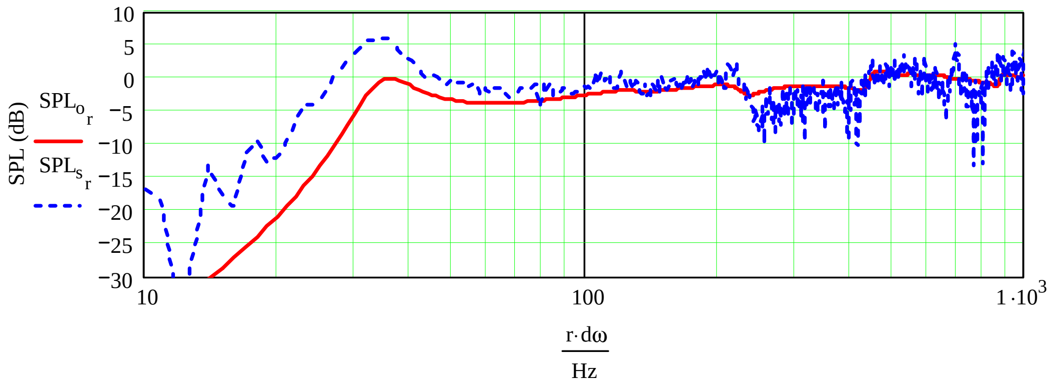

Frequency (Hz)

Calculated and Measured Impedance

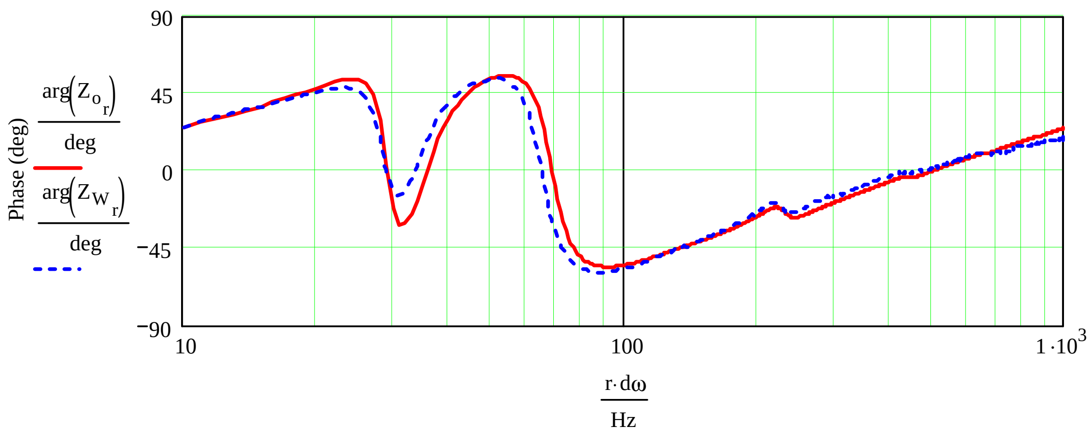

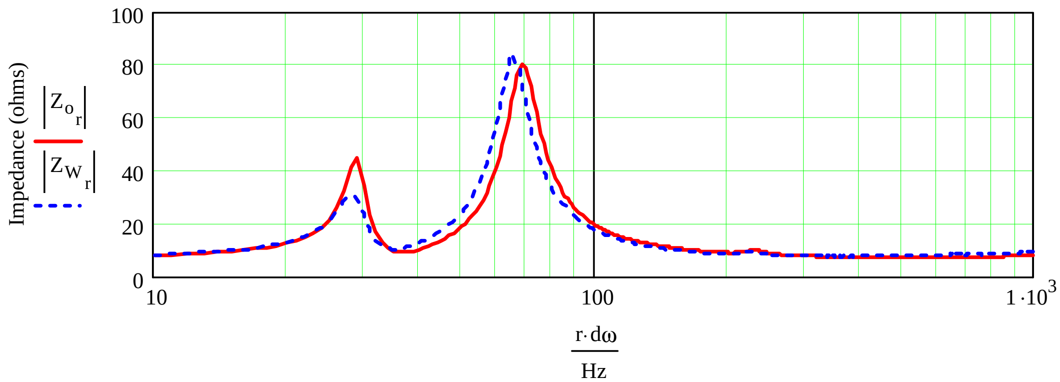

Adjusting the LAUD Measurements and Correlating with the MathCad Near Field Calculations

Adjustments :

1. Equal Level Offset to both Driver and Terminus Data.
2. Acoustic Center Offset Applied to the Driver Data Only.
3. Size Correction of -2.502 dB Applied to Terminus Data.

Import Driver Measured Data and Adjust for Level Offset and Acoustic Center

$\text{Data} := 0 \quad f := 0 \quad \text{Temp} := 0$

$\text{Data} := \text{READPRN}(\text{"Driver.prn"})$

$k_{max} := \text{rows}(\text{Data}) \qquad k := 0, 1 .. k_{max} - 3$

$f_k := \text{Data}_{k,0}$

$\text{Temp}_k := \text{Data}_{k,1}$

$\text{smooth} := \text{cspline}(f, \text{Temp}) \qquad \text{Mag}(r) := \text{interp}\left(\text{smooth}, f, \text{Temp}, \frac{r \cdot d\omega}{Hz}\right) \qquad M_r := 2 \cdot 10^{-5} \cdot 10^{\frac{\text{Mag}(r)}{20}}$

$\text{Temp}_k := \text{Data}_{k,2}$

$\text{smooth} := \text{cspline}(f, \text{Temp}) \qquad \text{Phase}(r) := \text{interp}\left(\text{smooth}, f, \text{Temp}, \frac{r \cdot d\omega}{Hz}\right) \qquad P_r := \text{Phase}(r)$

$W_r := \left(M_r \cdot Pa\right) \cdot \exp\left(j \cdot P_r \cdot deg\right) \qquad SPL_{w_r} := 20 \cdot \log\left(\frac{\left|W_r\right|}{2 \cdot 10^{-5} \cdot Pa}\right) - 5 + 6$

Import Terminus Measured Data and Adjust for Level Offset

$\text{Data} := 0 \quad f := 0 \quad \text{Temp} := 0$

$\text{Data} := \text{READPRN}(\text{"Terminus.prn"})$

$k_{max} := \text{rows}(\text{Data}) \qquad k := 0, 1 .. k_{max} - 3$

$f_k := \text{Data}_{k,0}$

$\text{Temp}_k := \text{Data}_{k,1}$

$\text{smooth} := \text{cspline}(f, \text{Temp}) \qquad \text{Mag}(r) := \text{interp}\left(\text{smooth}, f, \text{Temp}, \frac{r \cdot d\omega}{Hz}\right) \qquad M_r := 2 \cdot 10^{-5} \cdot 10^{\frac{\text{Mag}(r)}{20}}$

$\text{Temp}_k := \text{Data}_{k,2}$

$\text{smooth} := \text{cspline}(f, \text{Temp}) \qquad \text{Phase}(r) := \text{interp}\left(\text{smooth}, f, \text{Temp}, \frac{r \cdot d\omega}{Hz}\right) \qquad P_r := \text{Phase}(r)$

$T_r := \left(M_r \cdot Pa\right) \cdot \exp\left(j \cdot P_r \cdot deg\right) \qquad SPL_{t_r} := 20 \cdot \log\left(\frac{\left|T_r\right|}{2 \cdot 10^{-5} \cdot Pa}\right) - 5$

Driver Calculated and Measured Near Field Sound Pressure Level Response - After Adjustments

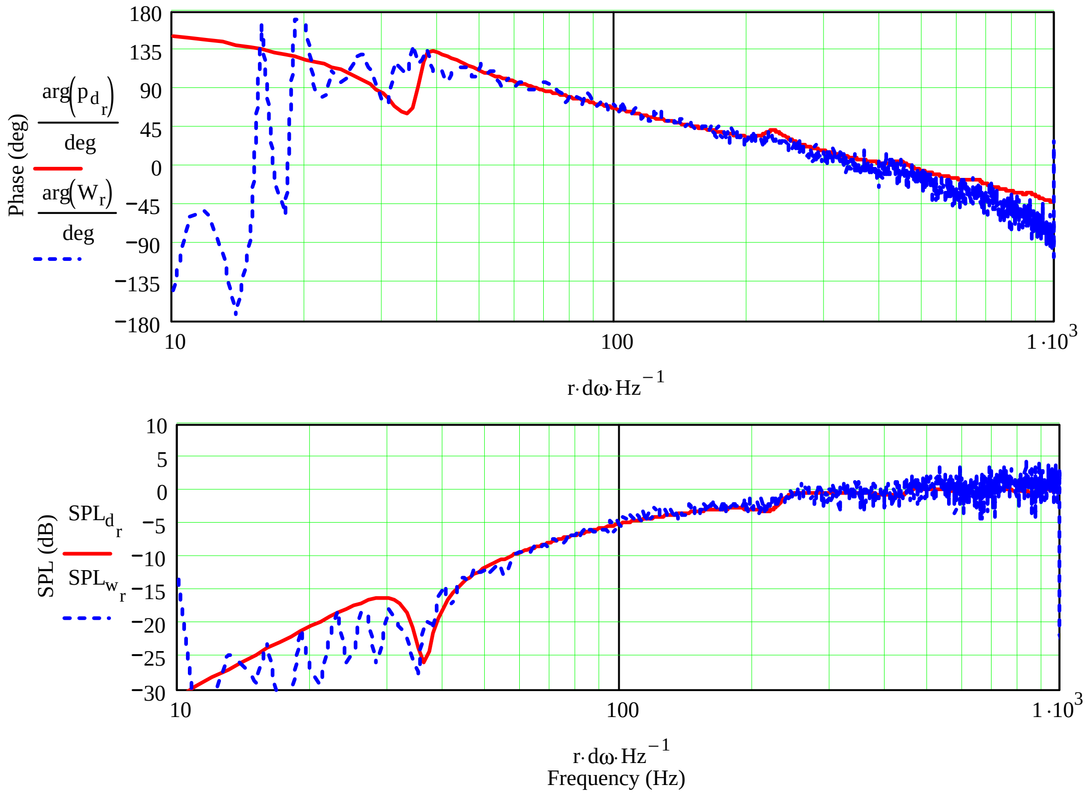

Terminus Calculated and Measured Near Field Sound Pressure Level Response - After Adjustments

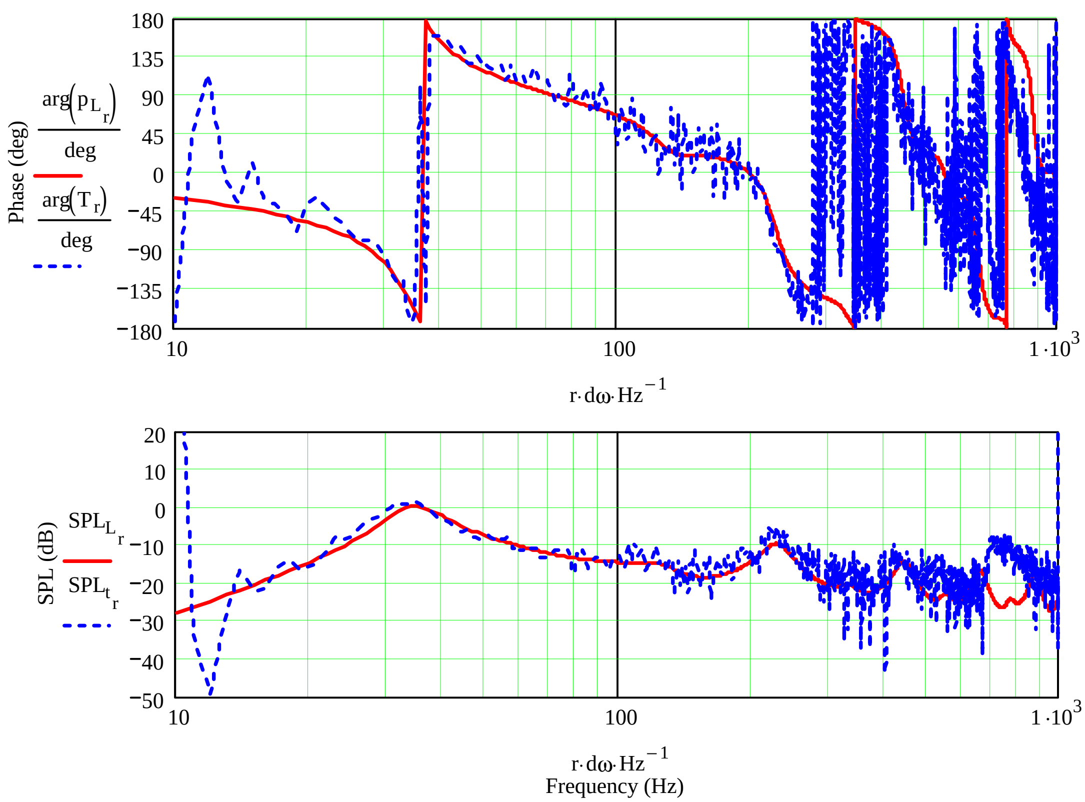

System Measured Data with Adjustments for Level, Driver Acoustic Center, and Relative Size

$$\exp\left(\frac{-1}{20}\right)^{-1} = 1.051$$

$$\exp\left(\frac{5 + 2.502}{20}\right)^{-1} = 0.687$$

$$Sys_r := 1.051 \cdot W_r + 0.687 \cdot T_r \qquad SPL_r := 20 \cdot \log\left(\frac{\left|Sys_r\right|}{2 \cdot 10^{-5} \cdot Pa}\right)$$

System Calculated and Measured Near Field Sound Pressure Level Response - After Adjustments